ENDOCARDIAL CELLS ARE A DISTINCT ENDOTHELIAL LINEAGE DERIVED FROM MULTIPOTENT CARDIOVASCULAR PROGENITORS

By

Andrew Michael Misfeldt

Dissertation

Submitted to the Faculty of the

Graduate School of Vanderbilt University

in partial fulfillment of the requirements

for the degree of

DOCTOR OF PHILOSOPHY

in

Cell and Developmental Biology

December, 2008

Nashville, Tennessee

Approved:

Professor Christopher V. Wright, Chair

Professor H. Scott Baldwin

Professor Guoqiang Gu

Professor Tsutomu Kume

Professor Antonis Hatzopoulos

To my parents, Michael and Alice

and

To my wife, Amanda

ACKNOWLEGDEMENTS

Surprisingly, the hardest words to write are “thank you.” Reflecting back on these past few years, it is abundantly clear that the work presented in this dissertation was only accomplished with the support of several individuals, labs, programs, and departments.

First of all, without the Department of Cell and Development and its commitment to the educational needs of graduate students, none of this would have been possible. In addition, I would like to express my appreciation to the Program in Developmental Biology, particularly its director Chris Wright and its coordinator Kim Kane, who have established what I believe is the premiere scientific community here at Vanderbilt. Finally, I would like to thank the Vanderbilt Medical Scientist Training Program, especially its past and present directors David Robertson and Terry Dermody, for giving me the opportunity to experience a truly rare and immensely rigorous academic training regime.

I would like to thank my graduate mentor, Scott Baldwin, for his support and guidance. I am immensely grateful for all the opportunities that have provided for me to learn and grow as an independent researcher. These thanks extend to all members of the Baldwin lab past and present, particularly Melissa Langworthy, Kel Vin Woo, Kate Violette, Dan DeLaughter, Leigh Compton, Kathy Boyer, Lorene Batts, Kim Roberts, Kevin Tompkins, Xianghu Qu, Justin Grindley, and Kai Jiao, as well friends of the Baldwin Lab, including Lance Prince, Steve Goudy, Ryan Humphreys, Chris Brown, Jaime Hendrix, and Cyndi Hill.

I would also like to thank the members of my committee, Chris Wright, Guoqiang Gu, Antonis Hatzopoulos, and Tom Kume, for keeping me focused and pushing me down the right avenues of investigation. In particular, I am deeply grateful to the chair of my committee, Chris Wright for his advice and perspective.

In this day and age, I would be remiss in not acknowledging my sources of funding. This includes the Vanderbilt Medical Scientist Training Program (T32 GM07347), a Predoctoral Fellowship from the Southeast conference of the American Heart Association (0515191B), and a March of Dimes Birth Defects Foundation award (1FY07-513).

During the course of these studies, we have had several collaborators who have supplied essential reagents and expertise. Victoria Bautch provided us the basic skills and protocols for embryonic stem cell differentiation. Antonis Hatzopoulos and Mathias Lamparter also were extremely helpful in getting this system off the ground. Doug Mortlock and Michelle Southard-Smith provided all the reagents to establish BAC recombineering and transgenesis in the lab. The advice of Trish Labosky was critical for the derivation of ESC lines from our transgenic mice. I also want to express my gratitude to Lorene Batts and Kevin Tompkins for all their technical assistance. In addition, I am very appreciative of services of Kevin Weller, David Flaherty, and Brittany Matlock in the VMC Flow Cytometry Shared Resource.

I was exceptionally lucky to have been surrounded by people who have made the long hours and many failed experiments tolerable, and for that I am thankful. To Chris Brown, you have been a good friend and valuable scientific resource. To Dave Frank, I blame you for many lost hours of work. Without your less than gentle encouragement, I

am sure I would have generated more data, but my life would be less interesting for it. To Scott Boyle, building the BAC transgene could only have been done with your help. To Mel, we endured and came out stronger, I hope zebrafish treat you better than the kidney. I was fortunate to have you as a colleague and friend. To Kel Vin and Kate, I wish you the best of luck as you finish your studies.

I have also been blessed with immeasurable support from my family. To my parents Mike and Alice, your commitment to education made it possible for me to pursue this career path. Without you constantly pushing me to be the best I could be, I am not sure I would have made it this far. To my sister Kristin, I am so proud of all your achievements, and am thankful for our strong friendship. Finally, I want to thank my wife, Amanda, and express how much her love and support keeps me motivated. It is my daily goal to match your work ethic and dedication. As stated by others, you married down, but I am thankful everyday that you did. I cannot wait to see where life takes us next.

TABLE OF CONTENTS

LIST OF TABLES

LIST OF FIGURES

LIST OF ABBREVIATIONS

β-gal	Beta-galactosidase
a	Atria
AMP	Ampicillin
ANF	Atrial natriuretic factor
ao	Aorta
APC	Allophycocyanin
as	Aortic sac
ATCC	American Types Culture Collection
av	Aortic valve
AVC	Atrioventricular canal
AVE	Anterior visceral endoderm
avs	Atrioventricular septum
BABB	Benzyl alcohol: benzyl benzoate
BAC	Bacterial artificial chromosome
bHLH	Basic helix-loop-helix
BL-CFC	Blast colony-forming cell
BMP	Bone morphogenic protein
bp	Base pair
bvf	Bulboventricular fold
Ca	Caudal
CAD	Coronary artery disease
CAM	Chloramphenical
cc	Cardiac crescent
CDK	Cyclin dependent kinase
CHD	Congenital heart disease
CHF	Congestive heart failure
Cm	Cardiomyocyte
CNC	Cardiac neural crest
Cr	Cranial
CRAC	Calcium-release-activated calcium channels
ct	Conotrunus
cTnT	Cardiac troponin T
Ctsk	cysteine protease cathepsin K
cz	Compact zone
D_	Differentiation day
da	Dorsal aorta
DAB	Diaminobenzidine
DAPI	4',6-diamidino-2-phenylindole
DCS	Directly conjugated secondary antibody
Dkk-1	Dickkopf-1
DM	Differentiation media
dmc	Dorsal mesocardium

DMEM	Dulbecco's modified eagle medium
DMSO	Dimethyl sulfoxide
e	Endocardium
E_	Embryonic day
EB	Embryoid body
Ec	Endocardial cell
ECC	Endocardial cushions
ECD	E-cadherin
ECE	Endothelin-converting enzymes
ECM	Extracellular matrix
EDTA	Ethylene diamine tetraacetic acid
eEPCs	Embryonic endothelial progenitor cells
EGF	Epidermal growth factor
EGTA	Ethylene glycol tetraacetic acid
EMT	Epithelial-to-mesenchymal transition
ep	Endocardial precursor
ESC	Embryonic stem cell
Et	Endothelial cell
ET	Endothelin
FACS	Fluorescence activated cell sorting
FBS	Fetal bovine serum
FGF	Fibroblast growth factor
GAG	Glycosaminoglycans
GCV	Gancyclovir
GFP	Green fluorescent protein
GSK3β	glycogen-synthase kinase 3
HBSS	Hank's balanced salt solution
hCG	Human chorionic gonadotropin
HPRT	Hypoxanthine-guanine phosphoribosyltransferase
HSVtk	Herpes simplex virus thymidine kinase
ht	Heart tube
iec	Intraembryonic coelom
IGF	Insulin-like growth factor
IMDM	Iscove's modified Dulbecco's medium
IP_3	Inositol-1,4,5-trisphosphate
iPS	Induced pluripotent stem cell
ivs	Intraventricular septum
KAN	Kanamycin
Kb	Kilobase
KDR	Kinase domain region
Klf4	Kruppel-like factor 4
la	Left atria
LB	Luria broth
LIF	Leukemia inhibitory factor
lv	Left ventricle
m	Myocardium

M	Molar
MCP	Multipotent cardiovascular progenitor
MCS	Multiple cloning site
Mef	Myocyte enhancer factor
MHC	Myosin heavy chain
MI	Myocardial infarction
MLC	Myosin light chain
mM	Millimolar
mp	Myocardial precursors
msc	Mesenchymal cells
mv	Mitral valve
NBF	Neutral buffer formalin
ne	Neuroectoderm
NEO	Neomycin
Nf1	Neurofibromin
NFAT	Nuclear factor of activated T-cells
NF-κβ	Nuclear factor-κβ
NHR	NFAT homology region
NICD	Notch intracellular domain
NLS	Nuclear localization sequence
Nrg1	Neuregulin1
O/N	Overnight
OFT	Outflow tract
pb	Pulmonary bud
PBS	Phosphate Buffered Saline
PDGF	Platelet-derived growth factor
PE	Proepicardium
PFGE	Pulse field gel electrophoresis
PHF	Primary heart field
PI	Propidium iodide
PIP_2	Phosphatidylinositol-4,5-bisphosphate
PLC-γ	Phospholipase C-γ
PMAGE	Polony multiplex analysis of gene expression
PMEF	Primary mouse embryonic fibroblast
PMSG	Pregnant mare serum gonadotropin
PS	Primitive streak
pv	Pulmonary valve
qRT-PCR	Quantitative real-time PCR
RA	Retinoic acid
ra	Right atria
RHR	Rel homology region
Rosa	Reverse orientation splice acceptor
RT	Room temperature
RT-PCR	Reverse transcriptase PCR
rv	Right ventricle
SAGE	Serial analysis of gene expression

SCID	Severe combined immunodeficiency
SDS	Sodium dodecyl sulfate
SHF	Secondary heart field
Shh	Sonic hedgehog
Sm	Smooth muscle
sv	Sinus venous
T	Brachyury
t	Trabeculea
Tet	Tetracycline
Tet^R	Tetracycline resistance cassette
TGF	Transforming growth factor
TRAP	Tartrate-resistant acid phosphatase
tz	Trabecular zone
UTR	Untranslated region
v	Common ventricle
VEGF	Vascular endothelial growth factor
VSMC	Vascular smooth muscle cell
vWF	von Willibrand Factor
YFP	Yellow fluorescent protein
µM	Micromolar
µm	Micrometer or micron
Ys	Yolk sac
ZPA	Zone of polarizing activity

CHAPTER I

INTRODUCTION

Overview

Heart disease represents one of the most prevalent conditions in modern health care, impacting the morbidity and mortality of patients at every stage of life. Congenital heart disease (CHD), as the most common birth defect, affects 1 out of every 100 live births worldwide (Hoffman and Kaplan, 2002). Increasingly, subtle cardiac developmental anomalies and unfavorable genetic predispositions are being regarded as potent risk factors for adult onset heart disease. Despite improvements in the surgical and pharmacological management of these afflictions, there has been a concerted effect to discover new treatment modalities. Recently, embryonic and adult stem cells have been touted as potential tools for regenerative medicine, with the hope that they might be used to repair and regenerate lost and damaged tissues (Murry and Keller, 2008). Understanding the specification of cardiac lineages from progenitor populations and how these different components interact to achieve proper organogenesis is an essential first step to harness stem cells for the treatment of both congenital and adult heart disease.

While factors influencing cardiomyocyte specification and differentiation have been well documented, little is known regarding the origin of the endocardium, the endothelial component of heart chambers. Examination of endocardiogenesis, the process of endocardial endothelium arising from mesodermal precursors, has proven difficult without markers to distinguish endocardium from endothelium. The

transcription factor Nuclear Factor of Activated T-Cells calcineurin-dependent-1 (NFATc1) has been identified one of the few specific markers of this endothelial subpopulation. Our laboratory has previously focused on the transcriptional regulation of *NFATc1* in endocardial cells lining the presumptive valve cushions, where NFATc1 functions in the maintenance of the endocardial cell layer during epithelial-to-mesenchymal transformation (EMT). However, NFATc1 is also expressed in endocardial cells as they first emerge from the cardiac mesoderm. Characterization of the regulatory domains controlling expression of *NFATc1* could potentially be used as a genetic tool to label early endocardial precursors, allowing for in depth study of endocardiogenesis and the origin of the endocardium. Taking into account the unique role endocardium plays in cardiogenesis, we hypothesized that the endocardium is a distinct subpopulation of endothelium derived from a common cardiovascular precursor in the anterior cardiac mesodermal also responsible for generating the myocardium, and is essential for proper cardiac morphogenesis.

The primary focus of my research has been to identify and monitor endocardiogenesis *in vivo* and *in vitro* using an *NFATc1* reporter transgene. Chapter I will describe heart development and detail the contributions made by various cell lineages to the assembling heart. It will go on to discuss proposed models of endocardial differentiation, the role of endocardium in cardiac morphogenesis, and the role of NFATc1 in heart development. Finally, Chapter I will provide background on embryonic stem cell (ESC) differentiation, specifically how it has furthered our understanding of cardiovascular specification and differentiation. Chapter II documents the generation of *NFATc1-nuc-LacZ* BAC transgenic mice, which by faithfully recapitulating endogenous

NFATc1 expression identifies the endocardium at the earliest stage of cardiac development. Chapter III focuses on the establishment of ESC differentiation as an *in vitro* model of endocardial differentiation demonstrating spatial-temporal coordination of endocardial and myocardial differentiation that mirrors the pattern seen during embryogenesis. Chapter IV extends these observations by documenting that endocardium is a cardiac cell lineage distinct from the hematopoietic lineage and systemic vasculature. Furthermore, the isolation and characterization of Flk1+ multipotent cardiovascular progenitors (MCPs) provides evidence that endocardium and myocardium are derived from a common precursor. In Chapter V, I conclude by discussing the significance of a multipotent cardiovascular progenitor focusing on endocardial-myocardial interactions and highlight future experiments to explore the differences between endocardium and other endothelium, as well as characterize the role of endocardium in heart development.

Heart development

The heart is the first organ to function in vertebrate organisms, and the cessation of its function is used as the defining characteristic of clinical death. Cardiac development in the mouse begins at embryonic day 7.5 (E7.5) in the splanchnic layer of the anterior lateral plate mesoderm between the anterior visceral endoderm (AVE) and ectoderm (reviewed in Harvey, 2002; Srivastava, 2006). The cardiac mesoderm consists of two bilaterally symmetrical fields of precursors that extend cranially towards the extraembryonic mesoderm (Fig. 1.1A). This pattern, which is conserved across diverse species, was adopted as an alternative term for this region, the cardiac crescent. With

lateral folding of the embryo, occurring from E7.5 to E8.5, these precursors coalescence along the ventral midline to form a primitive heart tube with an outer myocardium and inner endocardium separated by an extracellular matrix (ECM) termed the cardiac jelly (Fig. 1.1B). This linear tube serves as the structural basis for subsequent morphogenesis, as the heart initiates a conserved program of patterned growth and dextrorotation. Cardiac looping forces the atria and venous system dorsally, while the primitive ventricle bulges towards the anterior aspect of the embryo.

In addition, looping establishes borders of the atrioventricular canal (AVC) and the conotrunus or outflow flow tract (OFT), where swelling of the cardiac jelly marks the location of future valve formation (Fig. 1.1C). By E10.5, endocardial cells of the AVC and OFT delaminate and invade the cardiac jelly to form the endocardial cushions (ECC) (reviewed in Armstrong and Bischoff, 2004; Barnett and Desgrosellier, 2003). Through a process of cell differentiation, apoptosis, and ECM remodeling, ECCs are modified into thin leaflets of endothelium over a core of collagen, elastin, and glycosaminoglycans (GAGs) (Schroeder *et al.*, 2003). Cushion formation is the first step in a process known as septation, the division of atria and ventricles into right and left sides to generate the four-chambered heart necessary for parallel circulation in warm-blooded animals. Septation also marks the formation of trabecular and compact myocardial layers in the ventricles (Fig. 1.1D). The rapidly proliferating outer compact layer of the myocardium is responsible for the majority of ventricular growth seen between E11.5 and E14.5. The inner trabecular layer generates myocardial outgrowths into the ventricular chambers that increase myocardial perfusion and aid in contraction (Ben-Shachar *et al.*, 1985).

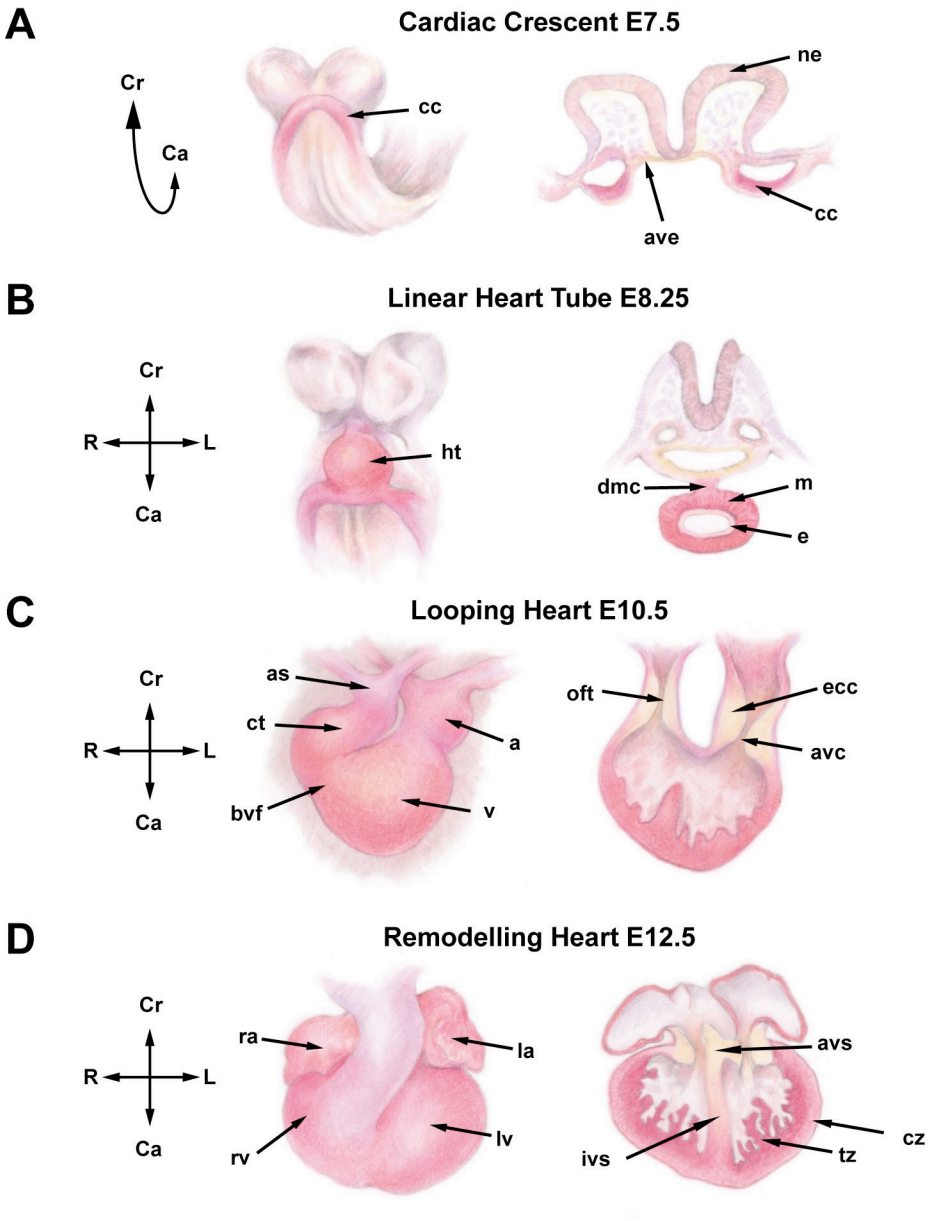

Figure 1.1. ***Morphogenic events in early cardiac development.*** Structural changes during the initial formation and remodeling of the murine heart. Figure modified from Harvey (2002).

Cranial, Cr; caudal, Ca; cardiac crescent, cc; neuroectoderm, ne; anterior visceral endoderm, ave; heart tube, ht; dorsal mesocardium, dmc; myocardium, m; endocardium, e; conotrunus, ct; bulboventricular fold, bvf; atria, a; atrioventricular canal, avc; aortic sac, as; common ventricle, v; endocardial cushions, ecc; left atria, la; left ventricle, lv; right ventricle, rv; right atria, ra; trabecular zone, tz; compact zone, cz; atrioventricular septum, avs; interventricular septum, ivs

In addition to the endocardium and myocardium, "extra-cardiac" lineages, populations not originating in the cardiac crescent, are crucial for complete formation of a functional heart, the two most notable being the Proepicardium (PE) and the Cardiac Neural Crest (CNC) cells. The PE originates at the septum transversum, migrating over the myocardium to form a single layer of cells by E10.5, at which it is becomes the epicardium (Mikawa and Gourdie, 1996). Epicardial cells undergo EMT and delaminate into the myocardium where they form endothelial cells, smooth muscle cells, and myofibroblasts. Formation of a functional coronary vascular plexus is essential for myocardial growth. CNC cells, as the other predominant extra-cardiac lineage, contributes to the OFT and parasympathetic innervation of the heart. Migrating CNC from somites 1-3 pass through pharyngeal arches 3, 4, and 6, where they play a role in remodeling the originally paired pharyngeal arch arteries into the aortic arch and its tributaries (Waldo *et al.*, 1998; Waldo *et al.*, 1999). Continuing on to the heart, cells of the CNC enter the distal OFT between the endocardium and myocardium to participate in OFT septation, becoming incorporated into the semilunar valves, and through myocardialization, generate myocardium and smooth muscle in the aortic and pulmonary arteries (reviewed in Brown and Baldwin, 2006).

Mesodermal origin of cardiac lineages

Heart development is dependent on the coordination of several distinct cell lineages. These interactions occur during specific developmental windows, at precise spatial locations, deviation from which can result in numerous development abnormalities. To understand how these lineages interact, it is necessary to examine their

developmental origins and how they are specified. Gastrulation transforms uncommitted embryonic epiblast into three germ cell layers: ectoderm, which forms skin and neural tissue; mesoderm that generates blood, bone, and muscle; and endoderm, the source of the respiratory and gastrointestinal systems (Tam and Behringer, 1997). Precursors of the cardiac mesoderm are derived from epiblast cells that reside lateral to the *brachyury* positive primitive streak (PS) (Fig 1.2Ai). These cells, which will come to populate the cardiac crescent, pass through the primitive streak during mid-gastrulation (Kinder *et al.*, 1999). As this population leaves the PS to form the anterior and lateral plate mesoderm, it transiently upregulates the basic helix-loop-helix (bHLH) transcription factor *Mesp1* (mesoderm posterior 1); fate mapping of *Mesp1*+ cells indicate they localize to the cardiac and paraxial mesoderm to generate the heart and skeletal muscle of the head and neck (Fig 1.2Ai). Loss of *Mesp1*, does not impact mesodermal formation or migration, or cardiac induction, but inhibits linear heart formation (Saga *et al.*, 1999). However, a double knockout of *Mesp1* and the closely related bHLH transcription factor *Mesp2* results in failure of mesodermal cells to migrate away from the PS, indicating functional redundancy between the two transcription factors (Kitajima *et al.*, 2000). Recent studies in embryonic stem cell models suggest that *Mesp1* is essential for the initial commitment of mesoderm towards a cardiac fate (Bondue *et al.*, 2008; Lindsley *et al.*, 2008).

Cardiogenic progenitors express neither *Mesp1* nor *Mesp2* upon reaching the anterio, though the cell surface receptor Flk1 is ubiquitously present in the cardiac mesoderm (Fig. 1.2Ai). Flk-1 (fetal liver kinase1, also known as Vascular Endothelial Growth Factor Receptor 2, VEGFR-2; or kinase domain region, KDR) was originally classified as one of the four Vascular Endothelial Growth Factor (VEGF) receptors

(Ferrara *et al.*, 2003). Targeted disruption of *Flk1* was embryonic lethal at E8.5-9.5 caused by a lack of vasculogenesis, *de novo* creation of blood vessels from mesodermal precursors (angioblasts), and impaired blood/vascular lineage development (Shalaby *et al.*, 1997; Shalaby *et al.*, 1995). Initially, Flk1 was viewed as an endothelial-specific receptor functioning in vascular formation and maintenance, in part due to the endothelial-restricted expression pattern of an Flk1 transgenic reporter targeted with the Beta-galactosidase (β-gal) gene *LacZ*.

However, subsequent lineage tracing with a transgenic mouse expressing Cre recombinase under the *Flk1* promoter suggested cell populations other than just endothelium expressed Flk1. When crossed with the *Rosa26 LacZ* reporter (*R26R*) mouse that activates β-gal in cells where Cre is actively being produced, as well as their progeny, expression was observed in skeletal and cardiac muscle, populations not previously associated with Flk1 expression (Motoike *et al.*, 2003; Soriano, 1999). At first met with skepticism, further examination indicated that Flk1 was expressed much earlier and in a broader pattern than previously described. By removing the neomycin selection cassette from the *Flk1* locus already possessing *LacZ*, expanded expression was detected in mesodermal cells departing the PS during early and mid-gastrulation (Ema *et al.*, 2006). These populations localized to blood islands in the extraembryonic mesoderm, the site of early vasculogenesis and hematopoiesis, and the cardiac crescent at E7.5 (Fig. 1.2Ai,ii). Though present in all cardiac progenitors, Flk1 is downregulated in myocardial cells over the course of cardiogenesis, yet retained in endocardium. Interestingly, *Flk1*$^{-/-}$ mice possess no observable defects in cardiomyocyte differentiation

or early morphogenesis, as the primitive heart forms and initiates looping prior to succumbing to vasculature insufficiency (Shalaby *et al.*, 1995).

Primary and secondary heart fields

Until recently, segmentation of the primitive heart tube was thought to reflect primordial regionalization that through growth and remodeling generated all aspects of the mature heart (reviewed in Srivastava and Olson, 2000). Through a combination of ablation studies, gene targeting, and lineage tracing it has become accepted that the adult heart is fashioned from two distinct heart fields (reviewed in Buckingham *et al.*, 2005; Kirby, 2002). The primary or first heart field (PHF), in the anterior lateral plate splanchnic mesoderm, represents the cells that generate the primitive heart tube of endocardium and myocardium (Fig. 1.2Aii). This linear tube then acts as a scaffold for another population of heart progenitors, referred as the secondary or anterior heart field, to enter the arterial and venous poles (Fig 1.2Bi). The terms anterior and secondary heart field are used interchangeably, but actually represent two different classifications of this second progenitor population. The secondary heart field is positioned behind the OFT in the pharyngeal mesoderm, while the anterior heart field encompasses both the secondary heart field and cranial mesoderm that extends into the pharyngeal arches; for simplicity, secondary heart field (SHF) will be used to designate this combined population of heart progenitors (Fig 1.2Aii) (Kelly *et al.*, 2001; Mjaatvedt *et al.*, 2001; Waldo *et al.*, 2001; Zaffran *et al.*, 2004). A retrospective clonal analysis with a α-cardiac actin laacZ reporter demonstrated the two lineages segregated soon after gastrulation from a common precursor (Meilhac *et al.*, 2004). How this divergence is regulated remains unknown.

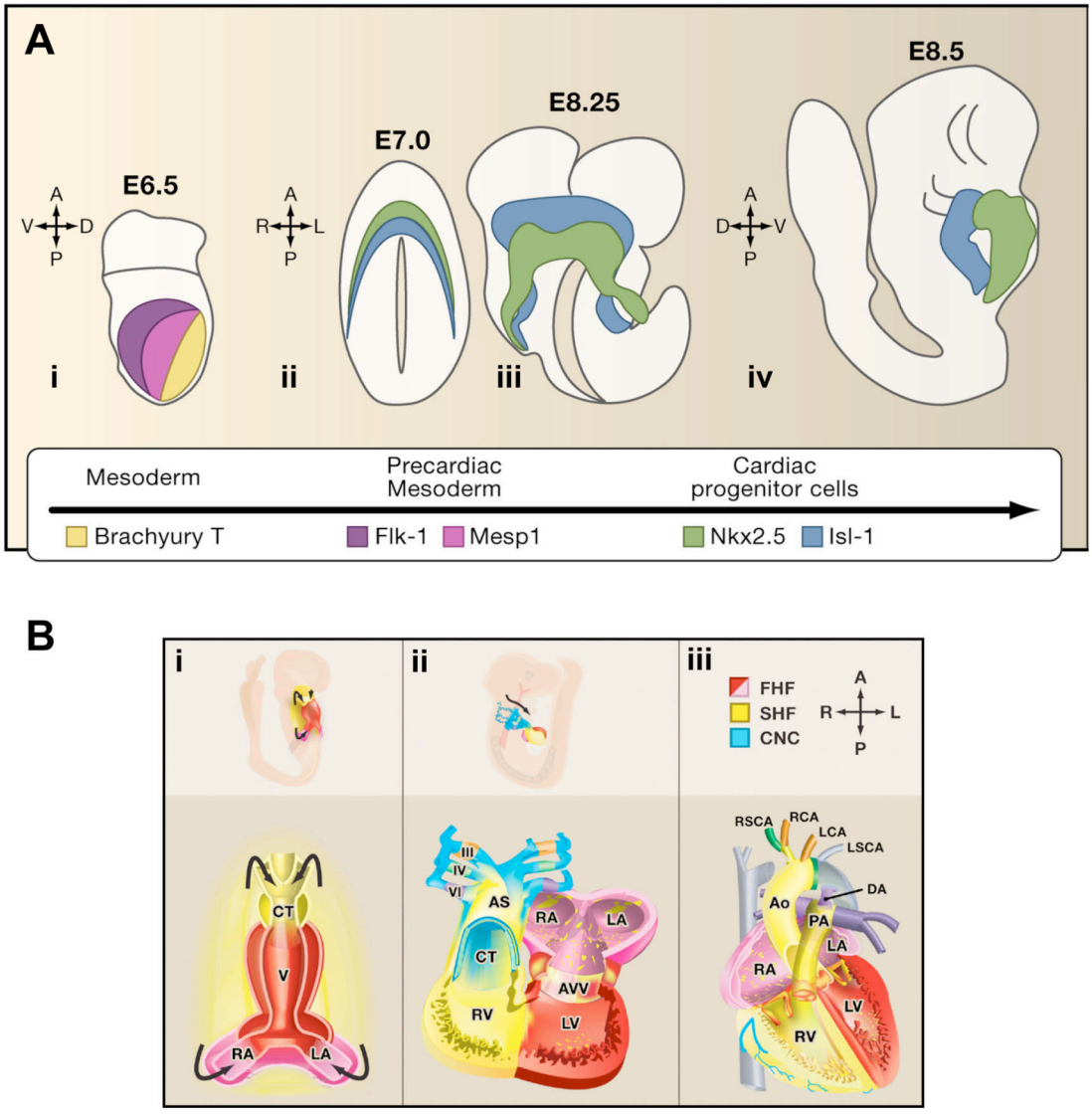

Figure 1.2. ***The origin and contribution of mesodermal and extracardiac lineages to the developing heart.*** **A.** Migration of mesodermal cells to the cardiac mesoderm from the primitive streak following gastrulation with associated gene expression (**i**). Location and orientation of the PHF (green) and the SHF (blue) at the cardiac crescent stage (**ii**) through the formation of the primitive linear heart tube (**iii**,**iv**). Figure adopted from Wu *et al.* (2008). **B.** Contribution of the PHF (red), SHF (yellow), and CNC (blue) to structures of the developing and adult heart. Figure adopted from Srivastava (2006).

In mice, the SHF was initially revealed by expression of an *FGF10* reporter active in the pharyngeal mesoderm (Kelly *et al.*, 2001). Analysis at a later developmental time point in this reporter mice documented β-gal+ cells in the right ventricle and outflow tract of the looped heart (Fig 1.2Aiii). This same study utilized Di-I labeling to track the pharyngeal mesoderm, confirming that this population did contribute to the myocardium. Studies of the LIM homeodomain transcription factor *islet1* (*isl1*) further supported the existence of a SHF and clarified its contribution to the developing heart. *Isl1* is expressed at E7.5 in the pharyngeal mesoderm, and later at the poles of the E8.5 linear heart; however, by E10.5 *isl1* is not expressed in the heart (Cai *et al.*, 2003). Fate mapping with a Cre recombinase targeted to the *isl1* locus demonstrated early isl1+ populations in the pharyngeal mesoderm generated structures associated with the SHF. In addition, deletion of *isl1* resulted in embryonic lethality caused by a failure of the right side of the heart to form.

Present models contend that the PHF, traditionally defined by its mesodermal location and expression of *Nkx2.5*, first identified as a homologue of the Drosophila *tinman*, generates the atria and left ventricle (Fig. 1.2Bii,iii). The SHF, marked by its prototypical transcription factor *isl1*, is instrumental to the development of the right ventricle and OFT. Asymmetrical gene expression in two sides of the heart had been observed prior to the discovery of the SHF. Disruption of the T-box transcription factor *Tbx5* or the bHLH *Hand1/eHand* result in left ventricle hypoplasia, while lose of *Mef2c* (myocyte enhancer factor 2) or *Hand2/dHand* cause right ventricular hypoplasia (Bruneau *et al.*, 2001; Firulli *et al.*, 1998; Lin *et al.*, 1997; Srivastava *et al.*, 1995). But with the advent of the multiple heart field model, these transcriptional networks can be

categorized as being downstream effectors of Nkx2.5 and isl1 in the PHF and SHF, respectively.

Cardiac induction from mesodermal progenitors

These studies detail a stepwise process by which epiblast cells transition to cardiac mesoderm, but it is important to note that ingression through the PS is not required for cardiac specification. Epiblast cells transplanted directly to the cardiac mesoderm can adopt a cardiac fate (Tam *et al.*, 1997). This implies that the environmental signals present at the cardiac crescent are the critical step for cardiac induction, not mesoderm progression. Elucidating the instructive/permissive signals required for cardiac specification, differentiation, and proliferation has been the focus of extensive inquiry and considerable debate. Early studies of cardiac specification were largely conducted with avian model organisms. Both ease of access and plentiful tissue made the avian model an attractive system for manipulation, but also paved the way for future studies in mammals (Yutzey and Kirby, 2002). Cardiac specification and terminal differentiation are now acknowledged to occur uniquely in the cardiac crescent because of the convergence of both inductive and inhibitory soluble growth factors; Wnts from the neural ectoderm and Bone Morphogenic Proteins (BMP) antagonists Chordin and Noggin from the notochord inhibit cardiogenesis, while BMPs, Fibroblast Growth Factors (FGF), and Wnt inhibitors Crescent and Dickkopf-1 (Dkk-1) from the endoderm are inductive signals (Fig. 1.3A,B) (Brand, 2003).

Commitment of mesoderm to the cardiac fate is initiated by the release of Activin, a member of the Transforming Growth Factor-β (TGF-β) family, from the hypoblast in

chicks, and the analogous AVE in mice (Ladd *et al.*, 1998; Yatskievych *et al.*, 1997). Early TGF-β primes the cardiac mesoderm for later signaling from the AVE in mice or definitive endoderm in chicks (Schultheiss *et al.*, 1995). As the AVE is a major source of BMPs, BMP2, -4, and -7 were initially cited as necessary for cardiomyocyte differentiation (Schultheiss *et al.*, 1997). However, further investigation found that BMPs alone were insufficient to induce myocyte differentiation, and could only do so in concert with FGF2, and -4 (Barron *et al.*, 2000; Lough *et al.*, 1996). FGFs are critical to cardiomyocyte differentiation; *FGFR1*$^{-/-}$ mice fail to form mesodermal structures, however *FGFR1*$^{-/-}$ ESCs can generate various mesodermal derivatives in teratomas and in embryoid body (EB) differentiation, but not cardiomyocytes (Dell'Era *et al.*, 2003; Deng *et al.*, 1994).

The Wnt signaling pathway has an important, yet dichotomous, role in cardiogenesis. Non-canonical Wnt11 originating from the mesoderm and endoderm acts to enhance cardiomyocyte differentiation, while canonical Wnt1, and -3A from the neural ectoderm inhibit cardiac differentiation along the midline and posterior aspects of the embryo (reviewed in Cohen *et al.*, 2008). A null mutation of β-catenin, the downstream effector of Wnt signaling, leads to additional cardiac tissue to form in endodermal layers, illustrating the function of canonical Wnt signaling in blocking cardiac differentiation (Lickert *et al.*, 2002). In contrast, Wnt inhibitors Crescent and Dkk-1 both act to enhance cardiogenesis from mesoderm progenitors. Crescent and Dkk-1 are unique among Wnt inhibitors in their ability to induced cardiac differentiation. Normally restricted to the AVE underlying the cardiac mesoderm, when missexpressed in other regions of the

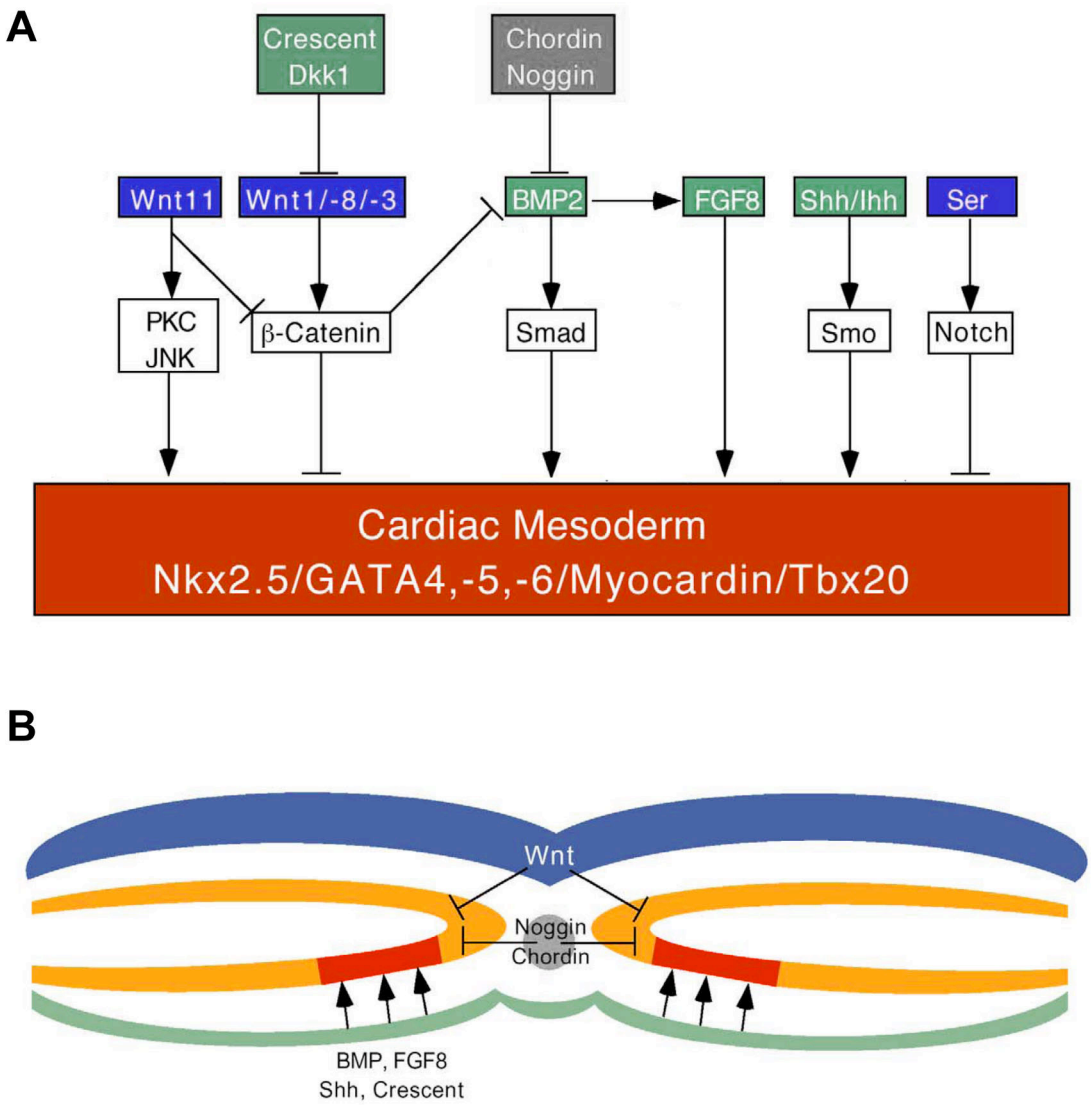

Figure 1.3. ***Extracellular signals regulating cardiac specification from mesoderm*****. A.** Extracellular growth factors and their relevant downstream effectors (white boxes) acting on the cardiac mesoderm to regulate cardiac gene expression. Lines with arrowheads represent inductive signals. Lines with perpendicular lines represent inhibitory signals. Box color denotes source of the paracrine signal. See below for color legend. **B.** Schematic depiction of E7.0-7.5 embryo displaying the origins of paracrine signals acting on the cardiac mesoderm (red). Inhibitory Wnts are derived from the neuroectoderm (blue). Inhibitory BMP inhibitors Noggin and Chordin are generated by the notochord (grey). The endoderm (green) is the source of BMPs, FGFs, and Wnt inhibitors Dkk-1 and Crescent that induce cardiac gene expression. Figure modified from Brand (2003).

embryo, they can convert non-cardiac posterior mesoderm to a cardiac fate (Marvin *et al.*, 2001; Schneider and Mercola, 2001).

A major caveat to the aforementioned studies is that cardiac is synonymous with cardiomyocyte, as few assess endocardial or endothelial differentiation from the cardiac mesoderm. Only a few studies have examined what factors are necessary to induce endocardial differentiation from cardiac mesoderm, and all have been done with chick explants. In chick cardiac mesoderm explants, endocardial cells, defined as endothelial cells expressing the QH-1 antigen, differentiated in the presence of lateral plate endoderm, either in direct contact or across a filter but not in its absence, suggesting a soluble factor originating from the endoderm initiates endocardial differentiation (Sugi and Markwald, 1996). Further work suggested that TGF-βs, but not BMP2 or FGF2, were the endodermal-derived growth factors enhancing endocardial precursor formation (Sugi and Markwald, 2003). Interestingly, VEGF alone had no effect on endocardial differentiation, but did synergize with TGF-βs.

The embryonic endocardium

Endocardial differentiation and development

With its seamless integration with systemic vasculature, the endocardium has in the past mistakenly been categorized as a specialized continuation of vascular endothelium. Advances in vascular and cardiac biology have revealed that the endocardium is a distinct cell population with a unique expression profile acting as a dynamic participant in cardiac morphogenesis. The endocardium is also notable as one

of the earliest cell lineages to develop during murine embryogenesis that retains its identity into maturity. Cells of the cardiac crescent are among the first mesodermal-derived populations to express N-cadherin, an epithelial cell surface marker, after gastrulation. As endocardiogenesis is initiated at E7.5, endocardial precursors downregulate N-cadherin expression to emerge from the ventral surface of the cardiac mesoderm into the fibronection-rich space between the presumptive myocardium and the AVE, where they can be distinguished from myocardial precursors still retaining N-cadherin expression (Fig. 1.4A) (Linask, 1992). Interestingly, deletion of *N-cadherin* does not hinder endocardial or myocardial differentiation in mice, but does result in cell adhesion defects in the myocardium (Radice *et al.*, 1997).

Endocardial cells first assemble into a vascular plexus, which coalesces through angiogenic remodeling and migration into the inner endocardial tube of the primitive heart (Fig. 1.4B) (reviewed in Baldwin, 1996). During this process, endocardial cells establish connections with system vasculature, which is critical to establishing blood flow through the beating heart (Coffin and Poole, 1988; Coffin and Poole, 1991). Endocardial precursors in the cardiac crescent express several vascular makers, including *Flk1*, *Tal1*, and *CD31/Pecam-1* (Baldwin *et al.*, 1994; Kallianpur *et al.*, 1994). As the endocardium is consolidated into an intact endothelial vessel and incorporated into the forming linear heart at E8.5, *Tal1* expression is lost, while other vascular markers, *VE-cadherin* and *Tie2* (*Tek*) are upregulated (Drake *et al.*, 1997; Lampugnani *et al.*, 1992).

The inherent problem of utilizing these genes to monitor endocardiogenesis is that they fail to distinguish endocardium from other endothelial populations. However, certain genes have been identified as being restricted to the embryonic endocardium,

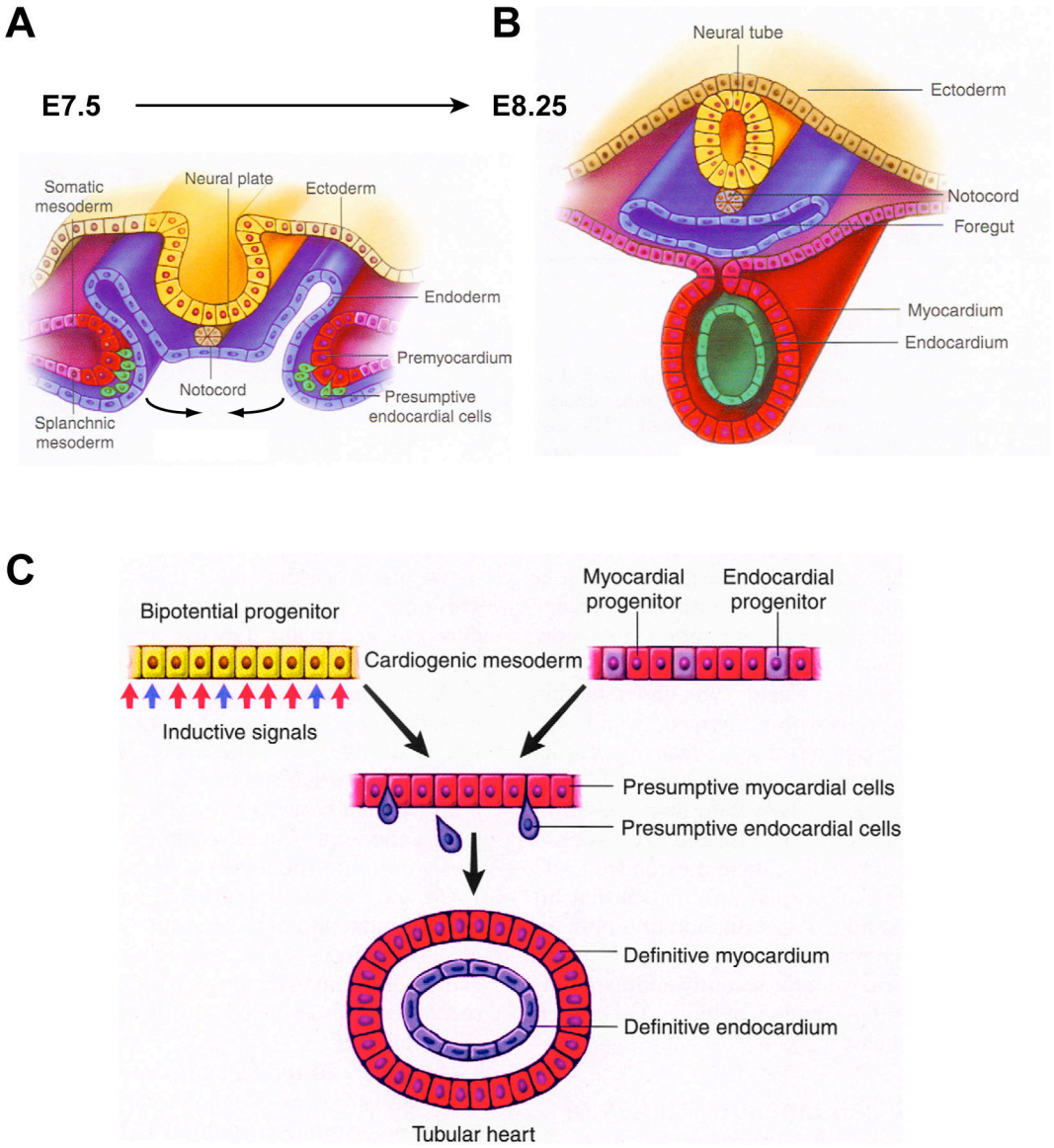

Figure 1.4. ***Models of endocardial specification and differentiation*****. A.** Endocardial precursors (green) delaminate from the cardiac mesoderm (red) into the fibronection-rich space between the presumptive myocardium and the AVE. **B.** With lateral folding of the embryo from E7.5 to E8.5, cardiac precursors coalescence along the ventral midline to form the primitive heart tube consisting of an outer myocardium (red) and inner endocardium (green). **C.** Proposed models depicting the origin of the endocardium. The first states that endocardium and myocardium are derived a common multipotent progenitor present in the cardiac mesoderm. The second asserts that endocardium and myocardium are two spatially sequestered populations within the cardiac mesoderm that develop in parallel. Figure adapted from Harvey and Rosenthal (1999).

indicating that endocardial cells are a distinct subpopulation of endothelium subject to its own unique transcriptional regulation at the earliest stages of development. In avian systems, all embryonic endothelial cells are positive for the QH1 antigen, but endocardial cells are the only endothelium to express cytotactin and the fibrillum-like protein JB3 (Sugi and Markwald, 1995; Sugi and Markwald, 1996; Wunsch *et al.*, 1994). TGF-βRIII is also restricted in the endocardial endothelium of avian embryos, a reversed pattern from what had been observed with TGF-βRII (Brown *et al.*, 1999). This pattern is not conserved in mice, as TGF-βRIII expression is detected throughout the endocardium, myocardium, and epicardium, as well as in the developing liver (Stenvers *et al.*, 2003). In the mouse, several genes with embryonic endocardial expression patterns have been observed. *Irx5* and *Irx6*, Iriquious family related proteins, are expressed in atrial and ventricular endocardium at E9.5, but not cushion endocardium (Christoffels *et al.*, 2000; Houweling *et al.*, 2001). Members of the Inhibitors of differentiation (Id) family of transcription factors *Id1* and *Id3* are present throughout the endocardium, but are also expressed in the epicardium and in other endothelial populations (Fraidenraich *et al.*, 2004). The only gene expressed in endocardial cells at the earliest stage of their development not present in other vascular population, is NFATc1. Following sections will discuss the expression and function of NFATc1 in detail.

Genes implicated in endocardiogenesis

Accumulating evidence indicates that the endocardium is molecularly distinct from other endothelium. The most striking examples come from zebrafish (*Danio rerio*) models, where *cloche* and *faust* mutants generate normal body vasculature, but fail to

form endocardium. *Cloche* mutants lack endocardium and hematopoietic lineages, but form a myocardial heart tube and have only minor abnormalities in systemic vasculature (Stainier *et al.*, 1995). While no mammalian homologues for *cloche* have been identified, *cloche* has been determined to function cell autonomously early in vascular signaling, upstream of Flk1 and Scl/Tal1 (Liao *et al.*, 1997; Parker and Stainier, 1999). The *faust* zebrafish mutant also fails to generate endocardial cells in spite of normal vascular differentiation. However unlike the *cloche* mutant, *faust* mutants do not possess a midline heart tube as cardiomyocyte precursors fail to migrate resulting in two nonfunctional bifid heart tubes (Reiter *et al.*, 1999). *Faust* has been mapped to the *GATA5* locus, which in mice is expressed in the early endoderm and endocardium. It remains unclear whether the lack of endocardial cells in the *faust* mutant is due to cell autonomous defects in endocardial differentiation, or more likely, non-cell autonomous deficits in endoderm patterning.

No genetic mutations in mice have been found to result in a complete lack of endocardium as seen in these zebrafish mutants. Nemer & Nemer demonstrated that inactivation of both *GATA5* and *NFATc1* could block endocardial differentiation from an immortalized mesodermal cell line treated with retinoic acid (Nemer and Nemer, 2002). However, as $GATA5^{-/-}$ and $NFATc1^{-/-}$ mice have no defects in endocardial differentiation, and double knockouts have never been generated, the *in vivo* relevance of this work is subject to question. While no mutants with endocardial ablation in concert with normal myocardial and systemic endothelial development have been documented, several genes that are crucial for endocardial development have been detailed. Global deletion of the Ets transcription factor *Er71*, which functions downstream of BMP, Notch, and Wnt

signaling in Flk1+ mesoderm and vasculature, disrupts all hematopoietic and vascular formation, including endocardial differentiation (Lee *et al.*, 2008). The severity of this phenotype, in terms of vascular development, exceeds even the *Flk1* knockout, in which endocardial and endothelial cells differentiate but fail to undergo proper vasculogenesis to form lumenized vessels and remain as aggregates of immature endothelial cells. The receptor tyrosine kinase (RTK) *Tie2* (*TEK*), while not involved with the initial specification of endocardium and endothelium, does transduce a proliferative and organizing signal to the endocardium; deletion of *Tie2* in the endocardium greatly reduces the number and cohesion of endocardial cells, causing circulatory collapse and embryonic death (Puri *et al.*, 1999). Proper endocardial development is dependent not just on growth factor transduction, but also on a permissive environmental structure. Loss of the ECM protein, fibronectin, indicates it is essential for formation and/or maintenance of the lumen of the endocardial tube (George *et al.*, 1997).

The role of endocardium in cardiac morphogenesis

Endocardial-myocardial interactions in early heart development

Examination of endocardial-myocardial interactions in mammalian models has been limited. The majority of what is known about the role of the endocardium in early cardiac organogenesis has been generated from studies of zebrafish development. As discussed in the previous section, *cloche* mutants fails to form endocardium and hematopoietic lineages, but normal endothelial cells line body trunk vessels. Early cardiac morphogenesis is relatively normal; the heart tube forms without the

endocardium, undergoes septation and looping, though does have reduced atrial and ventricular thickness (Stainier *et al.*, 1995). Detailed analysis of myocardial migration in the *cloche* mutant indicated that the fusing bilateral heart fields lacked angular motion in the most cranial and caudal regions compared to wild types (Holtzman *et al.*, 2007). Direct medial motion was not impaired, thus a single heart tube formed. Another zebrafish mutant *miles apart* (*mil*) was found to be deficit in medial motion resulting in a bifid heart phenotype with two independent heart tubes of myocardium and endocardium. *Cloche* and *mil* double mutants lacked both angular and medial migration, resulting in complete inhibition of migration of the bilateral heart fields and heart tube formation.

While these analyses suggest the endocardium is responsible for inducing angular motion of the migrating heart fields, the cardiac phenotype of the *cloche* phenotype suggests endocardium is not necessary for proper specification and growth of cardiomyocytes. However, another zebrafish mutant, *heart of glass* (*heg*), which encodes an endocardial transmembrane protein, suggests the endocardium is vital for patterned growth of the heart. In *heg* mutant embryos, the endocardium is present but myocardial cells fail to proliferate in the normal concentric direction, resulting in dilated chambers consisting of a single myocardial layer with negligible cardiac jelly (Mably *et al.*, 2003). It is not known whether *heg* is sufficient to drive myocardial growth, or is it represents a link in early reciprocal endocardial-myocardial signaling. Taken together, these studies of cardiac development in zebrafish suggest that the endocardium is an active participant in early cardiac moprphogenesis, serving as a reciprocal, and not passive, signaling partner with cardiomyocytes (Colvin *et al.*, 2001; Lavine *et al.*, 2005).

Patterned growth and differentiation of the myocardium

Targeted gene disruptions in mice underscore the critical role of endocardium in later cardiac morphogenesis, where endocardial-myocardial interactions appear critical for normal patterned growth of the myocardium, trabeculation, and valvulogenesis. FGFs and FGFRs not only act to induce myocardial specification, but also regulate cardiomyocyte proliferation and terminal differentiation during later stages of heart development. Lavine *et al*. described how FGF9, -16, and -20, induced by retinoic acid, are secreted from the endocardium, and transmit a proliferative stimulus through alternatively spliced FGFR1c and FGFR2c isoforms expressed in the myocardium. While it was previously demonstrated that *FGF9*$^{-/-}$ mice die at birth with hypoplastic lungs and thin, dilated hearts, this work clarified that it was specifically the loss of endocardial-derived FGF9 that caused premature terminal differentiation of myocardium, most dramatically at the ventricular apex (Colvin *et al.*, 2001; Lavine *et al.*, 2005). In addition to FGFs, other endocardial signaling molecules transmit patterning signals to various cardiac lineages. Endothelins (ET) are small peptides that act as paracrine signals for G-protein coupled receptors, ET_A and ET_B. ETs and endothelin-converting enzymes (ECE), which are responsible for converting ETs into an their active form, are widely expressed in endocardial cells and the mesenchyme of endocardial cushions and brachial arches (Yanagisawa *et al.*, 1998a). Mutations in *ET1* or *ECE-1* result in aberrant patterning of brachial arch derivatives, defective conotruncal septation, and ventricular septal defects (Yanagisawa *et al.*, 2000; Yanagisawa *et al.*, 1998b). Since ET receptors are expressed in migrating CNC, as well as in the myocardium, it suggests that endocardial-derived ETs act on CNC and myocardium to regulate septation.

Trabeculation

The development of trabecula is a defining characteristic of ventricular chamber morphogenesis. In this process, myocardial cells proliferate and migrate into ECM-rich pockets covered by endocardium (Sedmera *et al.*, 2000). The formation of these highly muscularized radiations increase surface area for blood flow and enhance the force that can be generated with ventricle contraction. In addition, trabecula are incorporated into the interventricular septum, the papillary muscles of the mitral and tricuspid valves, and contribute to the conduction system.

The first indication that endocardial-myocardial signaling plays an essential role in this process came with deletion of the epidermal growth factor receptor (EGFR) ligand *neuregulin-1* (*Nrg1*) and the EGFR receptors *ErbB2/ErbB4*. Nrg1 is normally expressed by ventricular, but not atrial, endocardium, while ErbB2/ErbB4 is restricted to the underlying myocardium. A null mutation in any one of these three genes resulted in embryonic lethality at E10.5 with an absence of ventricular trabeculation and decreased myocyte proliferation (Gassmann *et al.*, 1995; Lee *et al.*, 1995; Meyer and Birchmeier, 1995). Nrg1 released from endocardial cells induces heterodimerization of ErbB2 and ErbB4, which in concert with insulin-like growth factor-1 (IGF-1) also from the endocardium, controls trabecular myocardial growth and differentiation (Hertig *et al.*, 1999). Acting at an earlier developmental time point, endocardial Notch1 has been demonstrated to be required for trabeculation, modulating gene expression in both the endocardium and myocardium. The Notch1 intracellular domain (NICD) regulates EphrinB2/EphB4 signaling within endocardial cells, which in turn modulates *Nrg1* expression (Grego-Bessa *et al.*, 2007). NICD signaling through RBPJk in the

endocardium also activates *BMP10* expression in the trabecular myocardium through an unknown pathway to stimulate proliferation.

Regulating developmental growth depends on converging signaling pathways that stimulate growth, but also halt expansion at a certain threshold. While Notch1 and Nrg1 induce growth of trabecular myocardium, Platelet-derived growth factor-B (PDGF-B) restricts proliferation. PDGF is most commonly associated with vasculogenesis where it functions to recruit pericytes and vascular smooth muscle cells (VSMC) that expression the PDGFR-β to the endothelium (Hoch and Soriano, 2003). Global deletion of PDGF-B is perinatally lethal, due in part to microvascular dysfunction (Leveen *et al.*, 1994). Endothelial-specific deletion of PDGF-B is not fatal, but does highlight the role of endocardial-derived PDGF-B in cardiac morphogenesis as its loss results in myocardial thinning, chamber dilation, hypertrabeculation, and septal defects (Bjarnegard *et al.*, 2004). Collectively, these analyses of endocardial-derived signals demonstrate the critical role of the endocardial cell lineage plays in coordinating proper septation and trabeculation.

Valve Development

Valve formation is initiated when endocardial cells undergo EMT, delaminating into the cardiac jelly after downregulating vascular genes such as *CD31/Pecam-1* and *VE-cadherin* and activating mesenchymal genes like *Snail1* and *Twist*. Although this process was documented by developmental biologists decades ago, only recently has empirical proof been provided that demonstrates cushion mesenchymal cells are derived from endocardium. Lineage tracing with a Cre recombinase driven by the *Tie2* promoter

breed to the *R26R LacZ* reporter established that all mesenchymal cells of the AVC cushion and the proximal cells of the OFT cushion were derived from endocardium (Kisanuki *et al.*, 2001). The entire process of valve construction, from EMT to remodeling, relies on signals produced and received by the endocardium, myocardium, and cushion mesechyme (Armstrong and Bischoff, 2004; Barnett and Desgrosellier, 2003). Whereas EMT is induced by BMPs and TGF-βs from underlying myocardium, Notch signaling must be activated in the endocardium for cells to be receptive to those instructions (Timmerman *et al.*, 2004).

Accordingly, failure to undergo EMT or disruption of signals from the endocardium to cushion cells results in a variety of valve defects. Under normal physiologic conditions, heparin-binding EGF-like growth factor (HB-EGF), an EGF ligand secreted by the endocardium, activates the ErbB1/B2 complex to inhibit proliferation of cushion mesenchymal cells, but does not affect the ErbB2/3 complex conveying a parallel mitogenic signal (Iwamoto *et al.*, 2003). Loss of HB-EGF signaling through ErbB1/B2 in null mice results in prolonged Smad1, -5, -8 phosphorylation, the downstream effectors of BMP signaling, and increased proliferation of cushion mesenchymal cells that leads to the development of enlarged hyperplastic valve cushions (Jackson *et al.*, 2003).

Neurofibromin1 (Nf1) is transcription factor that has been implicated in valve development and remodeling. In humans, mutations in *Nf1* are responsible for von Recklinghausen neurofibromatosis, a genetic disorder causing café au-lait spots, neurofibromas, and potentially neural crest cell-derived malignancies. Global deletion of *Nf1* in mice results in a phenotype similar to neural crest ablation, consisting of valve

defects, increased cushion proliferation, decreased apoptosis, and decreased remodeling, in addition to double outlet right ventricle (Brannan *et al.*, 1994). Interestingly, CNC-specific deletion fails to recreate the observed phenotype, but endothelial-specific deletion of *Nf1* phenocopies null embryos (Gitler *et al.*, 2003). These studies also indicate that the Nf1 phenotype might be caused by misregulation of endocardial NFATc1.

Origin of the endocardial lineage

Despite their reciprocal signaling and close spatial-temporal relationship during embryogenesis, the question of whether endocardium and myocardium share a common progenitor in the cardiac mesoderm remains controversial. Drawing from observations made in different organisms, two models have been generated; one proposes that the endocardium and myocardium represent two spatially sequestered populations within the cardiac mesoderm that develop in parallel, while the second states that endocardium and myocardium are derived a common multipotent progenitor in the cardiac mesoderm (Fig 1.4C).

Evidence for the assertion that the cardiac mesoderm contains two distinct subpopulations of endocardial and myocardial precursors already committed to their fate comes from avian lineage tracing and zebrafish studies. Retroviral tracking of single cells in the cardiac mesoderm of chick embryos demonstrated that individual mesodermal cells in the heart field were capable of generating either myocardial cells (95.1% of clones) or endocardial cells (4.9% of clones), but never both cell types (Cohen-Gould and Mikawa, 1996). A following study that conducted retroviral lineage tracing of pre-

gastrulation PS cells also labeled only myocardial or endocardial cells (Wei and Mikawa, 2000). Pre-gastrulation blastomere transplantation in zebrafish also indicated that the two lineages were distinct prior to gastrulation (Lee *et al.*, 1994). This data is in agreement with a recent description of zebrafish with a mutation in the *Scl/Tal1* gene (tal^{t21384}). Bussmann *et al*. demonstrated that endocardial cells originate from a region in the lateral plate mesoderm that also generates cells of the primitive myeloid lineage (Bussmann *et al.*, 2007). Endocardial precursors then migrate to the bilateral heart fields where they invest the fusing primitive heart tube. In these *Scl/Tal1* mutants, endocardial precursors are specified, remain as aggregates at the ventricular pole of the heart, failing to properly migrate. These studies indicate that endocardial progenitors are derived from a small number of spatially sequestered precursors within a larger field of myocardial progenitors distinct not only in the cardiac mesoderm, but also identifiable prior to gastrulation.

Despites these findings, growing evidence suggests a common multipotent progenitor responsible for generating the endocardial and myocardial lineages does exist in the cardiac mesoderm. In the avian embryos, Linask & Lash identified a subpopulation in the cardiac mesoderm that co-expressed myocardial N-cadherin and endothelial QH-1 antigen (Linask and Lash, 1993). In addition, the QCE-6 cardiac mesoderm cell line, established from Quail cardiogenic mesoderm, was shown to be capable of differentiating into both endocardial and myocardial cells under certain treatment conditions (Eisenberg and Bader, 1996). The most compelling support for a common endocardial-myocardial precursor comes from lineage tracing in mice. Cre-mediated fate mapping of *Mesp1*+ cells, which is expressed in mesodermal cells exiting the PS to contribute to the lateral plate mesoderm, at first supported a model of two

separate progenitors of endocardium and myocardium. The initial characterization of the *Mesp1-Cre* crossed with the *R26R LacZ* reporter mouse indicated that only the myocardium was derived from *Mesp1*+ cells, while the endocardium was not (Saga *et al.*, 1999). Further analysis demonstrated this not to be the case and *Mesp1*-expressing mesoderm was shown to contribute to both endocardium and myocardium (Saga *et al.*, 2000). This study only demonstrated that endocardium and myocardium were generated by post-gastrulation mesoderm, and failed to address the question of whether a common progenitor resided in the cardiac mesoderm. With the discovery that Flk1 is expressed throughout the cardiac mesoderm during early development, lineage tracing demonstrated that myocardium and endocardium were both derived from an Flk1+ mesodermal population (Ema *et al.*, 2006; Motoike *et al.*, 2003). Further expression-based and lineage tracing analyses of *Nkx2.5*+ and *isl1*+ cardiac populations suggest that as late as the cardiac crescent, subsets of myocardium, endocardium, vascular endothelium, and smooth muscle were derived a common precursor (Cai *et al.*, 2003; Stanley *et al.*, 2002). These studies also indicated that the embryonic endocardium has two distinct developmental origins, with the endocardium of the atria, AVC, and left ventricle derived from the PHF, and the endocardium of the right ventricle/ OFT arising from the anterior SHF. These findings indicate that endocardium and myocardium share a common mesodermal precursor, but detailed examination has proven difficult due to the limitations of *in vivo* mouse models and the lack of specific markers for early endocardial cells.

NFATc1

The NFAT family of transcription factors

The Nuclear Factor of Activated T-cells (NFAT) family of transcription factors was initially described as activators of cytokine gene expression in the immune system, but have since been found to function in various tissues as an inducible transcriptional regulator (Crabtree and Olson, 2002; Hogan *et al.*, 2003; Macian, 2005; Rao *et al.*, 1997). The NFAT family consists of five members: NFATc1 (NFATc/NFAT2), NFATc2 (NFATp/NFAT1), NFATc3 (NFATx/NFAT4), NFATc4 (NFAT3) and NFAT5 (Fig. 1.5A). The structure of NFAT family members is highly conserved with each containing a NFAT homology region (NHR) and a REL homology region (RHR) (Fig. 1.5B). The NHR contains a transactivation domain with binding sites for calcineurin, NFAT kinases, and glycogen-synthase kinase 3 (GSK3β), as well as serine residues that can be phosphorylated to regulate its activity. The RHR consists of a DNA binding region with homology to the REL-family of transcription factors, also known as the nuclear factor-κβ (NF-κβ) family of transcription factors.

Calcium signaling (Ca^{2+}) regulates the transcriptional activity of all NFAT proteins, save for NFAT5. NFATc transcription factors are normally maintained in an inactive, phosphorylated state in the cytoplasm awaiting a cascade of Ca^{2+} release from intracellular stores and calcium-release-activated calcium channels (CRAC) in the plasma membrane (Fig. 1.5C). Activation of phospholipase C-γ (PLC-γ) downstream of receptor binding hydrolyzes phosphatidylinositol-4,5-bisphosphate (PIP_2) to inositol-1,4,5-trisphosphate (IP_3), which in turn initiates Ca^{2+} release via IP_3 receptors. Ca^{2+} binding

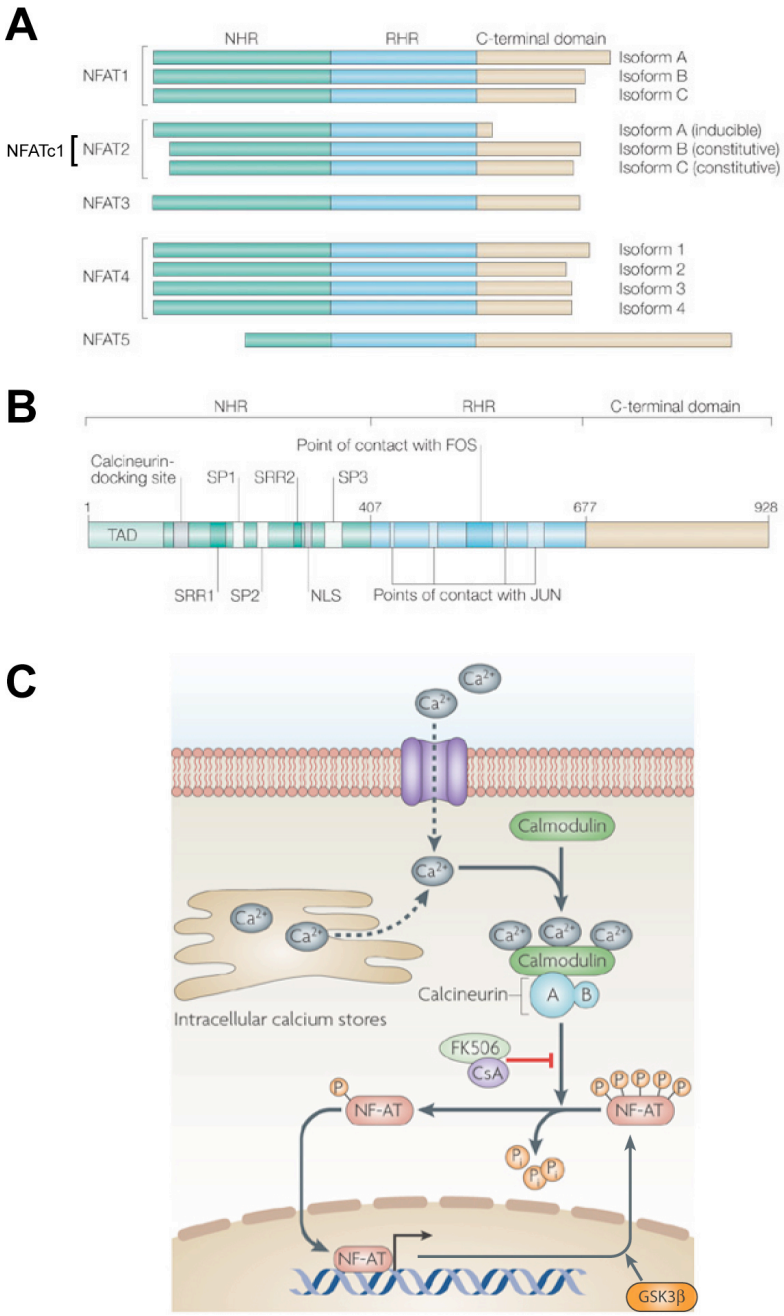

Figure 1.5. ***The structure and regulation of NFAT transcription factors.*** **A.** NFATc family members. **B.** Schematic representation of the transactivation, regulatory, DNA-binding and C-terminal domains of NFATc proteins. A and B adapted from Macian *et al*. (2005). **C.** Following an increase in intracellular calcium, the active calcium-calmodulin-calcineurin complex dephosphorylates NFAT, allowing nuclear localization and subsequent transcriptional activity. C adapted from Steinbach *et al*. (2007).

induces the formation of a phosphatase complex consisting of calmodulin and calcineurin A & B, which dephosphorylates NFATc, exposing a nuclear localization sequence (NLS) (Beals *et al.*, 1997). NFATc is shuttled into the nucleus and facilitates transcription by binding to 9-bp NFAT consensus elements ((A/T)GGAAA(A/N)(A/T/C)N) located in promoter regions (Rao *et al.*, 1997). The duration of NFATc transcriptional activity in the nucleus is ultimately controlled by GSK3β, which phosphorylates certain serine residues of the NHR, masking the NLS, resulting in nuclear export.

The role of NFATc1 in heart development

NFATc1 possesses three distinct transcriptional isoforms; NFATc1-A is the shortest isoform and is controlled from the strong P1 promoter 5' to Exon1 and the weak polyadenylation site pA1, while NFATc1-B and -C are expressed from either the P1 or P2 promoter and uses the strong polyadenylation site pA2 (Chuvpilo *et al.*, 1999a; Chuvpilo *et al.*, 1999b). While the B and C isoforms represent basal transcription, NFATc1-A can be induced in an autoregulatory loop where NFATc1 or NFATc2 binds to NFAT recognition sites in the P1 promoter yielding persistent NFATc1 transcriptional activation (Chuvpilo *et al.*, 2002; Zhou *et al.*, 2002).

In the developing heart, NFATc1 is expressed exclusively in endocardial precursors as they differentiate from the cardiac mesoderm, and throughout the endocardium of the E7.5-8.5 endocardial tube. Expression is subsequently restricted to the endocardium of the AVC and OFT by E10.5, and is undetectable after E14.5. Two separate groups concurrently generated null mutations in NFATc1, one mutating the RHR and other the NHR, both resulting in defects of the semilunar valves and

atrioventricular valves without obvious defects in the initial formation of endocardium. (de la Pompa *et al.*, 1998; Ranger *et al.*, 1998).

The function of NFATc1 in valve development is subject to debate. Early in valvulogenesis, it has been suggested that NFATc1 regulates EMT at sites of prospective valve development (Chang *et al.*, 2004). Chimeric analysis with *NFATc1*$^{-/-}$ ESCs suggests NFATc1 functions cell autonomously to maintain an endocardial phenotype during cushion formation, as chimeric valves lack *NFATc1*-/- endocardial cells and have an increased number of *NFATc1*$^{-/-}$ mesenchymal cells (unpublished observations). With ingression into the endocardial cushion, NFATc1 is rapidly downregulated, in agreement with this purported function. In *Foxp1*$^{-/-}$ and *Sox9*$^{-/-}$ mice, residual NFATc1 is present in mesenchymal cells, indirectly suggesting that NFATc1+ cells contribute to the cushions and expression silencing is aberrant in these genes' absence (Akiyama *et al.*, 2004; Wang *et al.*, 2004). EMT is not affected in *NFATc1*$^{-/-}$ mice, rather it is a failure to remodel the valve that causes embryonic lethality. This phenotype highlights the essential role of endocardial-to-mesenchymal signaling in valve development. NFATc1 is required as a transcriptional regulator of RANKL signaling, which activates tartrate-resistant acid phosphatase (TRAP) and the cysteine protease cathepsin K (Ctsk) to remodel ECM proteins in the cushion (Lange and Yutzey, 2006).

Previous promoter analysis of NFATc1 transcriptional regulation conducted in our laboratory identified a 250-bp region upstream of the p2 promoter in intron 2 responsible for autoregulation of *NFATc1* (Zhou *et al.*, 2005). In addition to multiple NFATc1 sites, putative consensus elements for GATA, HOX, and SMAD transcription factors are present in this conserved region. Mutatagenesis of these elements, followed

by transient transgenic analysis, indicted only the HOX site influences transcriptional activity from this element in the valvular endocardium. When this regulatory domain was inserted in front of a heat shock promoter (HSP), it was capable of driving reporter gene expression in the valvular endocardium beginning at E9.5 and persisting until E13.5, but failed to recapitulate endogenous *NFATc1* expression in the entire endocardium. Lineage analysis with this valvular enhancer driving Cre crossed to the *R26R LacZ* reporter suggests that this NFATc1+ cell population does not undergo EMT (unpublished observations). Nonetheless, as one of the few endocardial-specific gene transcripts, NFATc1 provides molecular evidence that the endocardium is a unique subpopulation of cells distinct from other endothelium and presents itself as an invaluable marker for tracking endocardial differentiation.

Embryonic stem cell differentiation

Murine embryonic stem cells (ESCs) were isolated from the inner cell mass (ICM) of E3.5 blastocyst stage mouse embryos (Evans and Kaufman, 1981; Martin, 1981). Cultured on primary mouse embryonic fibroblast feeders (PMEFs), these cells remain undifferentiated and exhibit self-renewal when maintained in growth media containing fetal bovine/calf serum (FBS/FCS) and leukemia inhibitory factor (LIF) (Smith *et al.*, 1988; Williams *et al.*, 1988). LIF functions by activating STAT3 through gp130, whereas FBS, or its substitute BMP4, mediates Smad activation and expression of the Id family of transcription factor (Ying *et al.*, 2003). Besides STAT3 and Id transcription factors, the OU domain class 5 transcription factor 1 (Oct-4), SRY-box containing gene 2 (Sox2), proto-oncogene c-Myc, and Kruppel-like factor 4 (Klf4), and

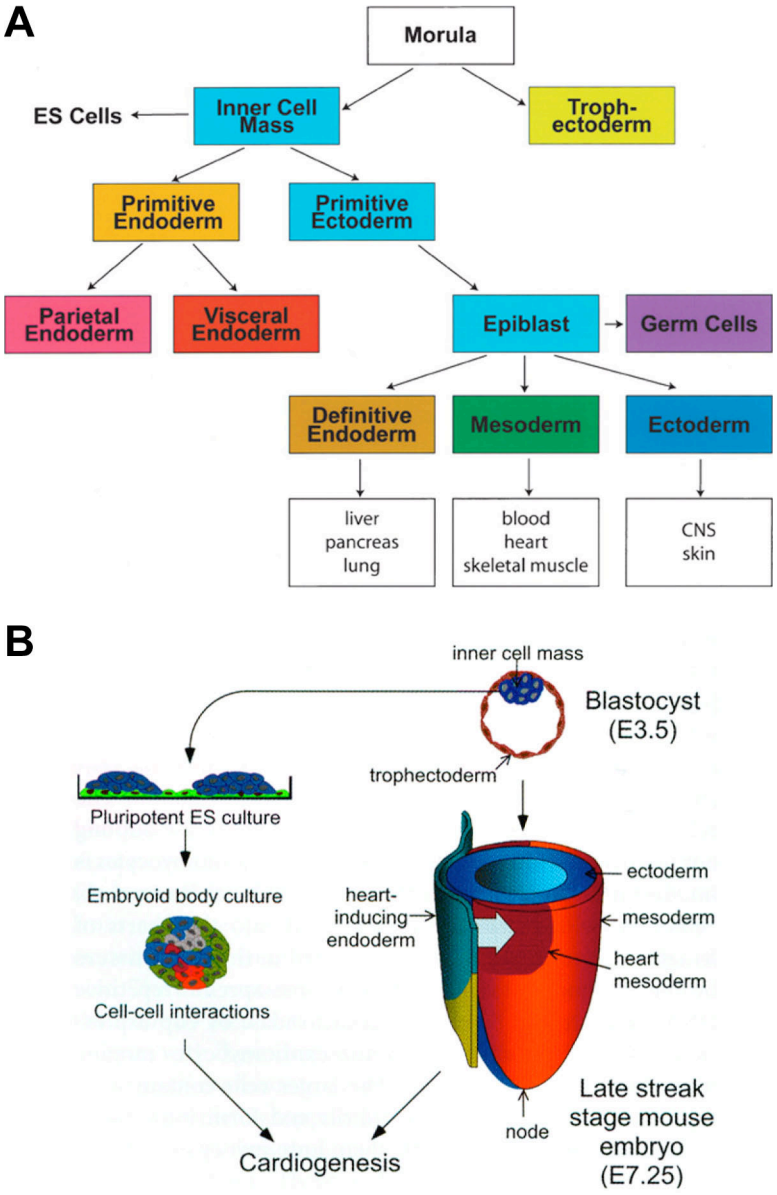

Figure 1.6. ***Potential of differentiating ESCs to generate ectoderm, mesoderm, and endoderm*****. A.** Relationship of early embryonic cell populations to the primary germ cell layers and their derivatives, with respect to the differentiation potential of embryonic stem cells (ESCs) isolated from the ICM. Figure adopted from Keller (2005). **B.** A comparison of cardiac induction in the E7.5 mouse embryo and in embryoid bodies generated from ESCs illustrating that the extracellular cues required for the stepwise process of lineage specification and differentiation *in vivo* are conserved *in vitro*. Figure adopted from Foley and Mercola (2004).

Nanog have all been implicated in stem cell self-renewal and pluripotency (reviewed in Jaenisch and Young, 2008).

When injected in a donor blastocyst, ESCs are capable of contributing to all tissues of the adult mouse, including germ cells, allowing germline transmission of ESC-derived genetic material from aggregation chimeras (Bradley *et al.*, 1984). *In vivo* pluripotency extends to *in vitro* culture, as demonstrated when ESCs were found to generate visceral yolk sac, blood islands, and myocardium when cultured in the absence of LIF under specific culture conditions (Doetschman *et al.*, 1985). ESC differentiation has since been documented to produced tissues derived from ectoderm, mesoderm and endoderm components (Fig. 1.6A). Most approaches to ESC differentiation involve one of three methods: either cell aggregation into three-dimensional colonies known as embryoid bodies (EBs), co-culture with stromal cells, or in a monolayer on ECM proteins. The system has come to represent a faithful *in vitro* model of lineage specification, where tissues develop in a sequential pattern mirroring embryonic development (reviewed in Keller, 2005). As noted, ESC differentiation generates cells from all three germ cell lineages, but for the purpose of the studies presented here only mesodermal-derivatives that comprise the cardiovascular system will be reviewed.

Hematopoietic and vascular differentiation

Hematopoiesis and vasculogenesis have been among the most extensively studied developmental programs in ESC differentiation. Genes that are required for the establishment of the hematopoietic lineages in the embryo, both primitive erythroid and definitive, serve similar functions in EBs. Utilizing ESCs with targeted mutations, the

particular roles of *Scl/Tal1*, *Runx1*, *GATA1*, and other transcription factors involved in hematopoiesis have been examined in detail. These studies highlight the strength of ESC differentiation to analyze lethal mutations *in vitro*, as well as identify new molecular targets and regulators. An additional beneficial feature of ESC differentiation in modeling hematopoietic and vascular commitment is that the system accurately recapitulates the temporal kinetics of lineage specification found in the yolk sac and embryo, as these lineages pass through the same stepwise pathway of specification *in vitro* that is observed *in vivo* (Keller *et al.*, 1993). Endothelial cells efficiently form non-lumenized vascular plexus in EBs grown in serum-containing media, moving through successive and routine stages of maturity (Vittet *et al.*, 1996). Differentiating ESCs thus are a valuable model of vasculogenesis; examination of targeted disruptions in *VEGF* and its receptors *Flk1* and *Flt1* has illuminated how these different components of the VEGF signaling pathway interact (Kearney *et al.*, 2002; Kearney *et al.*, 2004). Endothelial cell lines have isolated with the intent of studying endothelial cells at various stages of development (Balconi *et al.*, 2000). While vasculogenesis in EBs is generally accepted as a faithfully model, studies focusing on mature endothelium have been questioned as there is evidence that ESC-derived endothelial cells fail to achieve an equivalent level of functionality compared to their *in vivo* counterparts (McCloskey *et al.*, 2006).

This ability of the ESC model to assess early developmental stages that are difficult to access in the embryo led to characterization of the hemangioblast population, a common progenitor for both the hematopoietic and vascular lineages. The concept of the hemangioblast was indirectly supported by studies demonstrating that immature hematopoietic and vascular cells shared the expression of certain genes during

embryogenesis, but the actual proof and isolation of this common progenitor came from studies conducted using ESC differentiation. From EBs precisely dispersed after 3-3.5 days of differentiation, a population of cells termed blast colony-forming cells (BL-CFC) were characterized to generate hematopoietic, endothelial, and vascular smooth muscle cells in methylcellulose cultures upon exposure to VEGF (Choi *et al.*, 1998; Kennedy *et al.*, 1997). Using progressive cell sorting and culturing, lineage analysis further characterized the hemangioblast population by defining the point of divergence between endothelial and hematopoietic lineages (Nishikawa *et al.*, 1998). Bulk differentiation and dispersion EBs later was replaced with more accurate methods of isolating the hemangioblast population using Flk1 in conjunction with GFP expressed by the mesodermal genes *brachyury* and *Mixl1* (Fehling *et al.*, 2003; Ng *et al.*, 2005).

With these markers it became possible to not only isolate hemangioblasts from EBs to determine their lineage potential, but also to elucidate the mechanisms behind their specification from pluripotent ESCs and undetermined mesoderm. BMP4, Activin, Wnt, FGF, and VEGF have all been demonstrated to play specific roles at precise times in the stepwise specification of ESCs to a hematopoietic fate (Nostro *et al.*, 2008; Park *et al.*, 2004; Pearson *et al.*, 2008). These studies not only have advanced the understanding of the stages of hematopoietic and vascular development, in terms of the induction signals at play and the required sequence of transcriptional regulation, but have also established a framework in which to investigate the lineage specification of other populations.

Cardiomyocyte specification and lineage analysis using the ESC differentiation model

Since the original description by Doetschman *et al*. demonstrated contracting myocytes in EBs, ESC differentiation has emerged as the preferred *in vitro* model of cardiomyocyte specification and differentiation (Doetschman *et al.*, 1985). By understanding the basic processes of cardiac developmental biology in this system, it has been argued these cells might be used to repair and/or replace cardiac tissue damaged by coronary artery disease (CAD), myocardial infarction (MI), and congestive heart failure (CHF). Cardiomyocytes generated from EBs are both structurally and functionally mature, in terms of their expression of sarcomeric proteins and their electrophysiological attributes. Initially small and round with disorganized bundles of myofibrils, ESC-derived cardiomyocytes become elongated with well-developed myofibrils and sarcomeres. With this structural change, mononucleated cells begin to contract, and exhibit cell-cell junctions with neighboring cells consistent with those in myocardium *in vivo* (Westfall *et al.*, 1997). Expression of cardiac gene transcripts proceeds in a developmental controlled manner where genes encoding early markers of the cardiac mesoderm such as the transcription factors *GATA4* and *Nkx2.5* appear prior to the markers of cardiomyocyte maturation, including atrial natriuretic factor (ANF), myosin light chain ventricular isoform 2 (MLC-2v), α-myosin heavy chain (αMHC), and β-myosin heavy chain (βMHC) (reviewed in Boheler *et al.*, 2002). The appearance of these cardiac transcripts also indicates that myocardial chamber specification occurs in EBs (Miller-Hance *et al.*, 1993). Activation of chamber-specific genes transcripts without the positional cues that normally control patterning of the heart tube suggests that regional

specification of cardiomyocytes is a process inherent to cardiac cells, not entirely dependent on induction from extracellular signals.

The accessibility of early stages of development, which are difficult to visualize and manipulate in the embryo, makes the ESC differentiation model an attractive system to examine conditions that enhance or alter cardiac specification (Fig. 1.6B). Many of the same signaling molecules that specify mesoderm towards a cardiac fate *in vivo* have been demonstrated to induce cardiomyocyte differentiation in EBs. Temporally regulated administration of TGF-β2, FGF2, and BMP2 has been shown to enhance differentiation of cardiomyocytes, as has the inhibition of Notch signaling (Kawai *et al.*, 2004; Kumar and Sun, 2005; Nemir *et al.*, 2006). Constitutive overexpression of certain transcription factors in ESCs and EBs can influence the fate of undifferentiated cells. Oct-3/4, a stem cell transcription factor not previously associated with heart development enhances cardiac specification in a dose dependent manner by regulating the expression of mesodermal genes (Zeineddine *et al.*, 2006). These findings indicate early transcriptional regulation can influence the susceptibility of cells to inductive signaling, responding to certain cues and not others. In differentiating ESCs, the mesodermal transcription factor Mesp1 activities genes associated with cardiac specification, controlling mesodermal and endodermal cell fates (Bondue *et al.*, 2008; Lindsley *et al.*, 2008). One of genes Mesp1 regulates in EBs is Dkk-1, which also has been demonstrated to be an extracellular signal enhancing cardiomyocytes specification in EBs and during embryogenesis (David *et al.*, 2008; Naito *et al.*, 2006). It is yet to be determined how these finding relate to the observed phenotype of double *Mesp1* and *-2* knockout embryos.

Cardiac lineage analysis of multipotent cardiovascular progenitors

To fully delineate the mechanisms involved in cardiac specification, it is essential to elucidate the stepwise commitment of precursor populations to the cardiac fate. Mirroring approaches taken to define the hemangioblast as a progenitor of hematopoietic and endothelial cells, recent studies have utilized various genetically modified ESCs and cell surface markers in the attempt to identify multipotent cardiovascular progenitor (MCP) populations. As previously described, the VEGF receptor Flk1 is expressed in mesodermal progenitors of hematopoietic, endothelial, cardiomyocyte, and endocardial lineages. Using a GFP reporter under control of the *brachyury* locus with cell surface Flk1 to isolate Flk1+ mesoderm, only hematopoietic/vascular lineages, not cardiomyocytes, were generated from GFP-Bry+ Flk1+ cells at 3.5 days of differentiation (Kouskoff *et al.*, 2005). Further analysis using this methodological approach resorted the GFP-Bry+ Flk1- population after reaggregation to identify Flk1+ MCPs (Kattman *et al.*, 2006). When isolated after the equivalent of 4.5 days of differentiation, Flk1+ MCPs did not express cardiac markers, but after a short time in culture began to express *Nkx2.5*, *isl1*, *Tbx5*, and *Mef2c*. Clonal analysis of these Flk1+ MCPs indicated this second wave of Flk1+ mesoderm represented a cardiovascular progenitor capable of generating cardiomyocyte, smooth muscle, and endothelial cells. Another study utilizing Flk1 as a marker of cardiac progenitors found that Flk1+ in conjunction with CXCR4, but not c-kit, Sca-1, CD44, or CD90, could isolate cardiomyocyte-restricted precursors (Yamashita *et al.*, 2005). Though these studies were conducted in murine ESCs, Flk1+ MCPs have been isolated from human ESCs as well, based on differential levels of Flk1 and the stem cell marker c-kit (Yang *et al.*, 2008).

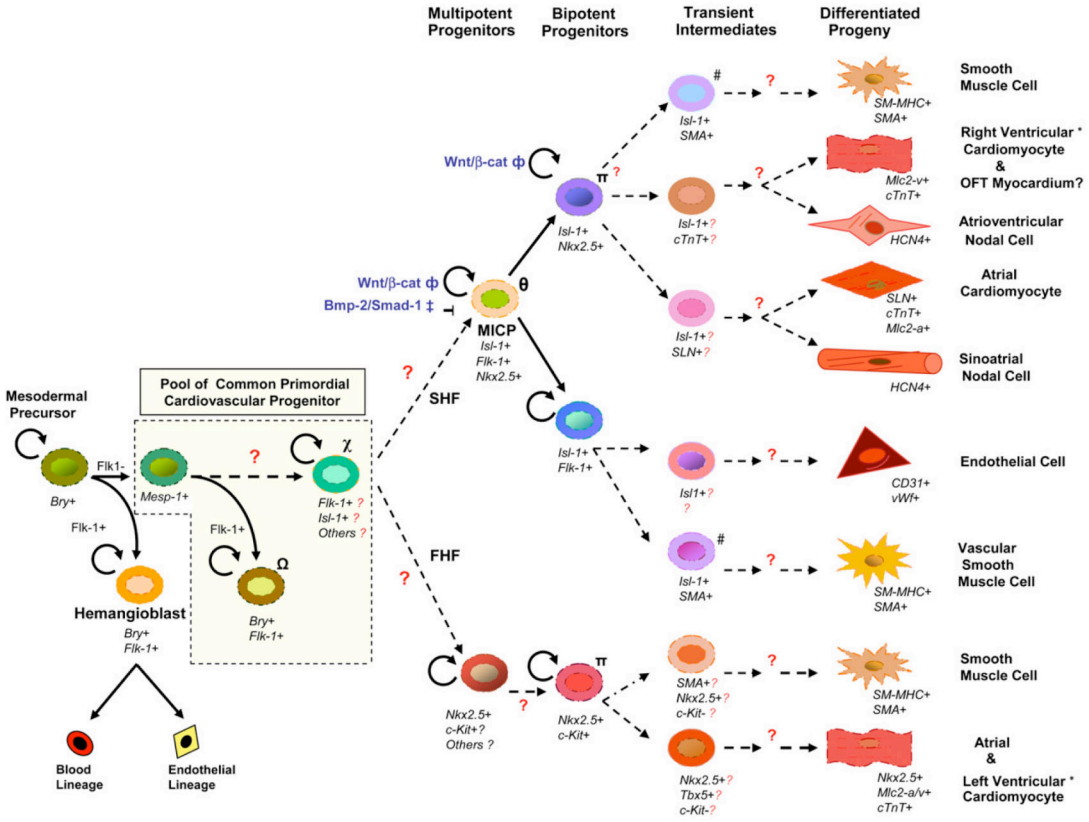

Figure 1.7. ***Hierarchical model of cardiac lineage diversification from mesodermal multipotent cardiovascular progenitors (MCPs).*** Schematic of cardiovascular progenitors and their progeny based on previous studies in murine ESCs, as well as *in vivo* fate mapping. Hematopoietic and vascular lineages diverge early from other cardiovascular lineages, which are generated from a common progenitor (yellow box). The separation of the PHF and SHF establishes two distinct pools of multipotent progenitors that undergo further diversification to bipotential progenitors. These progenitors pass through yet undefined transitional states to produced the terminally differentiated cell populations of the cardiovascular system. Denote the absence of NFATc1+ endocardium from this model. Figure adopted from Martin-Puig *et al*. (2008).

MCP populations have also been characterized using genetically modified ESCs with GFP reporters controlled by the early cardiac genes *Nkx2.5* or *isl1*. Using the SHF transcription factor *isl1* as a marker, MCPs were isolated from EBs and developing embryos capable of giving rise to cardiomyocytes, smooth muscle, and endothelial cells (Moretti *et al.*, 2006). Clonal expansion of these *isl1*+ MCPs found all three lineages were formed in only 12% of colonies, with the majority containing one or two cell types, suggesting that these *isl1*+ MCPs were more restricted in their lineage commitment compared to Flk1+ MCPs. The use of a GFP reporter driven by the PHF marker *Nkx2.5* instead of *isl1* also was capable of successfully identifying a MCP population from differentiating ESC with cardiomyocyte, smooth muscle, and endothelial cells potential (Christoforou *et al.*, 2008). Yet in another study, when *Nkx2.5*-GFP+ cells were sorted with c-kit, a bipotential myogenic precursor capable of giving rise to cardiomyocytes and smooth muscle cells, but not endothelium was obtained (Wu *et al.*, 2006). Collectively, these studies has allowed for the assembly of a working model of cardiac lineage diversification, in which any mention of the endocardial cell lineage is noticeably absent.

Aims of dissertation

The studies presented in this dissertation were initiated by a broad question; how is the endocardium different from other endothelial populations during development? To specifically identify the endocardium at the earliest stage of cardiac development, we generated a novel *NFATc1-nuc-LacZ* BAC transgene to faithfully recapitulate endogenous NFATc1 expression. This work is summarized in Chapter II. To better characterize endocardiogenesis, *in vitro* ESC differentiation was developed as a model of

endocardial differentiation. We demonstrate that endocardial and myocardial differentiation is spatial-temporal coordinated in EBs, an association that mirrors cardiogenesis in the developing embryo. This work is detailed in Chapter III. Given our observations of endocardial-myocardial interactions in differentiating ESCs, in conjugation with an emerging model of cardiac lineage specification that failed to address the endocardial lineage, we investigated the specification of endocardial cells from mesodermal precursors. Endocardial cells are distinct from the hematopoietic lineage and systemic vasculature, derived from an Flk1+ MCP population that also generates the myocardial lineage. This work is covered in Chapter IV. Taken together, this work clarifies endocardium is a unique cardiac lineage and provides further evidence that endocardium and myocardium are derived from a common precursor.

CHAPTER II

AN *NFATC1-NUC-LACZ* TRANSGENE IDENTIFIES ENDOCARDIUM AS A UNIQUE ENDOTHELIAL SUBPOPULATION DURING EARLY EMBYROGENESIS

Introduction

Many of the outstanding questions regarding the lineage classification and origin of the endocardium in murine heart development have been stymied by a dearth of specific endocardial markers in the face of an abundance of pan-vascular markers. *NFATc1* is one of the few endocardial-specific gene transcripts, and its unique expression pattern makes it an attractive target to study endocardial differentiation. As discussed, our previous efforts to analyze the transcriptional regulation of *NFATc1* characterized a 250 bp conserved region of intron 1 responsible for autoregulation of *NFATc1* in only the endocardium of valve forming region, (Zhou *et al.*, 2005). These experiments indicate that different regulatory mechanisms are involved in activating NFATc1 expression in endocardial precursors prior to heart tube formation in the cardiac crescent from those that direct transcription in endocardium lining the valve cushions.

Transcriptional cis-regulatory elements typically reside outside the core promoter region, and have been identified within introns and in distant untranslated segments of genomic DNA (reviewed in Kleinjan and van Heyningen, 2005). Prominent examples of this latter phenomenon include *Sox9*, *Pax6*, and *Sonic hedgehog* (*Shh*), as they possess distant cis-regulatory elements required for proper regulation of gene transcription. Identification of these regulatory elements has largely been accomplished through chromosomal analysis of human disease states and mouse mutants. Disruption of *Pax6*

expression can result in aniridia, or an absence of the iris, which has been attributed not to mutations in the transcriptional unit, but rather chromosomal rearrangements downstream of *Pax6* (Griffin *et al.*, 2002; Kleinjan *et al.*, 2001). Using the mouse mutant Small eye as a model, rescue experiments and expression studies indicate the cis-regulatory domain required for *Pax6* expression in the developing iris is over 200 kb downstream of the transcriptional start site. As another example of distant transcriptional regulation, *Sox9* has been linked to autosomal sex reversal, even though *Sox9*$^{-/-}$ mice do not display this phenotype. The Odsex mouse mutant, displaying ocular degeneration and sex reversal, demonstrates how dysregulation of *Sox9* expression results in sex reversal (Bishop *et al.*, 2000). In this mouse model, the insertion of a random transgene 980 kb away consequently creates a 134 kb deletion that removes a long-range activator of the *Sox9* promoter (Qin *et al.*, 2004). In addition, the random insertion of a reporter transgene ~1 Mb upstream of the *Shh* gene generated a mouse mutant termed Sasquatch that displays mirror image duplication of the hands and feet (Sharpe *et al.*, 1999). This particular phenotype is associated with preaxial polydactyl, a defect linked to *Shh* function in the zone of polarizing activity (ZPA) of developing limbs. These findings indicate long-range regulation of *Shh* expression is necessary for the critical processes of limb patterning and development.

To recapitulate NFATc1's endocardial expression pattern, but without having to define the required regulatory region, we utilized *in vitro* bacterial artificial chromosome (BAC) recombination. BAC recombination relies on expression of the *exo*, *bet*, and *gam* proteins of a defective λ prophage from the λPL promoter inserted into the bacterial genome repressed by the temperature-sensitive repressor *cI857* at 32°C and derepressed

at 42°C. These proteins function to direct homologous recombination for the purpose of either retrieving DNA fragments from BACs or inserting exogenous DNA elements, in this case a reporter gene, into BACs containing approximately 200 kb of genomic sequence (reviewed in Copeland *et al.*, 2001; Court *et al.*, 2002; Liu *et al.*, 2003). For our purposes, this approach will generate a reporter transgene regulated by the *NFATc1* promoter that also incorporates a sizeable amount of surrounding genomic information, all of which can be accomplished without affecting endogenous gene expression required for proper cardiac development.

With this system, we generated an NFATc1 *BAC* transgene with a nuclear localized beta-galactosidase (β-gal), encoded by the LacZ gene, inserted behind the P1 promoter (Fig. 2.2). By creating transient and stable transgenic mice carrying the *NFATc1-nuc-LacZ* BAC transgene, we demonstrate that this BAC possesses the regulatory elements necessary to distinguish endocardium from other endothelium during early embryogenesis by faithfully recapitulating endogenous *NFATc1* expression.

Experimental Procedures

Construction of NFATc1 BAC targeting vector

A 300 bp *Sma*I/*Sac*II fragment 5' of the translational start site of *NFATc1* (N5') incorporating promoter elements and the 5' untranslated region (UTR) was blunt end filled with T7 DNA polymerase (NEB) and ligated with the Mighty Mix DNA ligation kit (Takara) into the *Kpn*I site of a pBluescript KS+ (pBSKSa) vector with modified *Asc*I sites flanking the multiple clone site (MCS). A 440 bp *Sca*I/*Pst*I fragment from introns

1-2 distal to the exon1 splice acceptor (N3') was blunt end filled and ligated in the *Not*I site of pBSKSa-N5'. The nuclear β-gal cassette (*nuc-LacZ*) with its polyA sequence was excised with *Xho*I/*Pst*I from pWhere (Invivogen) and subcloned into *Xho*I/*Pst*I of pBSKSa-N5'-N3'. Finally, the *FRT* flanked tetracycline resistance cassette (Tet^R) from pGFP-IBG-tetR (a gift from the Mortlock Lab, Vanderbilt) was removed with *BamH*I/*Spe*I and ligated into the same sites to generate the *NFATc1* BAC targeting vector pBSKSa-N5'-nuc-LacZ-Tet^R-N3'.

BAC recombination

BAC recombination was performed as previously described (Lee *et al.*, 2001). Bacterial containing BAC DNA was cultured in Luria Brooth (LB) with 12.5 μg/ml of chloramphenical (CAM) at either 37˚C (DH10B) or 32˚C (EL250). Glycerol stocks were made by mixing 200 μl of a bacterial culture with 800 μl glycerol and placed at -80˚C. Small-scale preparation of BAC DNA was carried out using standard alkaline lysis techniques. For BAC "fingerprinting," DNA was digested overnight (O/N) with restriction enzyme(s) and analyzed by pulse field gel electrophoresis (PFGE) on a CHEF-DR III System (Bio-Rad) in 0.5 % TBE, run for >12 hours. A BAC (RP23-189J14, mouse C57Bl/6J; Invitrogen) covering the entire *NFATc1* locus, as well as 50 kb 5' and 75 kb 3' surrounding genomic sequence, was electroporated into a specialized *E. coli* strain (EL250) carrying the temperature sensitive λ phage Red recombination system and an arabinose inducible Flpe recombinase in a 0.1 cm cuvette at 1.75 V, 100 Ω 25 μF on a Bio-Rad Gene Pulser.

The *NFATc1* BAC targeting vector, pBSKSa-N5'-nuc-LacZ-frt/Tet^R-N3', was linearized with *Asc*I (5-10 μg maxi-prepped DNA) and gel purified with the Qiaex II Gel Extraction Kit (Qiagen). 300-500 μg were electroporated into EL250 cells containing the *NFATc1* BAC in a .1 cm cuvette at 1.75 V, 200 Ω 25 μF on a Bio-Rad Gene Pulser after a 15 minute 42°C heat shock to induce transcription of the λ phage Red recombination genes. Recombined clones were selected on 6.25 μg/ml CAM and 5 μg/ml Tet. Positive clones were treated with arabinose to activate the inducible Flpe recombinase of the EL250 strain to excise the *Tet^R* cassette by recombination of the *FRT* sites. Diagnostic tests of BAC clones with PFGE following by Southern blot confirmed BAC integrity and recombination. Southern probes were generated from the N5' homology arm or the 1.1 kb *Xho*I/*EcoR*V N-terminal fragment of *nuc-LacZ* and performed as previously described (Nagy, 2003b).

To establish transgenic mouse lines, *NFATc1-nuc-LacZ* BAC DNA was prepared by cesium chloride gradient purification after alkaline lysis. The lower band containing intact BAC DNA was pulled with a 21-gauge needle. Ethidium bromide was extracted with TE/NaCl-saturated n-butanol, then dialyzed into BAC microinjection buffer (10 mM Tris, 15 μM EDTA pH 7.4) using Centriprep size exclusion columns (Millipore). Dilutions of purified BAC DNA were cut with *Not*1 and analyzed by PFGE against Lambda DNA/*Hind*III standards to estimate concentration. BAC DNA was diluted to 2 ng/μl in BAC microinjection buffer with 100 nM spermine/spermidine and 100 nM NaCl for pronuclear injection FVB oocytes (Vintersten *et al.*, 2004).

Generation of transgenic mice

To generate fertilized oocytes for BAC DNA microinjection, female FVB donor mice were superovulated with the hormones Pregnant Mare Serum Gonadotropin (PMSG) and Human Chorionic Gonadotropin (hCG) and bred to stud FVB males (Nagy, 2003b). Oocytes were injected and cultured overnight in M2 media at 37˚C before being transferred into the oviducts of pseudopregnant foster mothers at the 2-cell stage. Vasectomized males were used to sham-fertilize recipient females to induce pseudopregnancy, thereby making them receptive to receiving injected embryos and allowing implantation and normal development to occur.

Genotyping

At three weeks of age, tail samples from offspring were digested in 100 mM Tris pH 8.5, 5 mM EDTA, 0.2% SDS, 200 mM NaCl, 100 μg/ml of Proteinase K overnight at 55˚C; DNA was purified by isopranol precipitation with an ethanol wash, and dried DNA pellets were resuspended in TE (10 mM Tris pH 7.5, 1 mM EDTA). Mice were genotyped by PCR with DNA MasterMix TAQ polymerase (NEB) using the following primers: 5’ GCA GCA GGC AGG GTC ACA GAG A 3’ and 5’ ACC CCA GGC TGC AAG GAG GAT T. Animals were maintained in accordance with protocols approved by the Vanderbilt University Institutional Animal Care and Use Committee (IACUC).

Beta-galactosidase (β-gal) staining

For whole mount β-gal staining, embryos were dissected in cold PBS and fixed in 0.2% glutaraldehyde, 2 mM MgCl2, and 5 mM EGTA in PBS for E8.5 and younger

embryos or 10% neutral buffered formalin (NBF) for older specimens. Fixation times were 15 minutes for glutaraldehyde and 30 minutes for 10% NBF. Embryos were washed twice with X-gal wash buffer consisting of 2 mM $MgCl_2$, 0.02% NP40 in PBS before incubation in a X-gal staining buffer of 1 mg/ml X-Gal, 5 mM potassium ferro/ferricyanate, 2 mM $MgCl_2$, 0.02% NP40, 0.01% sodium deoxycholate in PBS at 37°C for 2-6 hours to prevent overstaining. Embryos were cleared using a glycerol gradient in PBS and stored at 4°C.

To section E8.5 and younger specimens, whole mount X-gal stained embryos were embedded in 3% agarose plugs and processed through an alcohol-xylene-paraffin series and sectioned at 8 μm. For sections of β-gal expressing transgenic embryos at E9.5 and older, embryos were dissected in cold PBS and fixed in glutaraldehyde, washed with PBS, and cryoprotected by passing them through a sucrose gradient, 15% sucrose in PBS for 2-4 hours, then 30% sucrose in PBS O/N. Specimens were embedded in OCT and cryosectioned at 10 μm, and stained as described above. Both paraffin and frozen sections were counterstained with eosin, dehydrated, and mounted.

Immunostaining

For immunofluorescence, embryos were dissected in cold PBS and fixed in 10% NBF for 30 minutes at 4˚C, washed with PBS, and cryoprotected in 15% sucrose in PBS for 2-4 hours, then 30% sucrose in PBS O/N. Specimens were embedded in OCT and cryosectioned at 10 μm and place on charged slides. For single immunofluorescence for NFATc1 or for dual labeling with NFATc1 and another antibody, the Mouse on Mouse kit (M.O.M.) (Vector Labs) was used as per manufacturer's instructions with the

following modifications. After Avidin/Biotin blocking (Vector) and application of the M.O.M. Ig Blocking Reagent, primary antibody against NFATc1 was added to M.O.M. diluent and incubated O/N at 4˚C. In dual labeling conditions, primary antibody to the second antigen was added along with the M.O.M. biotinylated anti-mouse IgG reagent for 30 minutes as room temperature (RT). M.O.M. Fluorescein Avidin DCS and Alexa-555 conjugated secondary antibodies were added and incubated at 37˚C for 15 minutes. For instances where NFATc1 was not used, slides were blocked in 10% goat serum (Jackson Labs) prior to incubation with primary antibodies overnight at 4°C, followed the next day by secondary antibodies for 1 hour at 37˚C. Samples were mounted with Vectashield containing DAPI (Vector Labs).

For whole mount immunohistochemistry, embryos were dissected in cold PBS and fixed in Dent's Fixative (4:1 methanol:DMSO) O/N at 4˚C. Embryos were bleached in 4:1:1 methanol:DMSO:H_2O_2 for 5-10 hrs at RT and stored in 100% methanol at -20˚C. Rehydrated embryos were washed twice for 1 hour in PSB with 2% BSA and 0.5% Triton-X (PBSBT) before addition of the primary antibody at a concentration of 1 µg/ml in PBSBT and rocked O/N at 4˚C. The next day, specimens were washed five times with PBSBT for 1 hour each before addition of a species-specific biotinylated secondary antibody. After another O/N incubation and five hour washes with PBSBT, embryos were incubated with the streptavidin:peroxidase complex from the ABC kit (Vector) in PBSBT, followed by signal detection with Diaminobenzidine (DAB; Vector). After dehydration into 100% methanol, embryos were cleared for photography in BABB (1:2 benzyl alcohol: benzyl benzoate). For whole mount immunohistochemistry on X-gal stained embryos, specimen were fixed and stained for β-gal expression as described

above, then washed with PBS, post-fixed with Dent's fixative, bleached, then stored in 100% methanol at -20˚C. Embryos were immunostained as described above. For signal detection, NovaRed peroxidase substrate (Vector) was used for color contrast with blue X-gal staining. Embryos were cleared through a glycerol/PBS series, as the NovaRed substrate is unstable in BABB.

For immunohistochemistry on paraffin slides, citrate antigen retrieval was performed before incubation with 3% H_2O_2. Slides were blocked in 10% goat serum prior to incubation with anti-NFATc1 antibody overnight at 4°C, followed the next day by the SuperPic secondary antibody (Zymed) for 1 hour at RT. DAB was used to detect antibody signal, and then slides were counterstained with Harris hematoxylin and desaturated with lithium carbonate. Samples were dehydrated through an alcohol-xylene gradient and mounted. Images were acquired using a Nikon Elipse E800 epifluorescence microscope or a Zeiss Upright LSM510 Confocal Microscope.

Antibodies

NFATc1 (mouse 7A6, BD Pharmingen, 1:200)

Cardiac troponin T (cTnT; mouse CT3, Developmental Studies Hybridoma Bank (DSHB) University of Iowa, 1 μg/ml)

Sacromeric myosin heavy chain (MHC; mouse MF20, DSHB, 1 μg/ml)

CD31/Pecam-1 (rat MEC13.3, BD Pharmingen, 1:500)

VE-cadherin (rat 11D4.1, BD Pharmingen, 1:500)

Von Willibrand Factor (vWF; rabbit, Dako, 1:200)

β-Gal (chick, Abcam, 1:1,000 or rabbit, Cappel, 1:5,000)

In situ hybridization

In situ hybridization for NFATc1 was performed as previously described (Hogan, 1994). P^{35} thio-UTP labeled sense and antisense probes were generated from a plasmid containing a 2 kb N-terminal fragment of the NFATc1 cDNA. Tissue was treated with 20 μg/ml Proteinase K for 8 minutes, and probes were hybridized O/N at 55°C. After extensive washing, signal was checked by O/N exposure on X-ray film. Slides were then developed with emulsion, washed, dried, and mounted.

Culture of embryonic endothelial progenitor cells (eEPCs)

Embryonic endothelial progenitor cells (eEPCs) were cultured in Dulbecco's Modified Eagle Medium (DMEM) supplemented with 20% FBS (HyClone), 25 mM HEPES, 2 mM L-glutamine, 100 U/ml Penicillin/Streptomycin, 100 μM non-essential amino acids, and 100 μM β-mercaptoethanol. Cells were grown on 0.1% gelatinized plates and passaged every 2-3 days at a ratio of 1:10. For transfection, 2-4 μg of $CsCl_2$ purified BAC DNA was mixed with 40 μl of Lipofectamine 2000 (Invitrogen) in 2 ml Optimem (Invitrogen/Gibco). This complex was added to 2 ml of fresh eEPC media in 6-well dishes with cells at 70% confluency. Differentiation of eEPCs was induced with addition of 1 μM all-trans-retionic acid (RA; Sigma) and 0.5 mM dibutyrul cyclic AMP (cAMP; Sigma) (Hatzopoulos *et al.*, 1998). Cells were allowed to differentiate for 48 hours before analysis.

Quantitative real-time PCR (qRT-PCR)

Samples of undifferentiated and differentiated eEPC cDNA were provided by Matias Lamparter (Hatzopoulos Lab, Vanderbilt). All qRT-PCR was performed using a Light Cycler (Roche) with the Light Cycler DNA Master SYBR Green I Kit, 0.5 μM of each primer, 3-5 mM $MgCl_2$, and 100 ng cDNA. Gene specific primer sets were designed to cross intron-exon boundries when possible to ensure mRNA, not genomic DNA, was amplified. The primers used for these experiments are listed as follows: *NFATc1*: 5' GGT GGC CTC GAA CCC TAT C 3', 5' TCA GTC TTT GCT TCC ATC TCC C 3'; *CD31/Pecam-1*: 5' ATC CGG AAG GTC GAC CCT AAT CTC AT 3', 5' ATA CCC AAC ATG AAC AAG GCA GCG 3'; *VE-cadherin*: 5' AAC TCA CCC TCC TTG TGG AAT CCT 3', 5' ACA TCT CAT GCA CCA GGG TGA CTA 3'; *GAPDH*: 5' CAC TGG CAT GGC CTT CCG TG 3', 5' AGG AAA TGA GCT TGA CAAAG 3'. The specificity of the amplified product was evaluated using the melting curve analysis and a no template control reaction. Each sample was done in triplicate and relative expression was calculated as $\Delta^{2\text{-ct}}$ with *GAPDH* as the internal control (Schmittgen and Livak, 2008).

Results

NFATc1 is restricted to the endocardial endothelial lineage during early embryogenesis

In situ hybridization with a radiolabeled probe demonstrated *NFATc1* is an endocardial-specific transcription factor, capable of distinguishing the endocardium as a unique subpopulation of endothelium (Fig. 2.1A). At E9.5, signal is detected in all

endocardial cells of the primitive atria and ventricle, as well as the OFT. Signal dissipated at the proximal and distal ends of the looped endocardial tube, and was observed to be mosaic in the sinus venous and aortic sac. Little to no *NFATc1* is observed in the myocardium or system vasculature. Immunofluorescence of NFATc1 and the endothelial marker von Willibrand Factor (vWF) in an E10.5 embryo also documents that NFATc1 is restricted to endocardial endothelium (Fig. 2.1B). While other vascular markers such as Flk1, VE-cadherin, and CD31/Pecam-1 mark the endocardium early in development, vWF appears unique in that it is excluded from the endocardium until E14.5, after the major morphogenic events of valvulogenesis and trabeculation (Fig. 2.1C-E). vWF is only expressed in the peripheral vasculature and distal portions of the OFT at E10.5, and not does extend into the endocardium (Fig. 2.1F-H). These finding, similar to previous studies of early endocardial NFATc1 expression, indicate NFATc1 is an endocardial-specific gene transcript, providing molecular evidence that the endocardium is a unique subpopulation of cells distinct from other endothelium (Chang *et al.*, 2004; de la Pompa *et al.*, 1998; Ranger *et al.*, 1998).

Generation of an NFATc1 BAC reporter transgene

As discussed, BACs contain large segments of genomic DNA, covering entire gene loci and upstream and downstream regulatory elements. The particular BAC chosen to serve as the basis for the *NFATc1* reporter transgene (RP23-189J14) was selected based on the relative position of the *NFATc1* locus. In addition to containing the entirety of the *NFATc1* genomic locus, this BAC has 50 kb upstream sequence that extends up to, but not including, the closet gene on chromosome 18, *Atp9b*, as well as 75 kb of genomic

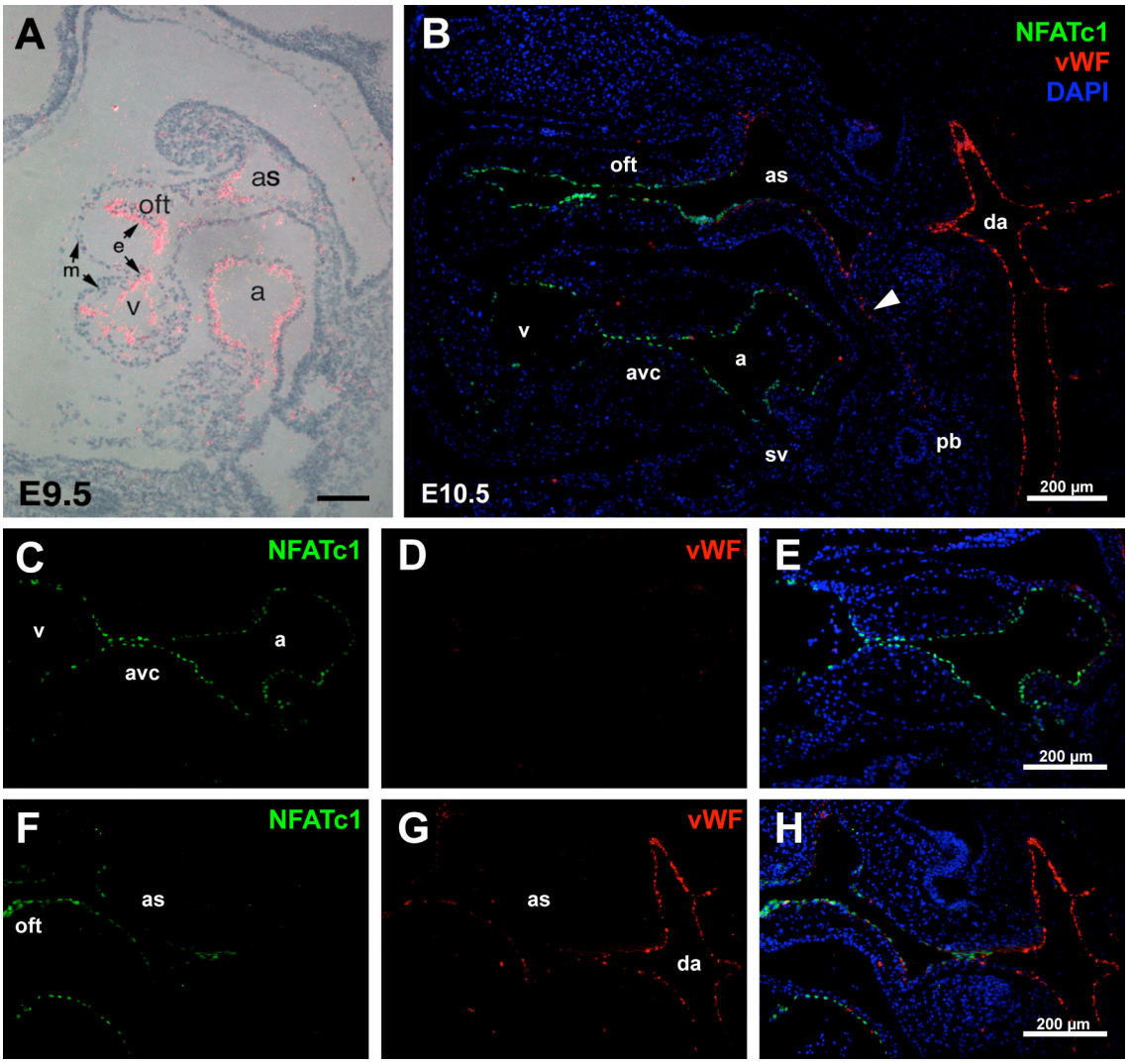

Figure 2.1. ***Endogenous expression of NFATc1 in the embryonic endocardium.*** **A**. *In situ* hybridization depicting *NFATc1* mRNA (magenta) localized to the endocardium at E9.5. **B.** Immunofluorescence of NFATc1 (green) and the endothelial marker von Willibrand Factor (vWF; red) in an E10.5 embryo. Nuclei were detected with DAPI (blue). The white arrowhead marks the forming pulmonary artery. **C-E.** NFATc1 (**C**, green) is present in the endocardium of the forming AVC valve cushion while vWF (**D**, red) is not expressed in this endothelial subpopulation. **F-G**. NFATc1 (**F**, green) is entirely restricted to the endocardial endothelium, dissipating at the aortic sac where the distal portion of the OFT intersects with the systematic vasculature as labeled by vWF (**G**, red).

Myocardium, m; endocardium, e; outflow tract, oft; common ventricle, v; atrioventricular canal, avc; aortic sac, as; atria, a; dorsal aorta, da; sinus venous, sv; pulmonary bud, pb

downstream sequence (Fig. 2.2A). With this coverage, there would be a high probability of containing the regulatory elements necessary to drive appropriate gene expression from the *NFATc1* locus.

BAC DNA was purified from the parental DH10B *E. coli* strain and electroporated into the EL250 strain engineered to carry both the heat inducible λ phage Red recombination gene and an arabinose inducible Flpe recombinase. DNA was prepared from resulting CAM resistant EL250 clones and digested with *BamH*1 to compare with the original BAC to confirm stable introduction of the NFATc1 BAC into the EL250 strain (Fig. 2.2C, panel i). A nuclear localized β-gal (*nuc-LacZ*) was chosen as the reporter gene for several reasons: X-gal staining yields a robust colorimetric stain for histology, specific antibodies exist to detect the β-gal protein for Immunostaining, PCR genotyping for *nuc-LacZ* is specific and efficient, and the nuclear stain is beneficial for cell counting. For targeting, a 5' homology arm (N5') was designed to contained upstream promoter elements of the *NFATc1* locus, as well as the 5' UTR up to the translational start site (Fig 2.2B). Inclusion of the *FRT* flanked Tet^R conferred tetracycline resistance to the construct, but also could be removed by the arabinose inducible *Flpe* recombinase in the final construct as to not interfere with reporter gene expression. For BAC targeting, the targeting construct excised from the vector backbone with *Asc*I and purified before electroporation into EL250-*NFATc1*-BAC cells heat shocked at 42˚C to induce expression of the recombineering genes. Dual resistant CAM and Tet colonies were screened by *Not*I digestion analyzed by PFGE. As rare cutter of the genomic region carried on the RP23-189J14 BAC, *Not*I sites flanking exon1 yielded a 7.3 kb band that increased to 13.0 kb with the introduction of *nuc-LacZ-*Tet^R (Fig. 2.2C,

panel iii). Following removing of the *Tet*^{R} cassette, this fragment was reduced in size at 10.5 kb. The BAC vector backbone, which possesses two *Not*I sites at its ends, is constantly visible at 8.7 kb. Confirming these shifts represented correct targeting, Southern blots with probes generated from the N5' homology arm or the 1.1 kb *Xho*I/*EcoR*V N-terminal fragment of *nuc-LacZ* localized to the expected bands (Fig. 2.2C, panels iii' & iii'').

Prior to use, two additional modifications were made to the targeted BAC via homologous recombination. The BAC vector (pBACe3.6) contains two cryptic *loxP* sites, one wild type and one *loxP511* mutant. Though these two sites rarely undergo recombination, BAC transgenes integrate into the host genome as concatamers, thus lining up similar *loxP* sites of different copies of the transgene that might undergo inappropriate excision in the presence of a Cre recombinase (Furuta and Behringer, 2005). The *LoxP* site in the pBACe3.6 vector backbone was replaced with a zeocin cassette flanked by 500 bp homology arms complementary to the sequence adjacent to the *LoxP* site (pLoxPOUTZeo). Subsequently, the *LoxP511* site was replaced with a kanamycin cassette (KAN) flanked by 50 bp homology arms complementary to the sequence adjacent to the *LoxP511* site (pLoxP511OUTKan). These plasmids were used in collaboration with the Southard-Smith lab (Vanderbilt University). These modifications resulted in an increase in the size of the vector backbone, from 8.7 kb to 9.2 kb to 10.3 kb, as observed by a band shift after *Not*I digestion (Fig. 2.2C, panel ii). These cassettes were not removed from the BAC since the distance between the BAC backbone and the first exon of NFATc1 was deemed sufficient enough as to not interfere with activity of the reporter gene.

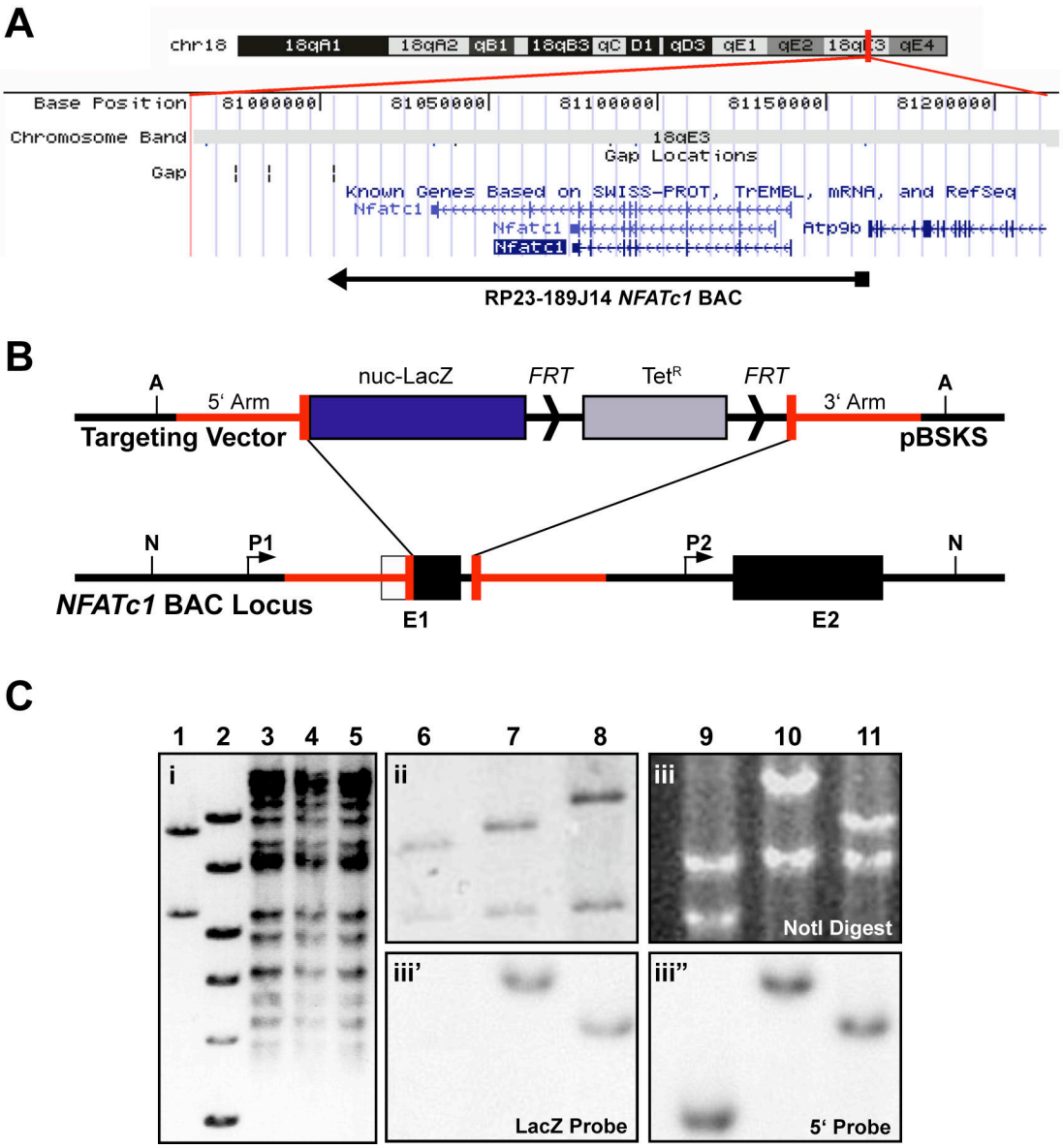

Figure 2.2. ***Generation of an NFATc1-nuc-LacZ BAC reporter transgene.*** **A.** Location of the NFATc1 locus on chromosome 18 and the coverage of RP23-189J14 *NFATc1* BAC. **B.** Schematic of the BAC targeting vector and its insertion into the mouse *NFATc1* BAC locus. Red bar, homology arms; E, exons; white box, 5'UTR; N, *Not*I; A, *Asc*I. **C.** PFGE of *BamH*1 digestion **(i)**. Lambda/*Hind*III ladder (1), 1 kb ladder (2), original BAC from DH10B (3), electroporated BAC from EL250 (4-5). PFGE of the *Not*I digestion after removal of the *loxP* sites **(ii)**. The upper band represents the 8.7 kb unmodified BAC backbone (6), the 9.2 kb backbone after ZEO insertion (7), and the 10.3 kb band after KAN insertion (8). The wild type 6.6 kb band of *NFATc1* remains unchanged **(iii)** PFGE of *Not*I digestion with the wild type 6.6 kb band of *NFATc1* (9), the 13.3 kb *NFATc1-nuc-LacZ-tetR* (10), and the final 11.5 kb band left after Tet^R removal. Southern blotting for *LacZ* **(iii')** and the 5' homology arm **(iii")** confirmed insert of the targeting construct and the removal of the Tet^R cassette.

NFATc1-nuc-LacZ is expressed in differentiating eEPCs

To validate whether the targeted *NFATc1-nuc-LacZ* BAC constituted a functional construct, confirmation *in vitro* prior to its introduction into transgenic mice was deemed necessary. However, while a number of cell lines have been established to express high levels of NFATc1, including the Jurkat T cell line and several osteoclast cell lines, no embryonic endocardial endothelial cell line exist (Heymann *et al.*, 1998; Shaw *et al.*, 1988). The differentiation of embryonic endothelial progenitors cells (eEPCS) represented a potential model to test the *NFATc1-nuc-LacZ* BAC transgene. Isolated from E7.5 mouse embryos, eEPCs possess self-renewal capability, but upon treatment by RA and cAMP, differentiate into mature endothelial cells (Hatzopoulos *et al.*, 1998). Xenoplantation of these eEPCs into chick embryos demonstrate these cells preferentially integrate with the endocardium, suggesting eEPCs might contain endocardial precursors. Though differentiated eEPCs express numerous vascular gene transcripts, it had not yet determined whether they expressed endocardial transcripts, such as *NFATc1*. Comparison of gene transcripts by qRT-PCR from undifferentiated and differentiated eEPCs indicated that endothelial markers *VE-cadherin* and *CD31/Pecam-1* increased 4-6 fold, respectively (Fig. 2.3A). When transfected with $CsCl_2$ purified *NFATc1-nuc-LacZ* BAC DNA, undifferentiated eEPCs only sparsely expressed β-gal (Fig. 2.3B, panel ii). However after two days of RA and cAMP induction, significant β-gal expression could be detected (Fig. 2.3B, compare panel i vs iii). These findings suggested that the *NFATc1-nuc-LacZ* BAC not only functioned, but also was expressed in a manner that reflected changes of endogenous NFATc1 expression.

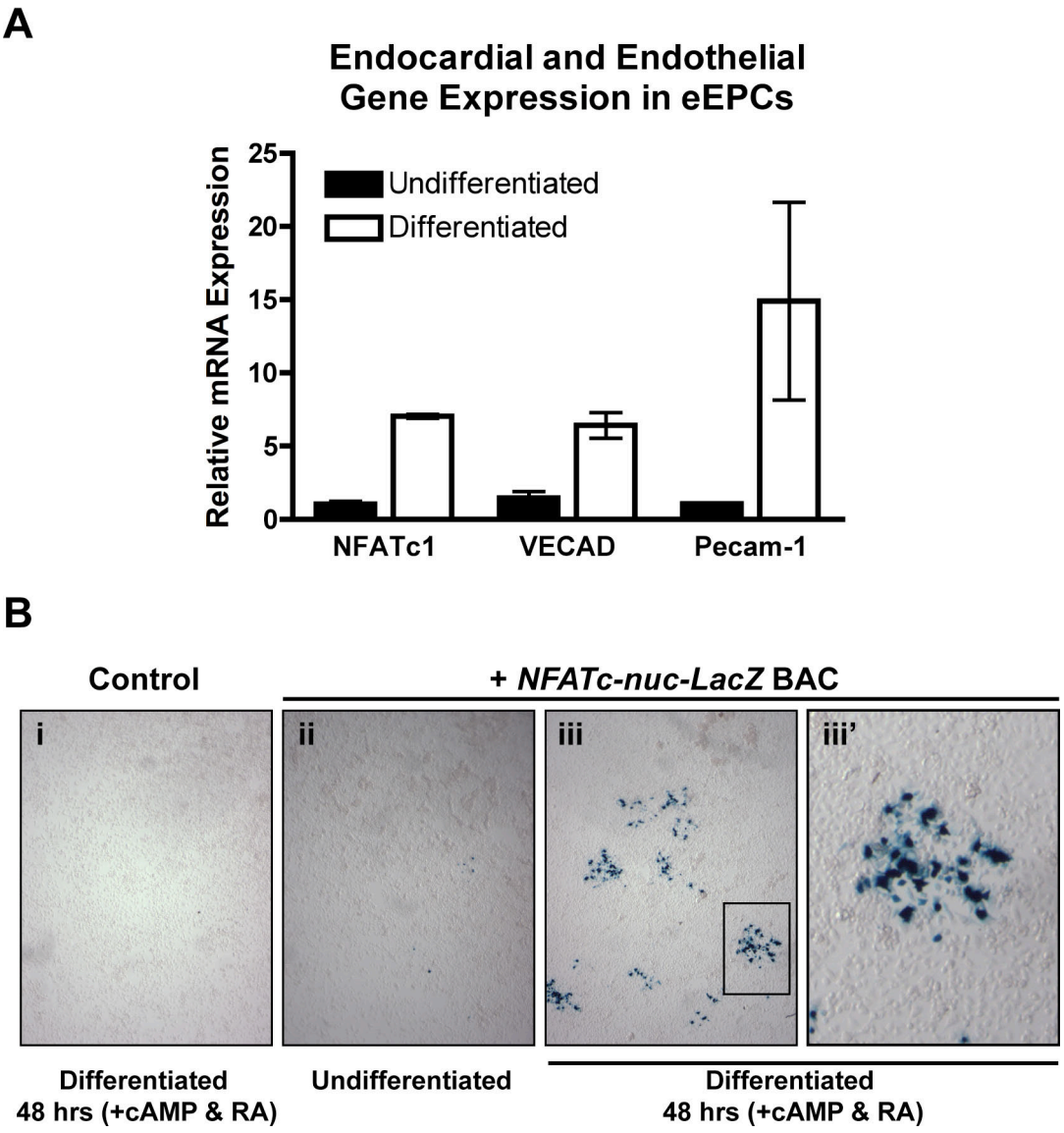

Figure 2.3. ***In vitro differentiation of endocardial cells from embryonic endothelial progenitors (eEPCs).*** **A.** qRT-PCR of endocardial (*NFATc1*) and endothelial (*VE-cadherin and CD31/Pecam-1*) gene transcripts in undifferentiated eEPCs compared to eEPCs differentiated for 48 hours with 1 μM RA and 0.5 mM dibutyrul cAMP. Endocardial and endothelial genes are upregulated with differentiation. **B.** Expression of the *NFATc1-nuc-LacZ* BAC transgene in eEPCs with no BAC DNA **(I)**, undifferentiated eEPCs transfected with the BAC transgene **(II)**, and differentiated eEPCs containing the BAC transgene **(III,III')**. Significant expression from the *NFATc1-nuc-LacZ* BAC transgene was only detected in differentiated eEPCs

The NFATc1-nuc-LacZ BAC contains the necessary regulatory elements for early endocardial expression

Expression of the *NFATc1-nuc-LacZ* BAC in differentiated eEPCs failed to assess whether the regulatory domains required for early endocardial expression are present on the modified RP23-189J14 BAC transgene. To determine the expression capacity of this transgene *in vivo*, transient transgenic embryos were obtained at E9.5. From pronuclear injection of ~50 zygotes, 8 embryos were recovered, 1 of which was determined by PCR to carry the *nuc-LacZ* cassette (data not shown). Whole mount X-gal staining demonstrates *NFATc1-nuc-LacZ* BAC expression was specific to the developing heart, with β-gal present in the endocardium of the primitive atrium and ventricle, as well as in the AVC and the OFT (Fig 2.4A-C). Sagital sections of this transient transgenic demonstrate β-gal is restricted to the endocardial tube, and absent from the outer myocardial layer, as well as from the systemic vascular endothelium (Fig 2.4D). In addition, β-gal is most robustly expressed on the endocardial lining the AVC, in accordance with endogenous NFATc1 restriction to valvular endocardium with the initiation of endocardial cushion formation (Fig 2.4E). Mesenchymal cell expression is also evident even though NFATc1 is normally downregulated in this population, most likely representing residual β-gal protein, not active transcription. Reporter expression is notably absent at the proximal and distal ends in the sinus venous and aortic sac (Fig 2.4F). As expression from the *NFATc1-nuc-LacZ* BAC transgene includes the entire endocardial population, and is not limited to the valvular endocardium as with the 250-bp intron 2 enhancer, it suggests that the distal regulatory elements required for early endocardial expression are present in this BAC.

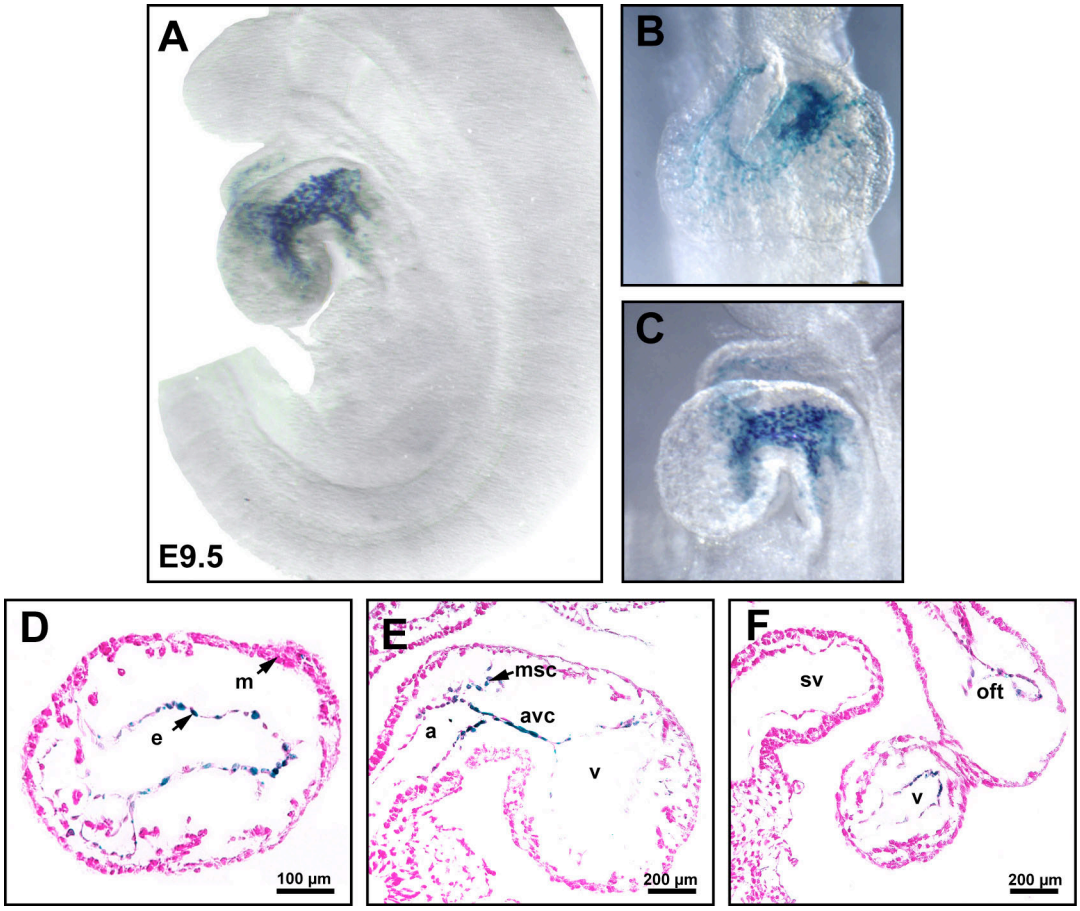

Figure 2.4. ***Transient transgenic analysis of early endocardial expression from the NFATc1-nuc-LacZ BAC transgene.*** **A.** Whole mount X-gal stained E9.5 transient transgenic embryo with β-gal expressed from the BAC transgene restricted to the looped heart. **B-C.** Higher magnification images of the ventricle and OFT **(B)** and the inflow tract and AVC **(C)**. **D.** Sagital sections counterstained with eosin demonstrating β-gal only in the endocardial tube, and not in the outer myocardial layer. **E.** Sagital section of endocardial β-gal expression the atria, ventricle, and AVC. Residual β-gal expression can also be detected in endocardial cells that have just undergone EMT to become mesenchymal cells of the ECC. **F.** Reporter expression is absent at the proximal and distal ends in the sinus venous and aortic sac.

Myocardium, m; endocardium, e; outflow tract, oft; common ventricle, v; atrioventricular canal, avc; aortic sac, as; atria, a; sinus venous, sv; mesenchymal cells, msc

NFATc1-nuc-LacZ BAC expression recapitulates endogenous NFATc1 during cardiogenesis

With confirmation that the *NFATc1-nuc-LacZ* BAC possessed the regulatory elements necessary to drive early endocardial expression, we proceeded to generate stable transgenic mouse lines. Two separate attempts to generate mouse lines through pronuclear injection using CD1/ICR donor oocytes failed to generate any PCR positive pups. CD1/ICR oocytes respond poorly to the microinjection of BAC DNA, and thus for further pronuclear injections, we utilized the inbred FVB/N mouse strain, characterized as being highly efficient for transgenic production with limited blocking at the 1-cell stage in response to the introduction of foreign (Auerbach *et al.*, 2003; Giraldo and Montoliu, 2001). Supercoiled BAC DNA, not linearized BAC DNA, was injected as supercoiled BAC DNA has been suggested to be more resistant to sheering during injection, as well as more likely to be introduced into the genome intact. The addition of polyamines to the microinjection buffer maintained the purified BAC in a supercoiled form. Pronuclear injection of ~200 zygotes resulted in 18 live births, 3 of which were determined by PCR to carry *nuc-LacZ* (data not shown). From these animals, a line that demonstrated germline transmission and robust expression was propagated as the founder line. Copy number analysis has not yet been conducted, but a method to do so in BAC transgenic mice has been described (Chandler *et al.*, 2007).

β-gal produced from the *NFATc1-nuc-LacZ* BAC is first detectable during embryonic development in the anterior portion of the E7.5 embryo as individual cells appear in the lateral plate mesoderm (Fig. 2.5A; white arrowhead). Further in development, these cells consolidate into a tightly organized band corresponding to the cardiac crescent extending across the midline (Fig. 2.5B; white arrowheads). As lateral

folding in the embryo at E8.0 brings the cardiac precursors towards the ventral midline to form the primitive heart tube, robust β-gal expression is observed in the heart-forming region of the PHF (Fig. 2.5C). In coronal sections of E7.5 transgenic embryos, nuclear-localized β-gal is restricted to endocardial precursors at the cardiac crescent that are organized as a distinct plate of cells positioned directly between the AVE and myocardial precursors rather than being interspersed with primitive cardiomyocytes (Fig. 2.5D,E). E7.75 X-gal stained transgenic embryos whole mount immunostained for myosin heavy chain (MHC) further illustrate how endocardial and myocardial precursors are dispersed throughout the cardiac crescent as the two populations migrate towards the midline to generate the primitive heart tube (Fig 2.5F,G).

By E8.25 the linear primitive heart has been completed by the merging of the bilateral precursors of the PHF; at this time β-gal expression is entirely localized to the developing heart (Fig. 2.6A,B). No expression was evident in the systemic vasculature, as illustrated by the comparison of a whole mount stained E9.5 *NFATc1-nuc-LacZ* BAC transgenic embryo against a comparable embryo whole-mount *in situ* stained for the endothelial marker CD31/Pecam-1 (Fig. 2.6C). X-gal staining in coronal section through the length of the linear heart demonstrates β-gal is limited to the endocardial tube and not in the surrounding myocardium (Fig. 2.6D). These findings indicate the *NFATc1-nuc-LacZ* BAC transgene specifically identifies the entire subpopulation of endocardial endothelium at its earliest stage of development as they differentiate in the cardiac mesoderm.

Given NFATc1's dynamic expression in endocardial cells across the window of cardiac development, we assessed β-gal expression during early murine embryogenesis.

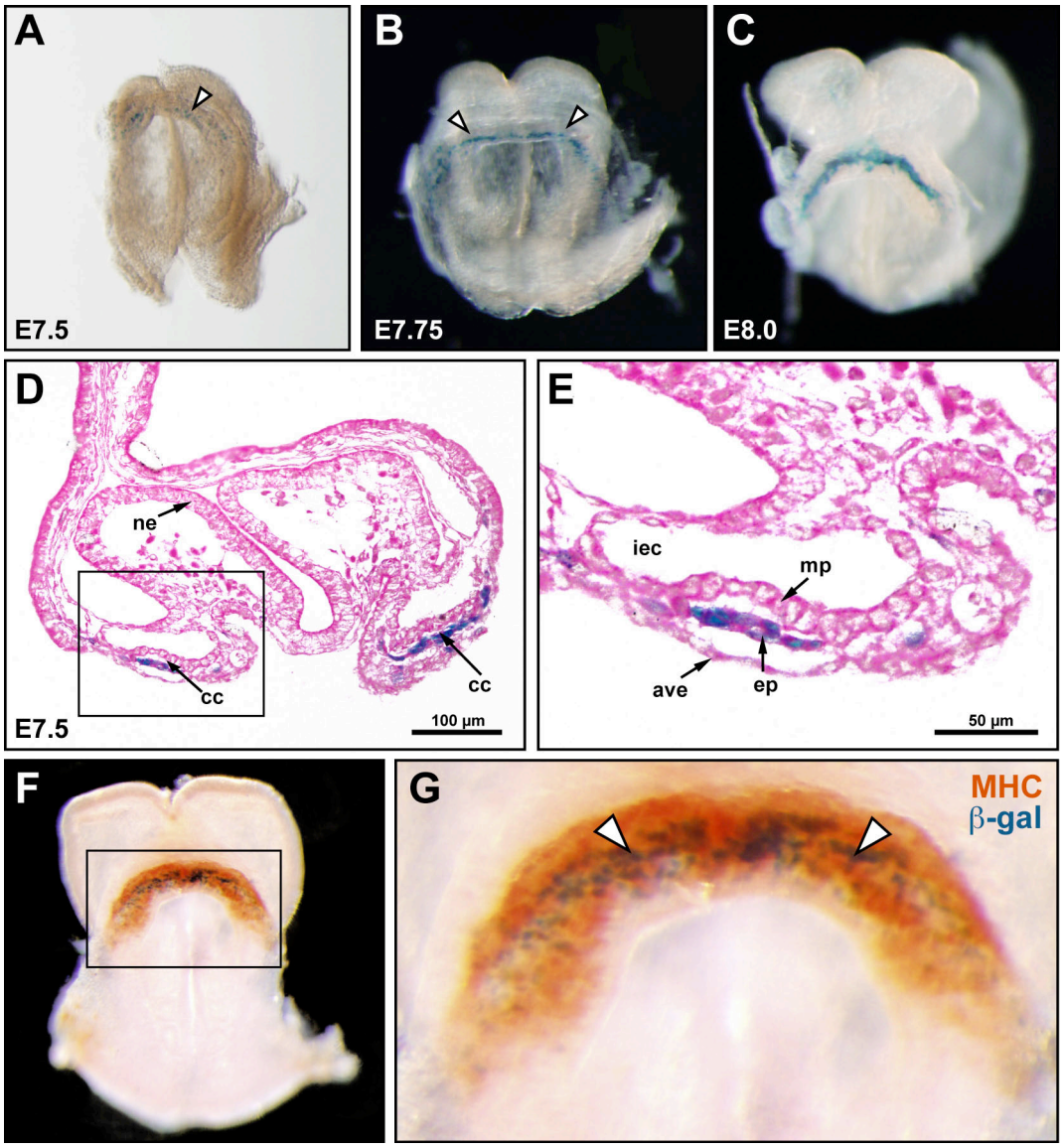

Figure 2.5. ***In vivo expression of the NFATc1-nuc-LacZ BAC transgene in differentiating endocardial precursors.*** **A.** X-gal stained E7.5 *NFATc1-nuc-LacZ* embryo with β-gal expression in the cardiac crescent (white arrowhead). **B.** E7.75 transgenic embryo with β-gal+ endocardial cells (white arrowheads) organized along the cardiac crescent **C.** Merging of the endocardial tubes with lateral folding at E8.0. **D,E.** Coronal section of β-gal+ endocardial cells positioned directly between the AVE and myocardial precursors **F.** Whole mount immunohistochemistry for myosin heavy chain (MHC; reddish-brown) marking myocardial precursors in the cardiac crescent of an E7.75 X-gal stained transgenic embryo. **G.** High magnification image demonstrating endocardial (white arrowheads) and myocardial precursors dispersed throughout the cardiac crescent.

Myocardial precursors, mp; endocardial precursor, ep; neuroectoderm, ne; cardiac crescent, cc; anterior visceral endoderm, ave; intraembryonic coelom, iec

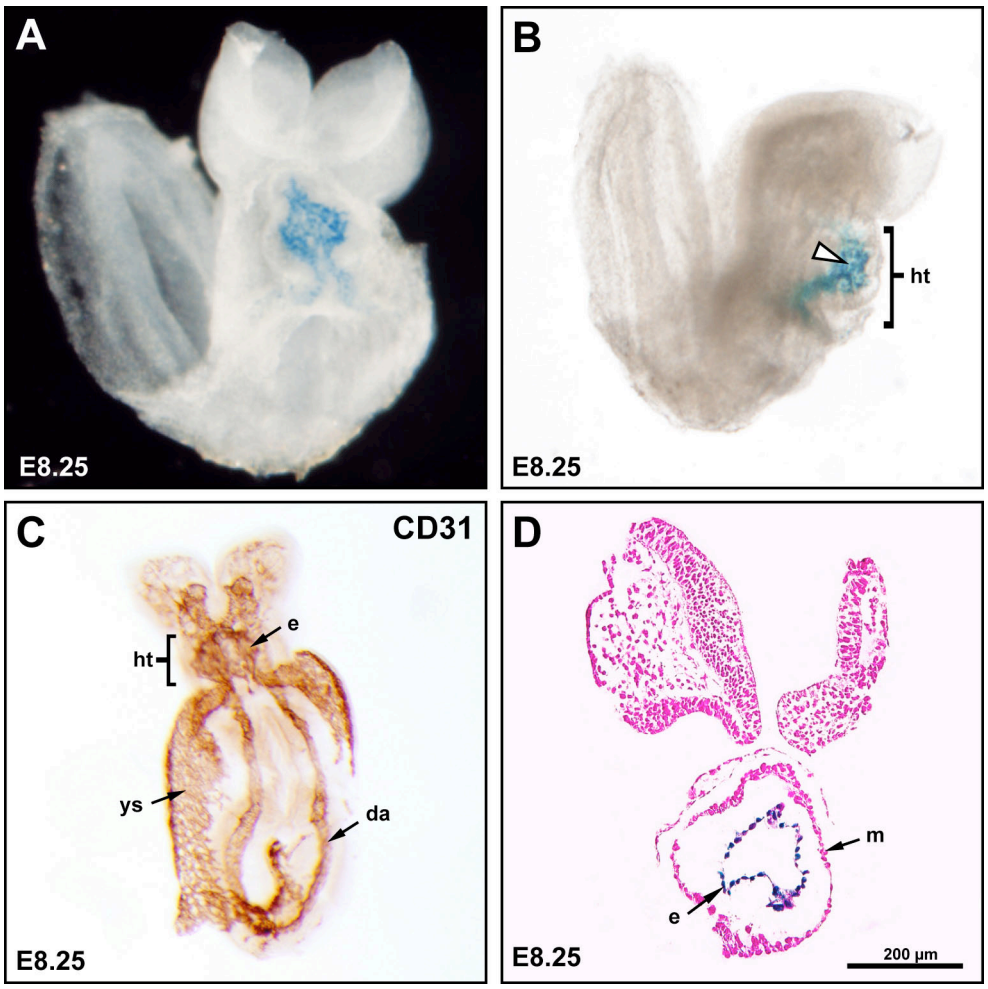

Figure 2.6. ***NFATc1-nuc-LacZ BAC transgenic expression in the endocardium of the E8.5 primitive heart tube.*** **A.** Frontal view of an E8.5 whole mount X-gal stained transgenic embryo. **B.** Lateral view of an E8.5 whole mount X-gal stained transgenic embryo with β-gal expression confined to the linear heart tube (white arrowhead). **C.** Whole-mount *in situ* for the endothelial marker CD31/Pecam-1 displaying the entirety of the embryonic vasculature at the E8.5 linear heart stage. **D.** Coronal section of E8.5 X-gal stained *NFATc1-nuc-LacZ* embryo documenting β-gal expression is present only in the endocardial layer, and not the myocardial layer.

Myocardium, m; endocardium, e; heart tube, ht; dorsal aorta, da; cardiac crescent, yolk sac, ys.

At E9.5, whole mount X-gal staining documents β-gal in all segments of the looped heart (Fig. 2.7A). Expression is present only in the heart and is absent from the other vascular populations as marked by whole mount immunohistochemistry for CD31/Pecam-1 and MHC at this developmental point (Fig. 2.7B,C). Robust expression was observed throughout the entire endocardium, present in the primitive atria, ventricle, AVC, and the OFT (Fig. 2.7D,E). Expression became mosaic at the proximal sinus venous and distal aortic sac as the endocardium meets the peripheral vasculature, where β-gal is not produced from by the BAC transgene (Fig. 2.7E). Though this pattern of expression matches previous descriptions of NFATc1 during early cardiogenesis, co-immunofluorescence of NFATc1 and β-gal was performed to assess their exact location at E9.5 (Fig. 2.7F-I). NFATc1 colocalizes with β-gal in endocardial cells of the looping heart, indicating transcription of *LacZ* from the BAC transgene faithfully recapitulates endogenous regulation of *NFATc1* during cardiogenesis.

With initiation of ECC formation at E10.5, the first alteration of expression was observed, as β-gal was downregulated in the atrial and ventricular endocardium. β-gal retained in the valvular endocardium, endothelium overlying the valve cushions that does not undergo EMT (Fig. 2.8A). The expression of cardiovascular markers during this stage of embryogenesis illustrates the unique expression pattern of NFATc1 in the developing heart. Immunofluorescence documents that NFATc1 and β-gal are colocalized in the AVC and OFT in the endocardium, (Fig. 2.8C-E). Furthermore, β-gal from the *NFATc1-nuc-LacZ* BAC transgene identifies a cardiac subpopulation of endothelium that expresses the vascular marker VE-cadherin, which also does not overlap with myocardium as identified by cardiac troponin T (cTnT) (Fig. 2.8B,F-H).

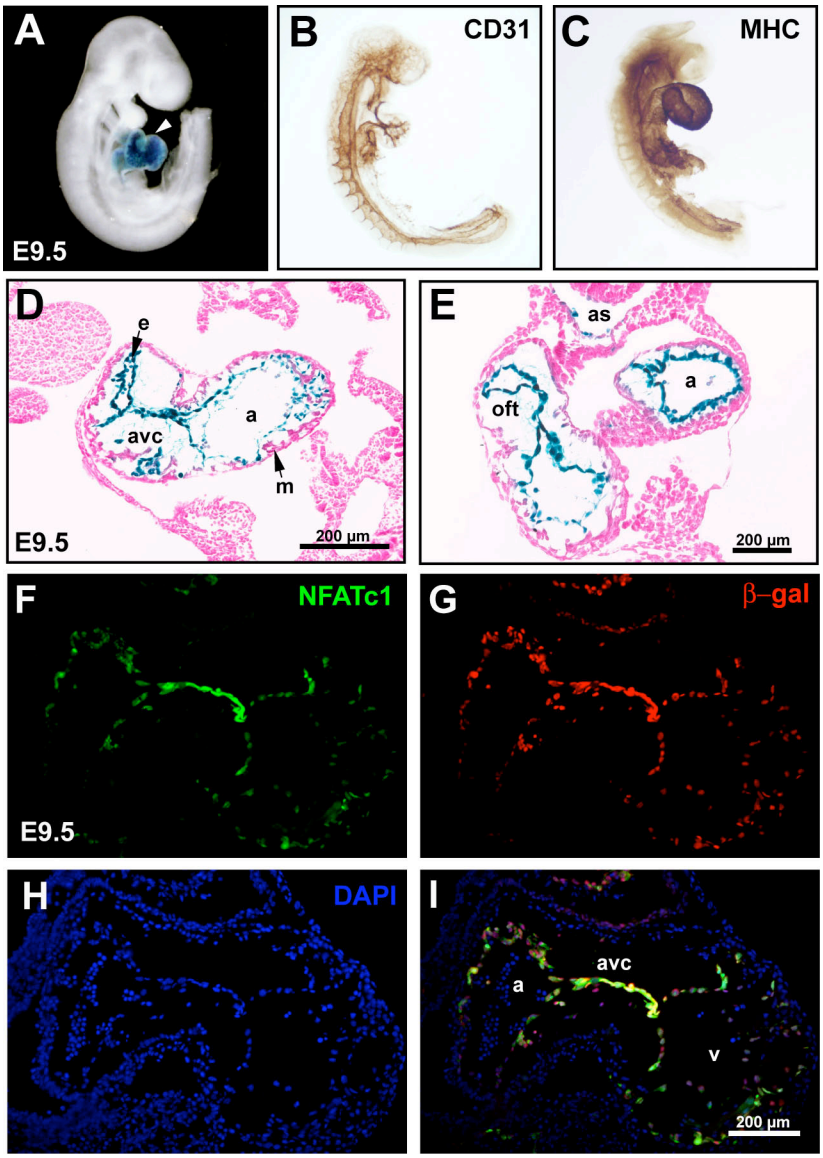

Figure 2.7. ***NFATc1-nuc-LacZ BAC transgenic expression in the endocardium of the E9.5 looped heart*****. A.** E9.5 whole mount X-gal stained transgenic embryo **B.** Whole mount immunohistochemistry for CD31/Pecam-1 labeling all embryonic endothelium **C.** Whole mount immunohistochemistry for cardiac MHC with the MF20 antibody **D,E.** Sagital and frontal sections of E9.5 *NFATc1-nuc-LacZ* embryos with β-gal expression in all endocardium of the looped heart tube, but in no other embryonic endothelium. **F-I.** Immunofluorescence of an E9.5 *NFATc1-nuc-LacZ* heart demonstrating cellular co-localization of endogenous endocardial NFATc1 (**F**, green) and β-gal (**G**, red). Nuclei were detected with DAPI (**H**, blue).

Myocardium, m; endocardium, e; outflow tract, oft; common ventricle, v; atrioventricular canal, avc; aortic sac, as; atria, a

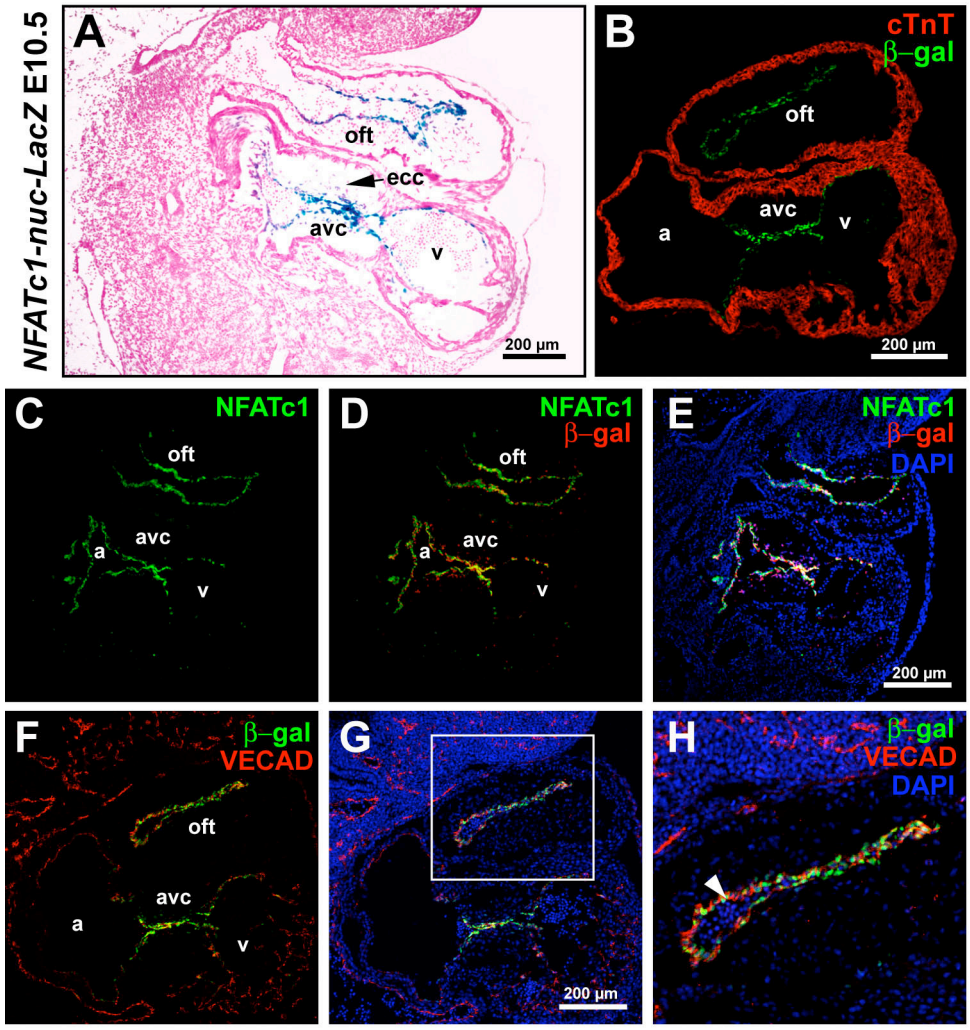

Figure 2.8. ***NFATc1-nuc-LacZ BAC transgenic expression in relation to other cardiovascular populations during embryogenesis.*** **A.** At E10.5, β-gal was retained in the valvular endocardium, but largely absent in the atrial and ventricular endocardium. **B.** Dual immunofluorescence for β-gal (green) and cTnT (red) marking non-overlapping endocardium and cardiomyocytes at E10.5 **C-E.** Immunofluorescence of an E10.5 *NFATc1-nuc-LacZ* heart demonstrates cellular co-localization of endogenous endocardial NFATc1 (**C**, green) and β-gal (**D**, red). Nuclei were detected with DAPI (blue). **F-G.** β-gal+ endocardium (green) at E10.5 identifies a cardiac subpopulation of endothelium distinct from system vasculature marked by VE-cadherin (VECAD, red). Nuclei were detected with DAPI (blue). **H.** Higher magnification image of nuclear-localized β-gal (white arrowhead) of the OFT endocardium.

Outflow tract, oft; common ventricle, v; atrioventricular canal, avc; aortic sac, as; atria, a; endocardial cushion, ecc

The process of restriction first observed at E10.5 was complete by E11.5, with expression entirely localized to the cushion endocardium in accordance with the role of NFATc1 in valve remodeling (Fig. 2.9A-D) (Chang *et al.*, 2004; Lange and Yutzey, 2006; Zhou *et al.*, 2005). With the onset of chamber septation, the resulting partition of the AVC and OFT forms four valve cushions that will comprise the mitral, tricuspid AV valves, and the aortic and pulmonary semilunar valves. β-gal was expressed on all four valve cushions formed with the onset of chamber septation at E12.5 (Fig. 2.9E,F). During valve remodeling and elongation, β-gal was retained in this endocardial subpopulation, and was undetectable by E16.5 (data not shown). Although expression from the *NFATc1-nuc-LacZ* BAC transgene is specific to endocardial cells during early development, later in development other populations are observed to activate transcription of β-gal (Fig. 2.10A-D). In the limb buds, beginning with the forelimb at E10.5 then the hindlimb at E11.5, LacZ expression is upregulated in the cartilaginous condensations of endochondral ossification (Fig. 2.10E-G). This same process is evident in cartilaginous condensations of prevertebral bodies and ribs (Fig. 2.10H). Immunoperoxidase staining of comparable sections of prevertebral bodies demonstrates NFATc1 expression in the same population at this stage of development (Fig. 2.10I). In addition, expression is also apparent in developing whisker follicles at E13.5 (Fig. 2.10J,K). These dynamic developmental expression patterns in the developing heart, and in other embryonic populations, confirm that the *NFATc1-nuc-LacZ* BAC transgene faithfully recapitulates endogenous NFATc1 expression.

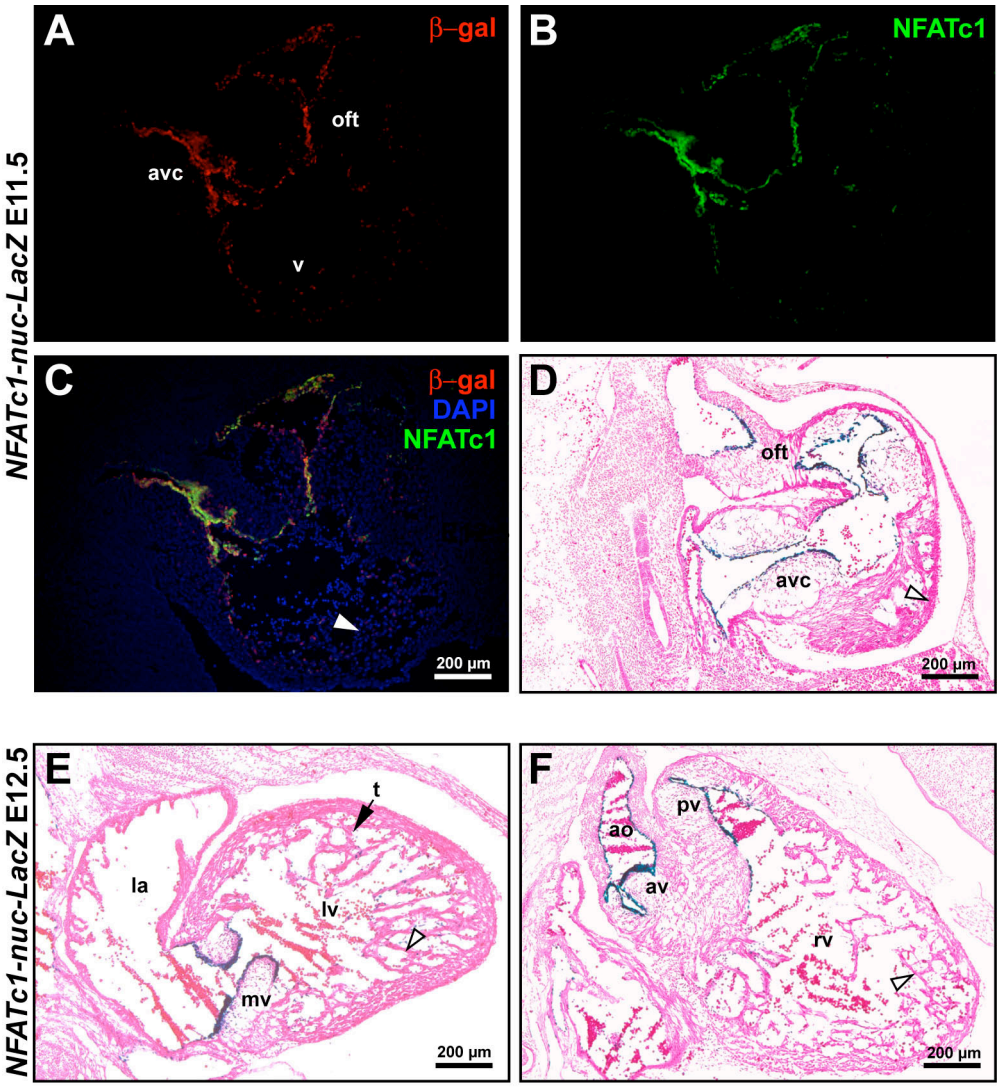

Figure 2.9. ***Expression of the NFATc1-nuc-LacZ BAC transgene during valve remodeling and septation.*** **A-C.** Immunofluorescence at E11.5 shows cellular co-localization of endogenous NFATc1 (**A**, green) and β-gal (**B**, red) at the valve cushion endocardium. Nuclei were detected with DAPI (**C**, blue). **D.** By E11.5, β-gal is restricted to endocardium overlying the valve cushions, with no expression in endocardial cells having undergone EMT to populate the cushions. Expression is absent in the atrial and ventricular endocardium (white arrowhead). **E-F**. After septation, β-gal expression is only evident in the endocardium of remodeling valves, and in no other endocardial cells (white arrowheads).

Outflow tract, oft; common ventricle, v; endocardial cushions, ecc; left atria, la; left ventricle, lv; mitral valve, mv; aortic valve, av; aorta, ao; pulmonary valve, pv; right ventricle, rv; trabeculea, t.

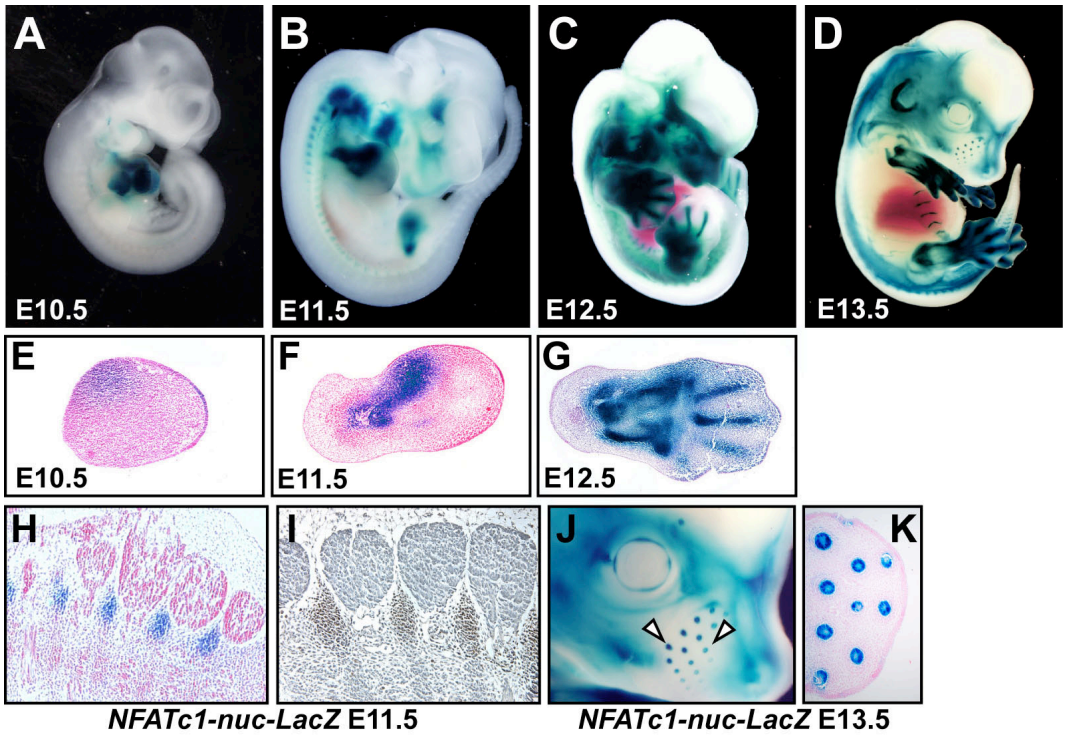

Figure 2.10. ***NFATc1-nuc-LacZ BAC transgenic expression in other cell populations during development.*** **(A-D)** Whole mount X-gal stained *NFATc1-nuc-LacZ* BAC transgenic embryos at E10.5 (**A**), E11.5 **(B)**, E12.5 **(C**), and E13.5 **(D)** demonstrating the onset of *NFATc1*'s complex developmental expression pattern during mid gestation. (**E-G**) X-gal stained cryosections documenting β-gal expression in cartilaginous condensations during the initial stages of forelimb development at E10.5 **(E)**, E11.5 **(F)**, and E12.5 **(G)**. **H,I**. Comparable sections of prevertebral bodies at E11.5 showing β-gal expression **(H)** or NFATc1 expression revealed by immunoperoxidase staining **(I)**. **J,K.** β-gal expression in developing whisker follicle epithelium (white arrowheads) at E13.5.

Discussion

Using BAC recombineering for targeted homologous recombination in bacteria, we generated a 220 kb transgene that allowed for maximum utilization of critical genomic regulatory elements of the *NFATc1* genomic locus to govern *LacZ* expression. Through *in vitro* differentiation of eEPCs, in addition to transient and stable mouse transgenesis, we confirmed this BAC contained the cis-regulatory domains required for activating transcription in endocardial precursors as they emerged from the cardiac mesoderm. Further analysis demonstrated that β-gal expression from the *NFATc1-nuc-LacZ* BAC transgene faithfully recapitulated endogenous *NFATc1* expression in the heart and other cell populations during development. With the ability to distinguish endocardium from other endothelium, this *NFATc1-nuc-LacZ* BAC transgene represents a novel and invaluable tool to monitor endocardiogenesis during early embryogenesis. In addition, these findings provide additional support for our hypothesis that the endocardium is a distinct cardiac subpopulation of endothelium with a unique molecular identity.

Since the discovery of its role in regulating valve development, NFATc1 has remained one of the few specific markers of this endothelial subpopulation. The studies presented here build off our previous promoter analysis of NFATc1, which characterized a transcriptional enhancer responsible for autoregulation of *NFATc1* in endocardial cushions (Zhou *et al.*, 2005). The restricted expression pattern exhibited by this enhancer implied that early endocardial expression of NFATc1 is controlled by regulatory elements that are distinctly separate from the one modulating transcription in valvular endocardium. These same analyses indicated that the early endocardial enhancer did not

reside within 25 kb surrounding the P1 promoter and exon 1. Thus BAC recombineering was selected as it represented an efficient means to harness a genes expression pattern without having to define individual regulatory elements. The resulting BAC transgene was advantageous compared to a direct knock-in generated by homologous recombination in ESCs as it would not affect endogenous gene expression and was a discreet unit that could be used for multiple purposes. An additional benefit of the BAC approach was its modularity; the NFATc1 targeting vector, pBSKSa-N5'-nuc-LacZ-Tet^{R}-N3', was constructed so that the different genes of interests could be rapidly inserted and targeted into the *NFATc1* BAC.

The *NFATc1-nuc-LacZ* BAC transgene demarcated differentiating endocardial cells in the anterior lateral plate mesoderm at the earliest stages of cardiac development (Fig 2.5A-C). β-gal+ cells were not observed at earlier stages and could not be detected along the path cardiac progenitors take as they migrate from PS. These observations are insufficient to determine whether the endocardium is derived from a shared progenitor with myocardium, from a distinct population, or even from an outside source that migrates into the cardiac mesoderm. However, these findings indicate that activation of expression from the *NFATc1-nuc-LacZ* BAC transgene coincides with the initial commitment of mesodermal cells to the endocardial lineage. In addition, the *NFATc1-nuc-LacZ* BAC transgene drives expression in all endocardial cells from both the PHF and SHF. At E8.5 in the linear heart the transgene identifies the entire endocardium, which is entirely derived from the PHF (Fig. 2.6). Yet at E9.5, β-gal expression is also present in the endocardium of the OFT, which is SHF-derived (Fig. 2.7). Whether extensive molecular differences exists between endocardium derived from the PHF

verses that derived from the SHF remains unknown. Collectively, these observations demonstrate the strength of this transgene to identify all endocardial cells during early cardiac morphogenesis.

In addition to identifying endocardial cells during early cardiogenesis, the *NFATc1-nuc-LacZ* BAC transgene documents *NFATc1* in other populations during development. The function of NFATc1 as an early transcriptional activator of chondrogenesis, as well as its role in the regulation of bone mass by controlling osteoclast differentiation, has been well established (Koga *et al.*, 2005; Ranger *et al.*, 2000; Winslow *et al.*, 2006). By mid-gestation (E11.5-13.5), β-gal is detected in cartilaginous condensations of limbs, prevertebral bodies, and ribs. Furthermore, β-gal expression is also apparent in developing whisker follicles at E13.5. Horsley et al. demonstrated that NFATc1 is responsible for governing hair follicle stem cell renewal (Horsley *et al.*, 2008). NFATc1, activated by BMP signaling, represses CDK4 to maintain stem cell quiescence, but under signals that activated hair follicle growth, NFATc1 is downregulated, and CDK4 repression is relieved to allow proliferation and differentiation. Our observations suggest NFATc1 might function as an early marker of follicle development, but a more detailed analysis of this expression pattern is needed.

Driven by our observations that eEPCs can be induced to form endocardial cells, we initially explored eEPC differentiation as an *in vitro* model of endocardiogenesis. However, there were certain caveats that reduced its viability as an appropriate system for our purposes. Only a small fraction of cells differentiate into endothelium, and no myocardial transcripts are upregulated upon differentiation, making it less then ideal to study endocardial-myocardial interactions. Also, introduction of reporter transgenes to

monitor endocardiogenesis would be inefficient, as it is difficult to obtain a clonal population from these cells. Chapter III details the characterization of *in vitro* differentiation of ESCs as a model of endocardiogenesis and endocardial-myocardial interactions that is not limited by these particular obstacles.

CHAPTER III

ENDOCARDIAL AND MYOCARDIAL SPECIFICATION ARE TEMPORALLY AND SPATIALLY COORDINATED IN EMBRYONIC STEM CELL DIFFERENTIATION

Introduction

Examination of cardiac cell lineage specification and early differentiation during murine embryogenesis has been complicated by limitations on the amount of tissue that can be obtained, as well as difficulties in accessibility. Since the discovery that embryonic stem cells (ESCs) isolated from the ICM of blastocyst-stage embryos can be induced to form all three germ cell layers and their derivatives, ESC differentiation has come to represent a faithful *in vitro* model of early embryonic development. Given the potential of ESCs to generate a broad spectrum of cell lineages in a pattern mirroring embryonic development, the system has provided new avenues in which to study lineage induction and development. In contrast to embryos *in utero*, differentiating ESCs can be easily manipulated either genetically or through modification of culture conditions. In addition, cell populations at different stages of development can be harvested for biochemical and functional assays in large quantities with proper markers for selection and isolation.

ESC differentiation has been particularly useful in elucidating the mechanisms involved in specification of the mesodermal-derived populations that comprise the cardiovascular system, including endothelium, hematopoietic cells, and cardiomyocytes (Keller, 2005). Through ESC differentiation, early processes and inductive signals required for hematopoietic and vascular lineage differentiation have been defined, and *in*

vitro analysis of targeted gene disruptions have clarified the transcriptional regulation of lineage specification. Modeling hematopoietic and vascular specification in ESC differentiation has also led to the characterization of the long hypothesized hemangioblast, a common mesodermal precursor to both hematopoietic and vascular populations (Choi *et al.*, 1998; Nishikawa *et al.*, 1998). Similarly, cardiomyocyte differentiation has been well documented in ESC differentiation, and as described in Chapter I, significant effort has been expended to devise how to enhance myocardial specification from stem cells in the hope of utilizing them as a therapeutic tool to treat heart tissue damaged by myocardial infarction and other ailments. Although these studies have significantly extended our understanding of cardiac lineage specification, they have either drawn no distinction between endocardium and endothelium or only obliquely addressed endocardiogenesis. This is due in part to the aforementioned absence of markers of endocardial cells, but also the fact that endocardiogenesis has not yet been defined in ESC differentiation.

As ESC differentiation has been widely used to study mesodermal lineage determination and cardiovascular cell differentiation, we investigated its ability to model endocardial differentiation. In this *in vitro* system, we documented that endocardial differentiation, as identified by NFATc1 expression, occurred at the same time as other cardiovascular cell types. In addition, we demonstrate that endocardial cells only appear at sites of myocardial cell differentiation, a finding that was validated using an ESC line derived from *NFATc1-nuc-LacZ* BAC transgenic embryos. Taken together, our findings document the close temporal-spatial relationship seen between endocardium and myocardium *in vivo* is reproduced *in vitro*.

Experimental Procedures

Mouse embryonic fibroblast culture

Neomycin resistant primary mouse embryonic fibroblasts (PMEF-N; Specialty Media/Millipore) were obtained at passage 3 and plated on 1000-mm Poly-D-Lysine treated dishes coated with 0.1% gelatin in 1x PBS for 30 minutes at RT. Cells were cultured in DMEM supplemented with 10% FBS (HyClone), 2 mM L-glutamine, 100 U/ml Penicillin/Streptomycin, 1 mM sodium pyruvate, 100 μM non-essential amino acids, and 100 μM β-mercaptoethanol at 37˚C, 5% CO_2. From a single vial, cells were plated to 3 plates, passaged the next day 1:4, then passaged two days later 1:3; from one vial, 36 100-mm dished could be generated. Cells were frozen at passage 5-6, one plate to one cryovial, by mixing resuspended cells in MEF media 1:1 with 2x Freezing media (60% MEF media, 20% FBS, 20% DMSO). Cryovials were placed in an isopropanol freezing container and stored at -80˚C for 1-3 days before transfer to liquid nitrogen. For growth cessation before use of PMEFs as feeders for ESC culture, confluent plates were exposed to 6-7 minutes (10-12 Gyr) of Cesium-137 irradiation. After irradiation, MEF media was changed and plates were replaced at 37˚C to be used within 2 weeks.

Embryonic stem cell (ESC) culture

Murine ESCs (R1) were cultured on irradiated PMEFS in DMEM supplemented with 15% FBS (ESC qualified; HyClone), 2 mM L-glutamine, 100 U/ml Penicillin/ Streptomycin, 1 mM sodium pyruvate, 100 μM non-essential amino acids, 1000 U/ml recombinant leukemia inhibitory factor (ESGRO, Millipore) and 100 μM β-

mercaptoethanol at 37˚C, 5% CO_2. ESC media was changed every day, with cells passaged every two days by 0.25% Trypsin-EDTA treatment for 2-4 minutes at 37˚C after a wash with PBS. Trypsin was inactivated by resuspension in ESC media, and the cell number counted with a hematocytometer. $2x10^6$ cells were replated onto fresh 100-mm dishes of irradiated PMEFS, an approximate dilution of 1:12. ESC were frozen at a density of $5x10^6$ cells by mixing resuspended cells in ESC media 1:1 with 2x Freezing media (60% ESC media, 20% FBS, 20% DMSO). Cryovials were placed in an isopropanol freezing container and stored at -80˚C for 1-3 days before transfer to liquid nitrogen. For plating of frozen stocks, cryovials were incubated in a 37˚C water bath and washed in pre-warmed ESC media, pelleted by spinning at 500xg for 5 minutes then resuspending in ESC for plating one vial to one 100-mm dish of irradiated PMEFs.

ESC differentiation

$1-3x10^6$ ESCs were transferred to 100-mm gelatinized plates 1-2 days prior to the initiation of differentiation in order to decrease PMEF contamination and maintained in ESC media with LIF. ESCs were washed with PBS prior to trypsinization to yield a single cell suspension that was then quenched by serum-contain media. ESC-derived EBs were formed by one of two methods, either by the hanging drop method or in suspension. To generate EBs by hanging drop, cells were brought to a density of $2.5x10^4$ cells per mL in ESC differentiation media (DM) consisting of Iscove's Modified Dulbecco's Medium (IMDM) supplemented with 15% FBS, 2 mM L-glutamine, 100 U/ml Penicillin/Streptomycin, 200 μg/m transferrin (Roche), 0.5 mM L-ascorbic acid (Sigma), and 4.5x10–4 M monothioglceryol. 20 μl drops (~500 cells) were deposited in

12-14 rows of 8 with an 8-well multichannel pipet onto 100x100-mm square Petri dishes (Thermo Fisher; 0875711A), and then gently inverted and returned to the at 37˚C, 5% CO_2 tissue culture incubator. After two days, plates were flooded with PBS, rocked back and forth to centralize the EBs to be picked up with a sterile pipet and transferred to a 50 ml conical. EBs were allowed to settle, the remaining PBS/DM was aspirated, and new DM was added to the EBs. EBs were transferred to 60-mm Petri dishes (VWR; 25384-328), approximately 3 hanging drop plates to 1 60-mm dish.

For EBs formed by suspension, ESCs were again diluted to a density of $2.5x10^4$ cells per ml in DM, and 5 ml (~ $1.25x10^5$ cells) was transferred to 60-mm Petri dishes (VWR). The use of this particular 60-mm non-tissue culture dishes from VWR was critical as EBs either attached to the bottom of the dishes (i.e. Fisher) or aggregated at the center, as occurred with Ultra-low attachment plates (Corning). Media was changed after 2 days in suspension. For both hanging drops and suspended EBs, after 1-2 days of further differentiation (3-4 days total), EBs were transferred to tissue culture plates for attachment; EBs collected for RNA, β-gal staining, or flow cytometry were deposited on 6 or 24-well gelatinized dishes, while EBs for immunofluorescence were deposited on Lab Tek II 4-well glass chamber slides (Nunc/Thermo Fisher). After plating, the media on attached EBs was changed every two days.

NFATc1-nuc-LacZ ESC derivation

ESC lines from *NFATc1-nuc-LacZ* BAC transgenic mice were derived from E3.5 blastocyst-stage embryos plated on irradiated passage 2-3 freshly isolated MEF feeders in RESGRO complete ES medium (Millipore) plus 50 μM MEK inhibitor (PD98059, Cell

Signaling Technologies) (Schoonjans *et al.*, 2003). Cultured blastocysts were not disturbed for 3-4 days to allow attachment, after which media was changed daily. After 5-6 days in culture, the inner cell mass outgrowth was selectively removed from the trophectoderm with a 20 µl pipet tip, dispersed with 0.25% Trypsin-EDTA and replated. Once colonies were visible, ESCs were transitioned to ESC media and expanded.

To prepare fresh MEFs, E13.5 embryos were dissected in cold PBS with 100 U/ml Penicillin/Streptomycin. The head and internal organs were removed and the remaining carcass was minced. Tissue was placed into a 50 ml conical, washed with PBS, allowing the tissue to settle not spun. PBS was aspirated and 0.25% Trypsin-EDTA with DNAse was added to digest tissue for 10 minutes at 37˚C before being passed through an 18 gauge needle 10 times. Cells were spun down and replated on gelatinized 100-mm tissue cultures dishes in MEF media and allowed to grow.

Generation of stable BAC transgene ESC lines

An NFATc1 BAC driving the red fluorescent protein mCherry was constructed as detailed in Chapter II. For selection purposes, a dual neomycin/ kanamycin cassette under the control of the mammalian *PGK* promoter and bacterial *Em7* promoter (*PGK-NEO*) was excised from the recombineering plasmid PL452 with *Nhe*I/*BamH*I. This cassette was inserted by blunt ligation between the two 500 bp homology arms of pLoxPOUTZeo after removal of the zeocin cassette with *Sal*I. This NEO targeting vector was electroporated into heat induced EL250 containing the *NFATc1-mCherry* or the NF*ATc1-nuc-LacZ* construct without the loxP modifications described in Chapter II. Recombined

BACs were selected with CAM and kanamcyin (KAN) and confirmed by *Not*I digest run O/N with PFGE.

For electroporation into ESCs, BAC DNA was prepared with the PsiClone Big BAC DNA kit (Princeton Separations) according to the manufacturer's protocol, and resuspended into microinjection buffer, stored at 4˚C to be used with 2 days. Low passaged wild type R1 were thawed and passaged two days prior to electroporation. The morning before electroporation, ESCs were fed with fresh media. To prepare cells for electroporation, ESCs were washed with PBS, trypinized, then resuspended in 10 ml to be re-plated on a fresh gelatinized 100-mm plate and incubated at 37˚C for to allow PMEFs to reattach. After 15-30 minutes, the media and the ESC still in suspension were pulled off, washed twice in ice-cold PBS by centrifugation at 500xg for 5 minutes, then counted. Approximately 30 μg of BAC DNA was electroporated into $5x10^6$ ESCs in a 0.4 cm cuvette at 250 V, 500 μF. Each electroporation was plated onto two 10 cm plates of PMEF-N. After two days, selection with 500 μg/ml Geneticin (Invitrogen) began, with the media changed every two days. Colonies were picked after 10-14 days of selection, and tested for expression.

Beta-galactosidase staining

For whole-mount β-gal staining, EBs were washed in cold PBS and fixed in 0.2% glutaraldehyde, 2 mM $MgCl_2$, and 5 mM EGTA for 6 minutes. EBs were washed twice with X-gal wash buffer consisting of 2 mM $MgCl_2$, 0.02% NP40 in PBS before incubation in a X-gal staining buffer of 1 mg/ml X-Gal, 5 mM potassium ferro/ ferricyanate, 2 mM $MgCl_2$, 0.02% NP40, 0.01% sodium deoxycholate in PBS at 37°C for

2-6 hours to prevent overstaining. EBs were cleared using a glycerol gradient in PBS and stored at 4°C.

For dual β-Gal/immunoperoxidase staining, cells first stained with X-gal as described above. After 3 washes with PBS, cells were treated with 3% H_2O_2, followed by Avidin/Biotin blocking. EBs were blocked with 10% goat serum in PBS (Jackson Labs) for 1 hour at RT. then incubated with primary antibody O/N in 10% goat serum in PBS. The following day, EBs were washed and treated with and HRP-conjugated secondary antibodies (BD Pharmingen; 1:100), before detection with DAB (Vector labs). Samples were washed and perserved in Crystal/Mount (Biomeda).

Immunofluorescence

For whole-mount immunofluorescent staining, EBs were washed in PBS and fixed in ice cold Methanol:Acetone (1:1) for 6 minutes on ice, then washed again. EBs were blocked with staining buffer consisting of 3% FBS and 0.1% sodium azide in PBS prior to incubation with primary antibodies diluted in staining buffer O/N at 4°C. For immunofluorescent staining of EBs from *NFATc1-mCherry/Venus-yfp* ESCs, EBs were fixed in 10% NBF on ice for 15 minutes, washed twice with PBS, then blocked in staining buffer consisting of 3% FBS and 0.1% sodium azide in PBS supplemented with 0.5% Triton-X. Species or isotype appropriate Alexa 350, Alexa 488, Alexa 555 and Alexa 647-conjugated secondary antibodies (Molecular Probes, 1:200) were added for 1 hour at 37˚C for signal detection. Samples were washed and mounted with Vectashield with or without DAPI (Vector Labs). Images were acquired using a Nikon Elipse E800 epifluorescence microscope or Zeiss Upright LSM510 Confocal Microscope.

Antibodies

NFATc1 (mouse 7A6, BD Pharmingen, 1:200)

Sacromeric myosin heavy chain (MHC; mouse MF20, DSHB, 1 μg/ml)

Cardiac troponin T (cTnT; mouse CT3, DSHB, 1 μg/ml)

CD31/Pecam-1 (rat MEC13.3, BD Pharmingen, 1:500)

β-Gal (chick, Abcam, 1:1,000 or rabbit, Cappel, 1:5,000)

Flow cytometry

EBs were dissociated using cell disassociation buffer (Gibco) for 30 minutes at 37˚C, resuspended in ice cold FACS buffer prepared from Hanks Buffered Salt Solution (HBSS) with 2% FBS (HyClone), and 25 mM HEPES, and filtered through a 42 micron sieve to produce a single cell suspension. Cells were resuspended $1x10^6$ per 100 μl and treated with an antibody against CD16/CD32 for 10 minutes (mouse, Ebioscence, 1 μg/ml) to block nonspecific binding prior to a 45-minute incubation at 4˚C with an Allophycocyanin-conjugated (APC) antibody against CD31/Pecam-1 (rat MEC13.3, BD Pharmingen, 0.5 μg/ml). Cells were analyzed on a 5-laser BD LSRII (Becton Dickinson).

RNA isolation

Total RNA from approximately $1x10^6$ cells or (surface area 35 mm) was extracted using 1 ml Trizol reagent (Invitrogen) following the manufacturers instructions. RNA pellets were resupended in 50 μl of nuclease-free H_2O and then treated with Turbo DNA-free (Applied Biosystems) to remove residual genomic DNA. An additional purification step was performed with the RNeasy Miniprep kit (Qiagen) following the RNA cleanup

protocol. RNA was collected from RNeasy columns in 20-40 µl of nuclease-free H_2O depending on the size of the pellet. RNA concentration and purity were analyzed on a NanoDrop spectrophotometer (Thermo Scientific). Samples with a 260/280 ratio > 1.8 (1.9-2.1 preferrably) and 260/230 ratio > 1.5 were deemed high enough quality for qRT-PCR. 2 µg of total RNA was reverse-transcribed into cDNA using the High Capacity cDNA Reverse Transcription kit (Applied Biosystems) in 20 µl as per manufacturers instructions, then resuspended into 80 µl to yield a final conentraton of 50 ng/µl.

Quantitative real-time PCR (qRT-PCR)

All qRT-PCR was performed using a Light Cycler (Roche) with the Light Cycler DNA FastStart SYBR Green I Kit, 0.5 µM of each primer, and 100 ng cDNA. Gene specific primer sets used for these experiments are listed as follows: *Brachyury*: 5' ACA GAT CAT GTT AAA CTC CTT GCA T 3', 5' TAC ATC TTT GTG GTC GTT TCT TTC T 3'; *NFATc1*: 5' GGT GGC CTC GAA CCC TAT C 3', 5' TCA GTC TTT GCT TCC ATC TCC C 3'; *βMHC*: 5' AGC CGC GCC AGT ACT TCA TAG GTG 3' , 5' TGT TCT TTT CCA GCC AGC CCA TAA 3'; *Nkx2.5*: 5' ACC TTT CTC CGA TCC ATC CCA CTT 3', 5' GCG TTA GCG CAC TCA CTT TAA TGG 3'; *Flk1*: 5' GGT TCT CTG TCA AGT GGC GGT AAA 3', 5' AGC ACA CAG GCA GAA ACC AGT AGA 3'; *VECAD*: 5' AAC TCA CCC TCC TTG TGG AAT CCT 3', 5' ACA TCT CAT GCA CCA GGG TGA CTA 3'; *CD31/Pecam-1*: 5' ATC CGG AAG GTC GAC CCT AAT CTC AT 3'; 5' ATA CCC AAC ATG AAC AAG GCA GCG 3'; *HPRT*: 5' AGT CAA CGG GGG ACA TAA AA 3' 5' TGC ATT GTT TTA CCA GTG TCA A 3'; *GAPDH*: 5' CAC TGG CAT GGC CTT CCG TG 3', 5' AGG AAA TGA GCT TGA

CAAAG 3'. The specificity of the amplified product was evaluated using the melting curve analysis and a no template control reaction. Each sample was done in triplicate and relative expression was calculated as $\Delta^{2\text{-ct}}$ with *HPRT* as the internal control.

Results

Endocardial cells differentiate in a similar temporal pattern to other mesodermal-derived cardiovascular cell populations

To confirm the presence of endocardial cells in ESC differentiation, and to define the particular window when they first emerge, RNA was obtained from undifferentiated ESCs and from EBs at 2, 4, 6, 8, 10, 12 days of differentiation in order to characterize gene transcripts associated with mesoderm and mesodermal-derived cell populations. In a preliminary study, *NFATc1*, as a specific endocardial transcript, was compared to *Flk1*, a marker of mesoderm early vascular development, and *VE-cadherin*, expressed by mature endothelium (Fig. 3.1A). *NFATc1* was first detected at differentiation day 6 (D6), peaked at D8-10, with its levels declining by D12. This pattern was similar to those seen with *Flk1* and *VE-cadherin*, suggesting that endocardial endothelium was present in EBs and arose during the same time period as other vasculature.

To further investigate the temporal pattern of endocardial differentiation in relation to mesodermal specification and the differentiation of other components of the cardiovascular system, particularly myocardium, molecular expression analyses were performed by quantitative real-time PCR (qRT-PCR). Supporting our earlier findings, *NFATc1* was absent in ESC colonies and in EBs during the first few days of differentiation. *NFATc1* expression was first observed at D6, reaching its highest

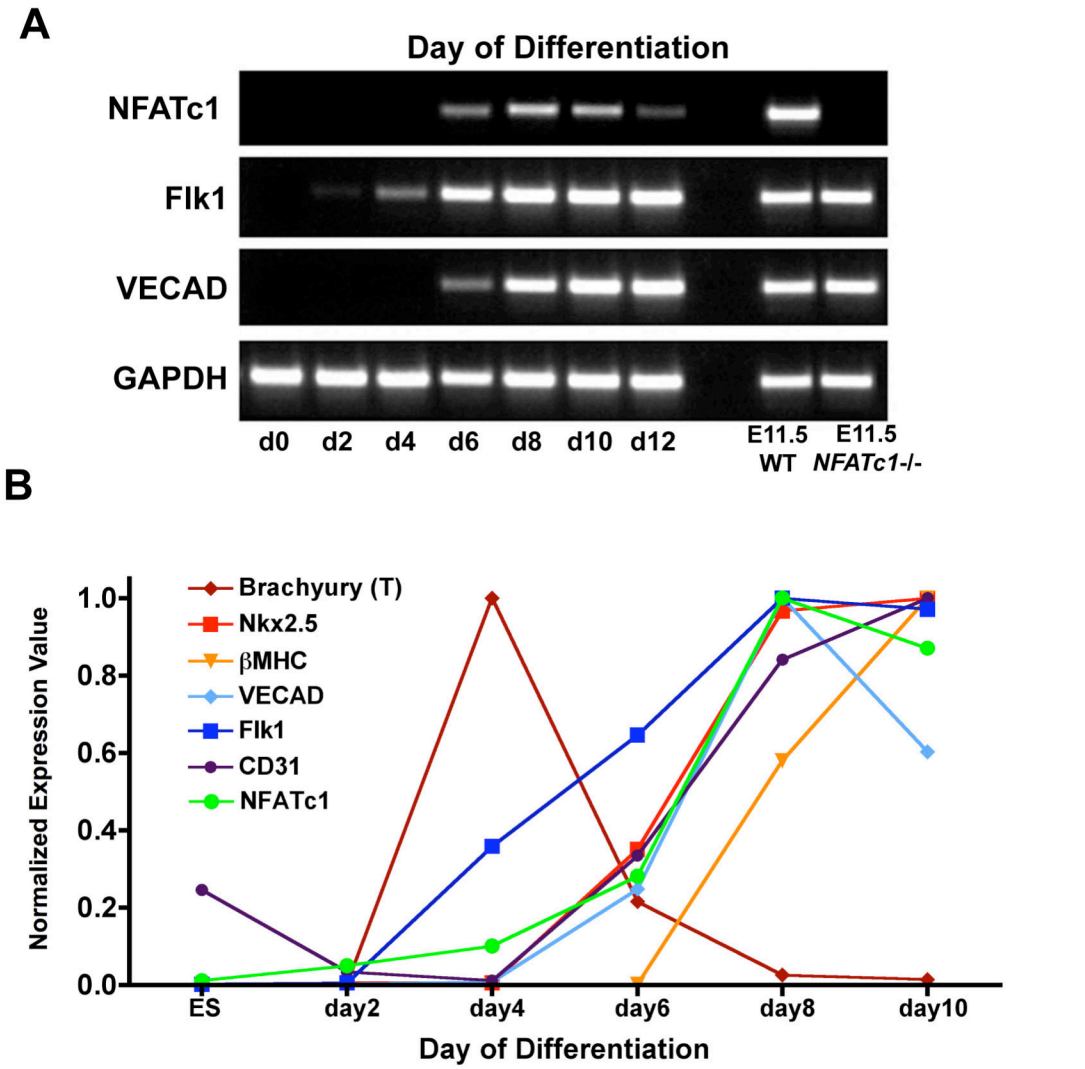

Figure 3.1. ***Temporal analysis of endocardial, myocardial, and vascular transcripts during ESCs differentiation*****. A.** RT-PCR documenting the temporal expression pattern of *NFATc1* compared to *Flk1*, a marker of mesoderm early vascular development, and *VE-cadherin*, expressed by mature endothelium in undifferentiated ESCs and EBs at 2, 4, 6, 8, 10, 12 days of differentiation. *NFATc1* is first observed at differentiation day 6 (D6), and peaks at D8-10, similar to *Flk1* and *VE-cadherin*. *GAPDH* was used as loading control. **B.** Normalized expression values from qRT-PCR analysis of the temporal expression of genes associated with mesoderm (*brachyury, Flk1*) and mesodermal derivatives, specifically cardiac (*Nkx2.5, βMHC*) and vascular lineages (*VE-cadherin, CD31, Flk1*), compared to endocardial *NFATc1* during ESC differentiation.

expression at D8-D10 (Fig. 3.1B). In contrast, *brachyury* (*T*), a transient marker of nascent mesoderm, was robustly expressed at D4, but sharply reduced by D6 (Wilson *et al.*, 1993; Yamada *et al.*, 1994). This indicates *NFATc1* expression, and by association endocardial differentiation, occurs subsequent to mesodermal specification. As endocardial differentiation is closely tied to myocardial differentiation in both time and space, we examined how the temporal kinetics of *NFATc1* expression in differentiating ESCs related to the genes expressed by cardiomyocytes (Fig. 3.1B). *Nkx2.5*, an early myocardial transcript that in vivo is observed in the PHF at the crescent stage was upregulated at D6 (Lints *et al.*, 1993). *βMHC* encoding a ventricular myocardial specific isoform of myosin heavy chain is first expressed at D8, coinciding with the appearance of contracting foci within EBs (Mahdavi *et al.*, 1987). In addition to cardiomyocyte transcripts, the pattern of *NFATc1* expression coincided with the appearance of several vascular markers, as had been indicated by our preliminary studies. *Flk1* expression at D4 again preceded *NFATc1*, consistent with its description as a marker of extraembryonic and embryonic mesoderm, as well as later vascular endothelial populations (Ema *et al.*, 2006). *NFATc1* expression was notably similar to *VE-cadherin*, and the late phase of *CD31/Pecam-1*, which is transiently expressed in the blastocyst ICM and therefore undifferentiated ESC colonies (Baldwin *et al.*, 1994; Lampugnani *et al.*, 1992; Robson *et al.*, 2001). These findings demonstrate differentiation of cardiovascular cell populations in ESC-derive EBs occur during the same temporally window, consistent with its expression during cardiogenesis *in vivo*.

To corroborate the qRT-PCR findings and establish the existence of NFATc1+ cells in ESC differentiation cultures when *NFATc1* message is detected, EBs were

immunostained with a monoclonal antibody raised against NFATc1. NFATc1+ cells were visualized with immunofluorescence at D8, where it was present in a subset of cells predominantly in its nuclear localized, transcriptionally active form (Fig. 3.2A). Positive cells were largely found in discrete groups and were not dispersed evenly throughout the attached EBs. The majority of these NFATc1+ cells were morphologically similar, consisting of a large nucleus and elongated polar processes (Fig. 3.2A, inset). Though NFATc1 is found exclusively in endocardial endothelium early in development, it is later expressed in numerous other tissues. To determine whether the NFATc1+ cells detected at D8 potentially represented endocardial cells or another cell population, we conducted dual immunofluorescence studies with NFATc1 and the vascular endothelial cell surface marker CD31/Pecam-1. This staining indicated NFATc1+ cells co-expressed the endothelial surface marker CD31/Pecam-1 at D8, thus suggesting these cells possessed an endocardial identity (Fig 3.2B).

Endocardiogenesis is spatially sequestered at sites of myocardial differentiation

While ESC-derived EBs maintain a pattern of sequential lineage progression that faithfully recapitulates development *in vivo*, EBs have generally been considered to lack the spatial complexity normally seen with in embryogenesis. These traditional assessments have been challenged by observations of required interactions between distinct cell populations in differentiating EBs that mirror *in vivo* spatial localization. The most prominent examples involve cardiovascular cell types, where one such study demonstrated contracting cardiomyocytes in EBs are spatially associated with conduction system tissue, as identified by a *minK-LacZ* transgene (White and Claycomb, 2005).

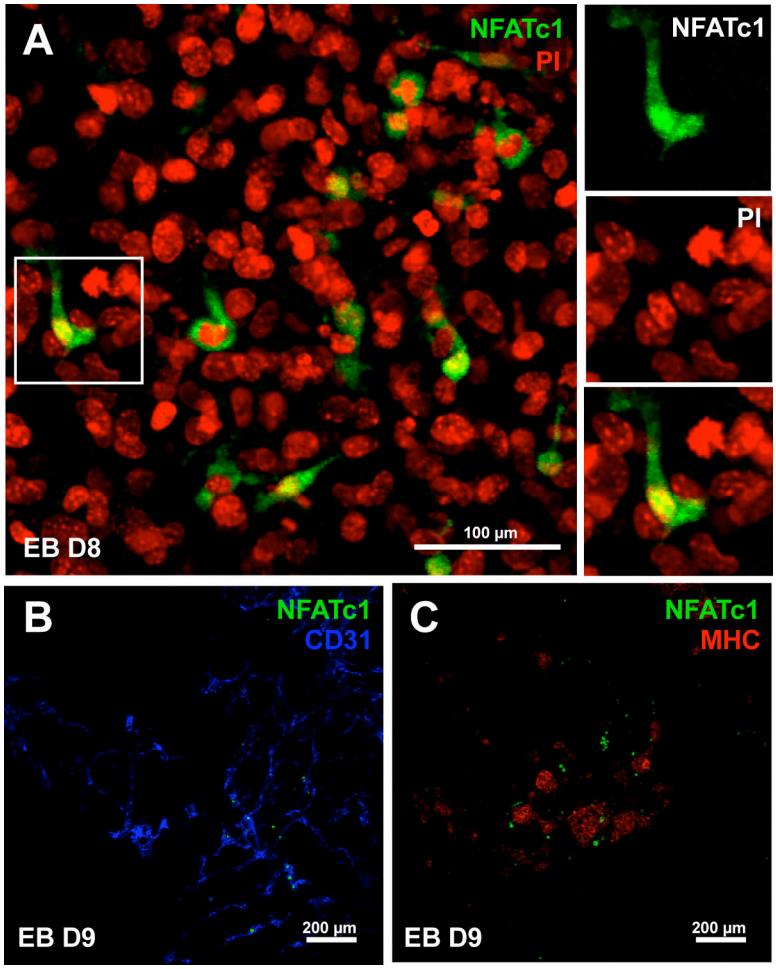

Figure 3.2. ***Identification of NFATc1+ endocardial cells in ESC differentiation cultures.*** **A.** Immunofluorescence of a D8 EB with cells containing nuclear localized NFATc1 (green). Nuclei were detected with PI (red). The inset contains higher magnification images of an NFATc1+ cells with a large nucleus and elongated polar processes. **B.** NFATc1+ cells (green) co-expressed the endothelial surface marker CD31/Pecam-1 (blue) at D9. NFATc1+/ CD31+ cells represent only a subset of the total CD31+ vascular plexus of the EB outgrowth. **C.** NFATc1+ cells (green) were found exclusively localized adjacent to developing cardiomyocyte foci as labeled by MHC (red) in differentiating EBs.

Another study characterized a sinusoid vascular-like network that integrated with hepatocytes to enhance the hepatic function of these layers (Ogawa *et al.*, 2005).

To explore whether spatial relationships between cardiovascular cell populations exist in ESC differentiation, we conducted immunofluorescence studies of EBs at the onset of cardiac differentiation as determined by qRT-PCR. The earliest cardiomyocyte contractions in attached EB cultures can be visually identified at D8-9, thus it was at this point we first investigated the spatial localization of myocardium and endothelium, using antibodies for sarcomeric myosin heavy chain (MHC) and CD31/Pecam-1. Cardiomyocytes at D8 are organized in contiguous groups of cells rather than being dispersed throughout the EB (Fig. 3.3A). These cardiomyocyte foci are completely enveloped by a network of endothelial cells, and rarely are cardiomyocytes not in direct contact with CD31+ cells, though the reverse is not true for endothelium, which forms an extensive plexus even in the absence of cardiomyocytes. This spatial relationship between endothelium and cardiac muscle was even maintained across time and through further growth and development, as at D12 juxtaposed cells could still be observed (Fig. 3.3B). Combined immunofluorescence of MHC, CD31/Pecam-1, and cTnT demonstrates this association is consistent using different cardiomyocyte markers (Fig. 3.3C-F). More intriguing was that the NFATc1+ cells we previously identified were located near cardiomyocyte foci, suggesting that the close proximity endocardium and myocardium shared in the developing embryo is reflected in vitro in differentiating EBs (Fig. 3.2C).

Using antibodies to designate early myocardium (MHC), endothelium (CD31/Pecam-1), and endocardium (NFATc1), we examined EBs from D8-D11 to determine if this spatial relationship between myocardium and endocardium was

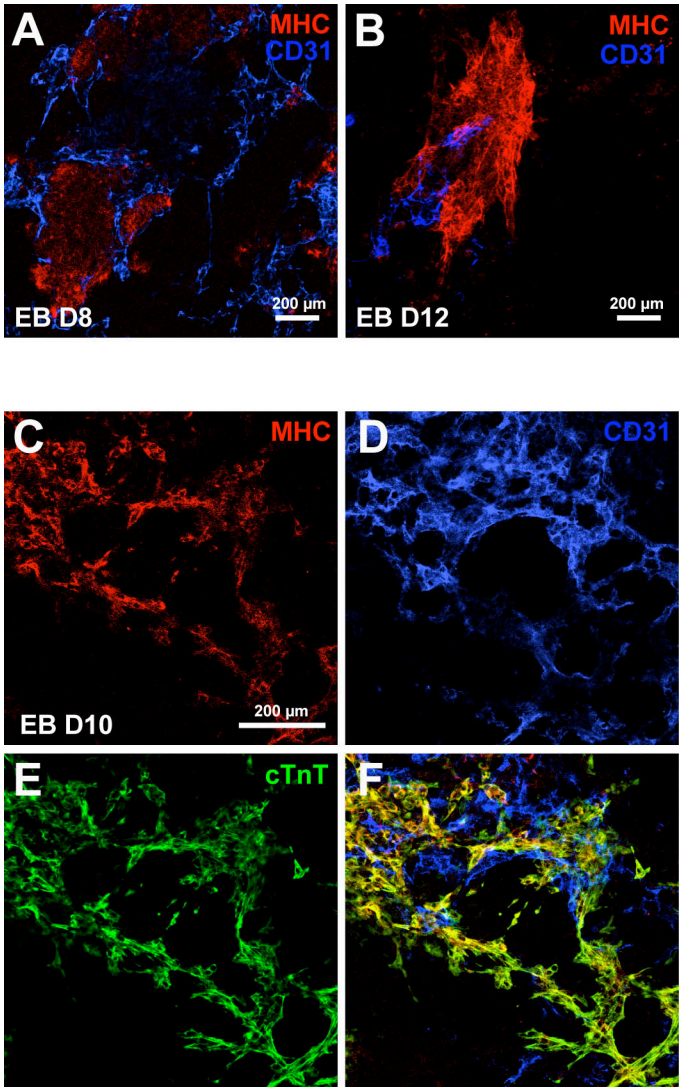

Figure 3.3. ***Spatial dynamics of differentiating cardiovascular cell populations in embryoid bodies.*** **A.** Cardiomyocytes at D8, labeled by MHC (red), are organized in contiguous groups of cells, and are morphologically small and round with disorganized bundles of myofibrils. Cardiomyocyte foci are completely enveloped by a network of CD31/Pecam-1+ endothelial cells (blue). **B.** By D12, ESC-derived cardiomyocytes have become elongated with well-developed myofibrils and sarcomeres. The spatial relationship between endothelium and cardiac muscle observed at earlier developmental time points was maintained at D12. **C-F.** Immunofluorescence of a D10 EB demonstrates that MHC (**C**, red) and cTnT (**E**, green) effectively co-labels all cardiomyocytes (**F**, Yellow) and that the association of myocardial cells with CD31/Pecam-1+ endothelial cells (**D**, blue) is consistent with various cardiomyocyte markers.

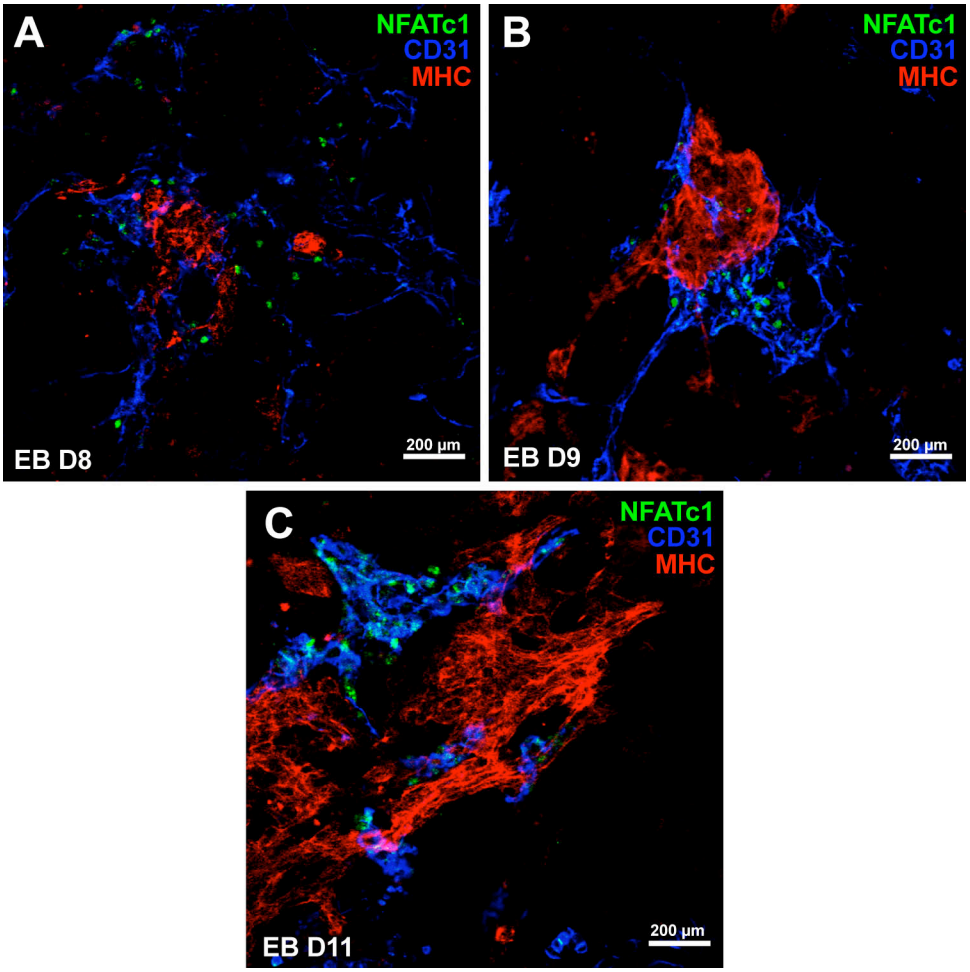

Figure 3.4. ***Spatial and temporal coordination of endocardium and myocardium in embryoid body outgrowths.*** Immunofluorescence images documenting myocardium (MHC, red), endothelium (CD31/Pecam-1, blue) and endocardium (NFATc1, green) in differentiating ESCs at D8, D9, and D11. **A.** At D8, NFATc1+/ CD31+ endocardial cells represent a subset of all endothelial cells restricted to regions adjunct to myocardial differentiation. **B.** At D9, NFATc1+/ CD31+ endocardial cells form a condensed epithelial-like sheet in close association with immature MHC+ cardiomyocytes. **C.** With the maturation of cardiomyocytes into elongated, contracting cells with well-developed myofibrils and sarcomeres at D11, NFATc1+/CD31+ endocardial cells were still detected at sites of myocardial differentiation. NFATc1+/ CD31+ endocardial cells were not detected in regions lacking cardiomyocyte differentiation at any of these time points.

preserved across the temporal window of cardiac differentiation. We observed that at D8 NFATc1+/ CD31+ cells were restricted to regions adjunct to myocardial differentiation, but were not in close association with one another (Fig. 3.4A). The association between endocardium and myocardium was consistent from when MHC was first detectable at D8, through the formation of larger contacting foci at D11. With maturation of cardiomyocytes, NFATc1+/ CD31+ endocardial cells transitioned from a diffuse vascular plexus to a condensed epithelial-like sheet, but always maintained their close association with MHC+ cardiomyocytes (Fig. 3.4B,C). NFATc1+/ CD31+ endocardial cells were not detected in regions lacking cardiomyocyte differentiation. These studies provide evidence to support the assertion that endocardium and myocardium exhibit and spatial coordination in ESC differentiation.

The NFATc1-nuc-LacZ BAC transgene identifies endocardial cells in ESC differentiation

Though antibody staining at the initiation of cardiac differentiation in EBs suggests endocardium and myocardium are coordinated both in time and space, these findings are circumstantial, using the *in vivo* association of these two cardiac subpopulations to explain our *in vitro* observations. Thus, to validate these findings and to further evaluate the temporal and regional differentiation of endocardium *in vitro*, ESC lines were derived from E3.5 blastocysts carrying the *NFATc1-nuc-LacZ* BAC transgene (Fig. 3.5A). E3.5 blastocysts were flushed from the uteri of wild-type FVB/N females breed to male *NFATc1-nuc-LacZ* BAC transgenics; females carrying the transgene produced poor number of blastocysts (Nagy, 2003a). Successful culturing of blastocysts was a difficult process that went through multiple iterations. Initially, blastocysts were

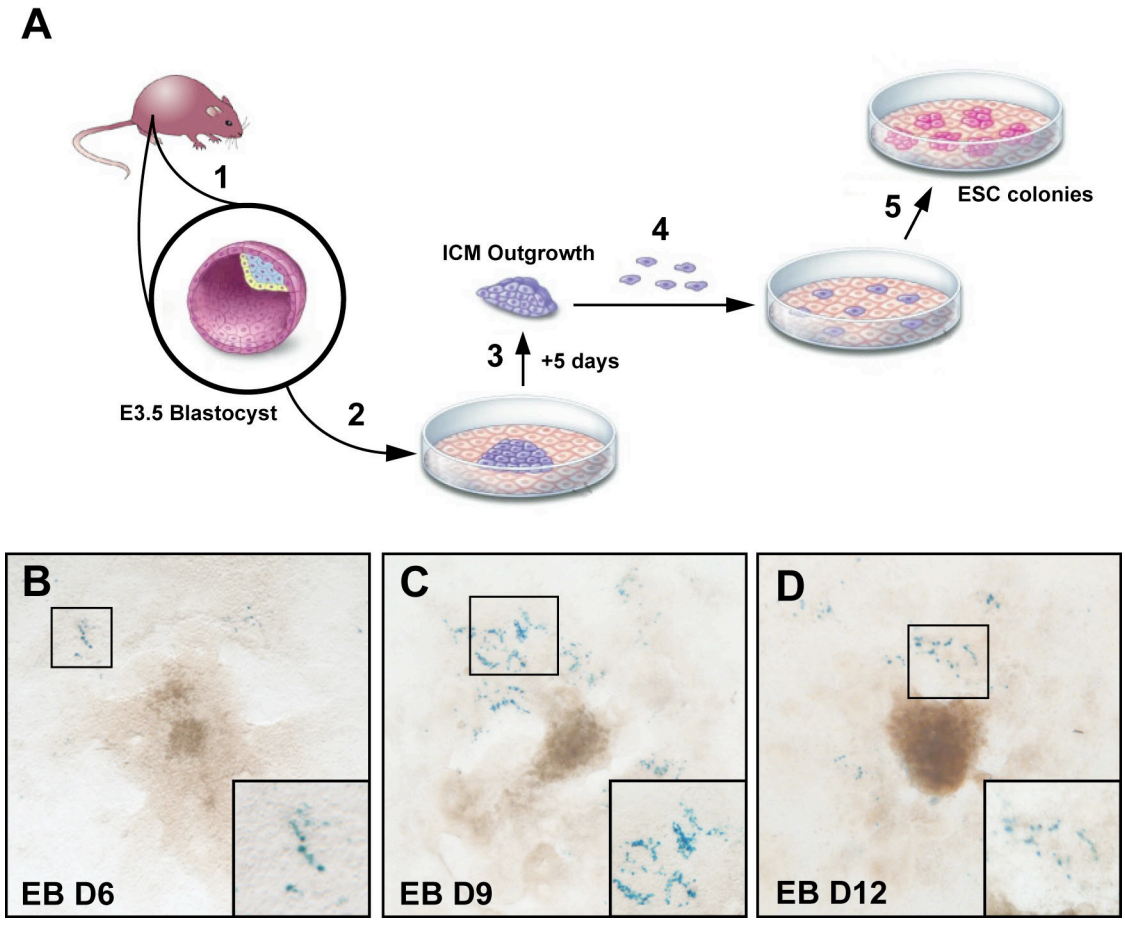

Figure 3.5. ***Derivation and differentiation of ESC lines from NFATc1-nuc-LacZ BAC transgenic mice.*** **A.** An ESC line from *NFATc1-nuc-LacZ* BAC transgenic mice was derived from E3.5 blastocyst-stage embryos (1) plated on irradiated passage 2-3 freshly isolated PMEF feeders (2). Cultured blastocysts were not disturbed for 3-4 days to allow attachment before changing the growth media. After 5-6 days in culture, the inner cell mass outgrowth was selectively removed from the trophectoderm (3), and dispersed (4), to generate ESCs colonies for expansion. Image modified from http://stemcells.nih.gov/info/scireport/appendixC.asp **B-D.** Low and high (insert) magnification images of X-gal stained EBs from *NFATc1-nuc-LacZ* BAC derived ESCs. β-gal+ endocardial cells are first detected at D6 (**B**), with robust β-gal expression consolidated in patches observable at D9 (**C**), but with noticeable reduction and dispersion by D12 (**D**).

deposited on STO feeders, a continuous line of mouse embryonic fibroblasts derived from the SLN/c mouse strain. The STO line, which were originally selected for 6-thioguanine and ouabain resistance, have been transfected to express LIF and possess neomycin resistance (Mann, 2001). Other groups have used STO cells to successful derive ESCs from blastocysts, however in our hands, once irradiated these cells produced excessive amounts of ECM that impaired ICM outgrowth and it subsequence removal, which prompted our switch to freshly prepared PMEFs. In addition, the use of RESGRO complete ES medium (Millipore) greatly facilitated blastocyst outgrowth compared to standard ESC media. However with this improved growth, tropohblast cell expansion had an adverse effect on ICM; the addition of the MEK1 inhibitor PD98059 blocked tropohblast growth with no discernible effect on the ICM outgrowth.

An ESC line derived from an *NFATc1-nuc-LacZ* BAC transgenic embryo was expanded and induced to form EBs. Upon differentiation, β-gal expression could be first observed at D6 (Fig. 3.5B). By D9, β-gal+ cells had increased in number and were consolidated in patches of cells, similar to what was observed in earlier immunofluorescence studies with NFATc1+/ CD31+ cells. After D12, β-gal+ cells were noticeably reduced and dispersed throughout the EB. The temporal expression of *NFATc1-nuc-LacZ* in EBs matched NFATc1's documented pattern from qRT-PCR analysis (Fig. 3.1B). Immunohistochemisty on X-gal stained EBs confirmed β-gal+ cells at D9 were CD31/Pecam-1+ endothelial cells and were spatially localized to sites of myocardial differentiation (Fig. 3.6A,B). To visualize multiple cells types and antigens, we employed an antibody against β-gal. Immunostaining of D9 EBs detected nuclear β-gal restricted to CD31+ endothelial cells (Fig. 3.6C). Further combined

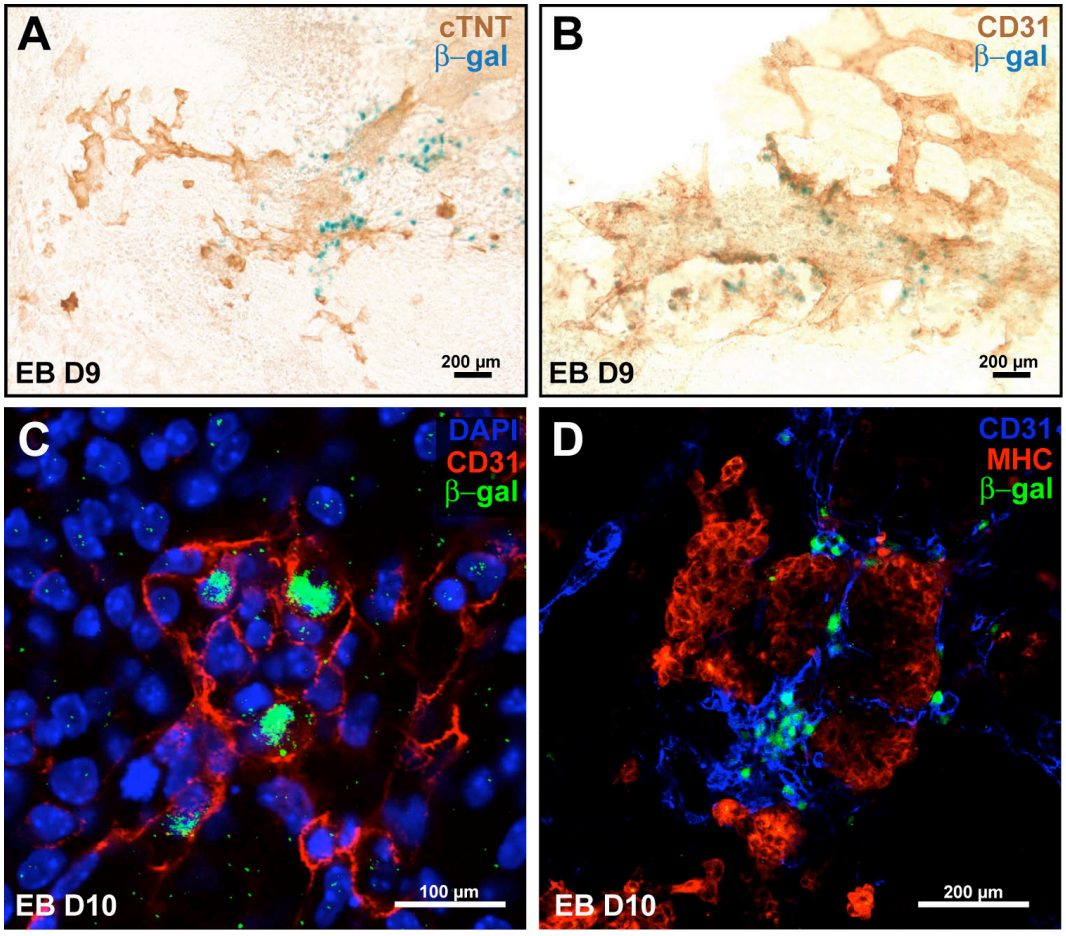

Figure 3.6. ***Characterization of β-gal expressing cells in embryoid bodies formed from NFATc1-nuc-LacZ BAC derived ESCs.*** **A.** Dual β-gal/immunoperoxidase staining of D9 EBs from *NFATc1-nuc-LacZ* derived ESCs with β-gal+ adjacent to sites of myocardial differentiation (cTnT, brown). **B.** Dual β-gal/immunoperoxidase staining documenting nuclear β-gal restricted to CD31+ endothelial cells. **C.** D9 EB from *NFATc1-nuc-LacZ* derived ESC stained with a β-gal (green) and CD31 (red) with nuclear β-gal restricted to endothelial cells. Nuclei were detected with DAPI (blue). **D.** Co-immunostaining for β-gal (green), MHC (red), and CD31 (blue) in D9 EBs from transgenic ESCs with β-gal+/CD31+ endocardial cells present in close proximity to myocardium, and not in regions lacking cardiomyocytes

immunofluorescence for cardiomyocytes, endothelium, and endocardium, confirmed that β-gal+/CD31+ endocardial cells were only present in close proximity to myocardium (Fig. 3.6D). Notably, cells expressing the *NFATc1-nuc-LacZ* were seldom detected in regions lacking cardiomyocytes, and non-endothelial NFATc1 expression was not observed over the period of differentiation investigated. The findings from differentiated *NFATc1-nuc-LacZ* BAC derived ESCs validates our initial immunofluorescence studies demonstrating temporal and spatial association of endocardium and myocardium in EBs, and furthermore establishes that the *NFATc1-nuc-LacZ* BAC transgene reflects *NFATc1* expression, allowing β-gal staining to be reliably used to monitor endocardial specification in ESC differentiation.

Electroporation of NFATc1 BAC transgenes generates stable ESC lines that faithfully monitor endocardiogenesis in EB differentiation cultures

As a routine method for generating new ESC lines stabling expressing BAC transgenes, the process of producing BAC transgenic mice via pronuclear injection followed by ESC deviation from transgenic blastocysts would be prohibitively difficult and time-consuming. In order to introduce BAC DNA directly into ESCs by electroporation, we modified a previously described method for the electroporation and selection of BAC transgenes (Tomishima *et al.*, 2007). Insertion of a *PGK-NEO* cassette between the homology arms of pLoxPOUTZeo conferred antibiotic resistance to *NFATc1-mCherry* and *NFATc1-nuc-LacZ* BAC constructs, allowing for selection with Geneticin (G418) in mammalian cells (Fig 2.7A). Given the large separation (50-75 kb) between the neomycin selection cassette in the BAC vector backbone from the reporter

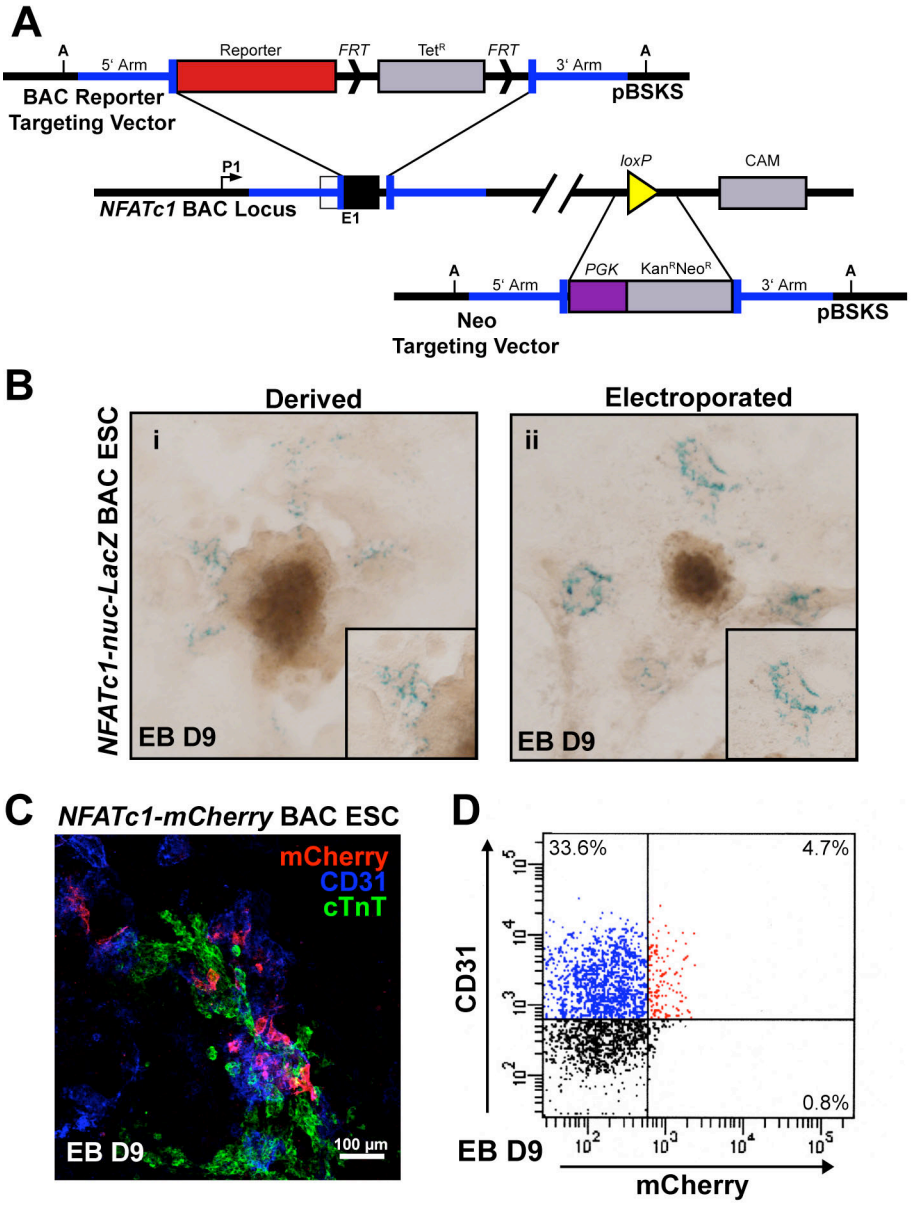

Figure 3.7. ***Stable NFATc1 reporter ESCs lines generated by electroporation of BAC DNA.*** **A.** Targeting schematic for the introduction of the fluorescent protein mCherry into the *NFATc1* BAC, and a strategy to convey neomycin resistance for selection in ESCs by introducing a *PGK-NEO* cassette into the BAC backbone (pBACe3.6). *Asc*I, A. **B.** Comparison of β-gal expression in D9 EBs generated from ESCs derived from *NFATc1-nuc-LacZ* BAC transgenic mice and from ESCs electroporated and selected for the neomyocin resistant *NFATc1-nuc-LacZ* BAC. **C.** Differentiated *NFATc1-mCherrry* BAC ESC line with mCherry (red) expression at D9 with immunostaining for cTnT (green), and CD31 (blue). mCherry+/CD31+ cells localize to regions of myocardial differentiation. **D.** Flow cytometry of D9 EBs from *NFATc1-mCherrry* BAC ESCs demonstrating mCherry (red) expression is largely restricted to endothelial cells, identified by CD31/Pecam-1 (blue).

gene inserted into exon 1, ESC colonies that survived selection and when differentiated expressed the reporter were assumed to contain an intact BAC transgene.

This process was first tested with an *NFATc1-nuc-LacZ* BAC transgene modified with the *PGK-NEO* cassette. After 10-14 days of selection, approximately 48 colonies were picked and tested. DNA was collected for PCR genotyping as described in Chapter II. Nearly 50% were PCR positive, but upon differentiation, only 30% expressed β-gal with X-gal staining. This ratio of 10-15% colonies of the total number surviving selection expressing the BAC transgene has proven consist for the majority of BAC electroporated into ESCs. When differentiated, the pattern of expression matched ESCs derived from *NFATc1-nuc-LacZ* transgenics in timing of expression and in the spatial relationships (Fig 3.7B). With these results, an ESC line containing an *NFATc1-mCherry* BAC was generated to monitor endocardiogenesis with a fluorescent reporter for live-cell imaging. Differentiated *NFATc1-mCherrry* BAC ESCs demonstrated that mCherry expression at D9 was colocalized with CD31/Pecam-1 adjacent to cTnT+ cardiomyocytes, in agreement with previous immunostaining and differentiation of *NFATc1-nuc-LacZ* derived ESCs that endocardial cells localize to regions of myocardial differentiation (Fig. 3.7C). Flow cytometry of mCherry against CD31/Pecam-1 at D9 demonstrated NFATc1+ cells (4.7%) were CD31/Pecam-1+ endothelial cells (Fig. 3.7D). This confirmed our earlier observations that the NFATc1 BAC reporter uniquely identified endocardial cells, and was not expressed in other cell populations during this window of differentiation.

Although mCherry signal was sufficiently luminous and photostable, its excitation/emission spectra were not compatible with lasers available for fluorescence

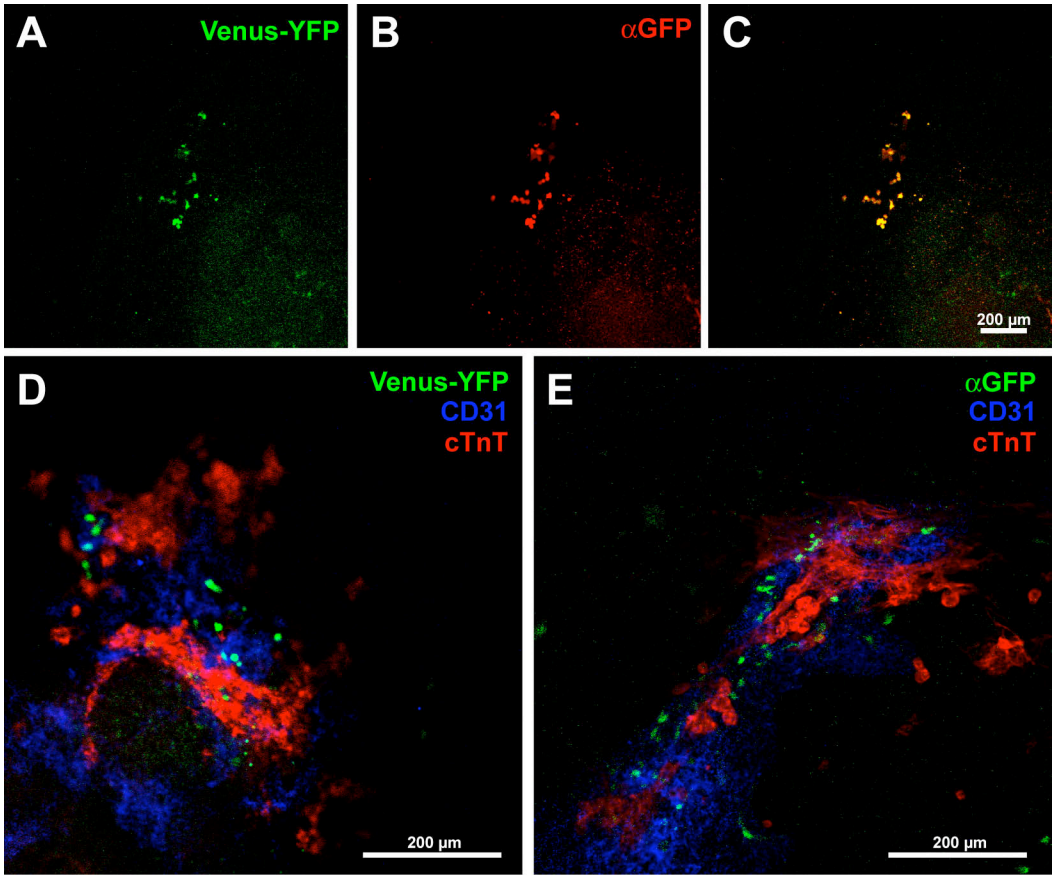

Figure 3.8. ***Preliminary characterization of differentiated NFATc1-Venus-yfp BAC ESCs.*** **A-C.** Native fluorescence of Venus-YFP (**A**, green) compared to detection with a primary antibody against GFP and an Alexa555 red fluorescent conjugated secondary (**B**, red) in a D8 EB. Signals from both detection methods colocalize to the same cells in the attached EB outgrowth (**C**, yellow). **D**. Immunofluorescent images of Venus-YFP (green) with cTnT (red) and CD31 (blue) in a D9 EB. YFP+ cells are CD31+ endothelial cells in close proximity to myocardium. **E**. Immunofluorescent images of αGFP (green) with cTnT (red) and CD31 (blue) in a D9 EB.

activated cell sorting (FACS). To correct this, an NFATc1 BAC was constructed driving the yellow fluorescent protein variant Venus (Nagai *et al.*, 2002). Initially, expression of Venus was comparable to other NFATc1 BAC reporters we had generated, displaying the spatial-temporal relationship to cardiomyocytes (Fig. 3.8). However, these lines quickly lost the ability to express Venus. The generation of new NFATc1-Venus ESC is currently in progress.

Discussion

With the ESC differentiation system, we have characterized an efficient and reproducible *in vitro* model of endocardiogenesis. Building off the extensive literature documenting mesodermal specification and subsequent differentiation of myocyte, endothelial, and hematopoietic populations in murine ESC-derived EBs, we provide evidence that endocardial differentiation occurs in a temporal pattern consistent with the mesodermal origin of endocardial cells, and their early emergence in mouse embryogenesis. Endocardial cells represent a fraction of the total vasculature plexus formed in outgrowths of attached EBs, but only appear at sites of myocardial cell differentiation. This spatial-temporal relationship between endocardial and myocardial cells as they arise from mesodermal progenitors, initially documented with immunofluorescence, was further validated using an ESCs derived from *NFATc1-nuc-LacZ* BAC transgenic embryos, and well as stable ESC lines containing *NFATc1-nuc-LacZ*, *NFATc1-mCherry,* and *NFATc1-Venus-yfp* BAC transgenes. Collectively, our findings document the close temporal-spatial relationship seen between endocardium and myocardium *in vivo* is reproduced *in vitro*, and provides a means to elucidate the origins

of the endocardial lineage and how endocardial-myocardial interactions shape early cardiac differentiation.

NFATc1 expression and function in ESC differentiation has been addressed in a select few studies, though its temporal expression pattern had never been properly defined. NFATc1$^{-/-}$ ESCs have been used to investigate the role of NFATc1 in osteoclast differentiation (Takayanagi *et al.*, 2002). Their data indicates NFATc1 is expressed in osteoclasts by D8-D10, which appears to be in conflict with our flow cytometry experiments on D9 EBs generated from *NFATc1-mCherrry* BAC ESCs where the majority of mCherry+ cells also express the endothelial marker CD31/Pecam-1. However, as osteoclastogenesis is somewhat late during ESC differentiation, and was only achieved with the addition of macrophage colony stimulating factor (M-CSF) and RANKL, the difference in experimental design might represent a potential explanation of this discrepancy. During the course of our studies, a report from Narumiya et al. maintained that NFATc1/CD31 double positive endocardial cells associated with GATA4-expressing myocardial cells in D8 EBs grown in suspension (Narumiya *et al.*, 2007). Though these findings seemingly confirmed observations we had made prior to its publication, NFATc1 and CD31/Pecam-1 immunofluorescence were not of high enough quality to make any definitive conclusion about the spatial association of endocardium and myocardium in EBs from their studies.

Monitoring endocardial differentiation in EBs with immunofluorescence provides only circumstantial evidence. Colocalization of vascular markers with NFATc1 only suggests an endocardial identity for this population. It is not possible to conclude they are in fact endocardial cells without additional validation. Chapter V describes future

experiments to further characterize NFATc1+ cells generated in EB outgrowths. ESCs derived from *NFATc1-nuc-LacZ* BAC transgenic embryos allowed for comparison between embryogenesis and during *in vitro* ESC differentiation. It was our intention to isolate by FACS NFATc1+ endocardial cells generated from EBs to confirm whether they possess the same expression profile and functionality as their *in vivo* counterparts. Unfortunately, technical difficulties prevented the use of *NFATc1-mCherrry* BAC ESCs for FACS, and no working *NFATc1-Venus-yfp* BAC ESCs have been generated. These experiments still remain as future experimental goals and are discussed in Chapter V.

In spite of the commonly held belief that EBs lack structural complexity, which in the embryo is essential for proper organogenesis, we observed that endocardial cells were only present in close proximity to cardiomyocytes in 2-dimensional EB outgrowths. Such consistency in organization of two distinct subpopulations implies that there might be required cell-cell signaling or physical interaction between the endocardium and myocardium that governs their association. The exchange of signals between endocardium and myocardium, as discussed in Chapter I, has been demonstrated during cardiac morphogenesis where it is essential for proper patterned growth and the development of structures of the mature heart. Furthermore, interaction between endothelial cells and cardiomyocytes is required for survival of these cell types *in vitro*, as cultured neonatal cardiomyocytes undergo less apoptosis and show increased contraction when co-cultured with HUVECs (Narmoneva *et al.*, 2004). Other potential explanations for the proximity between the endocardium and myocardium in EBs are that each lineage might be induced from similar cues present in the microenvironment, or they

directly share a common precursor. These two possibilities are explored in detail in Chapter IV.

CHAPTER IV

ENDOCARDIUM AND MYOCARDIUM ARE DERIVED FROM A COMMON MESODERMAL CARDIOVASCULAR PRECUSOR

Introduction

While comparisons of cardiogenesis in different model organisms across evolutionary diverse phyla have been largely consistent in describing the process of myocardial differentiation and early heart formation, observations of endocardiogenesis have yielded a convoluted picture of this cardiac subpopulation. As a result, the exact lineage classification of endocardium as either a cardiac or vascular cell population remains controversial. Two opposing models have been put forth to explain these observations, one which states that endocardial and myocardial precursors represent two distinct populations in the cardiac crescent, and another that asserts the two cardiac subpopulations are formed from a common multipotent mesodermal progenitor.

In non-mammalian systems, the endocardium appears to originate from the same common precursor as other vascular and hematopoietic cells, not from mesoderm generating the myocardium. Early retroviral tracing in the avian embryo indicated that the endocardium and myocardium exist as two distinct populations in the cardiac mesoderm, which separated prior to gastrulation (Cohen-Gould and Mikawa, 1996; Wei and Mikawa, 2000). Blastomere transplantation in zebrafish supported the hypothesis of two distinct lineages for the endocardium and myocardium prior to gastrulation, and suggested a shared origin of endocardium and other peripheral vascular components (Lee *et al.*, 1994). By examining *Scl/Tal1* mutant zebrafish, Bussmann *et al*. confirmed that

endocardial precursors migrate to invest the developing myocardial tube from a region in the lateral plate mesoderm that also generates cells of the hematopoietic lineage (Bussmann *et al.*, 2007).

These studies suggest that within the cardiac mesoderm, endocardial progenitors represent a small number of spatially sequestered precursors within a larger field of myocardial progenitors, each with its own distinct mesodermal origin. However, this viewpoint conflicts with accumulating evidence from mammalian systems suggesting endocardium and myocardium are derived from a common mesodermal progenitor. Cre-mediated lineage tracing of *Nkx2.5*+ and *isl1*+ cardiac populations suggests that myocardium, endocardium, vascular endothelium, and smooth muscle might be derived from common precursors in the cardiac mesoderm (Cai *et al.*, 2003; Stanley *et al.*, 2002). These findings insinuate a close developmental relationship, if not a common origin, between the endocardium and myocardium, though detailed examination has proven difficult due to the limitations of *in vivo* mouse models.

As discussed in Chapter I, ESC differentiation models have been used extensively to examine cardiac specification, focusing on the stepwise commitment of precursors to differentiated cardiac cell types. While few have addressed endocardiogenesis, these studies focusing on the cardiomyocyte lineage have revealed the potential of the ESC system to address the issue of endocardial origin. This is exemplified by work utilizing an ESC line expressing GFP under control of the *brachyury* locus along with the cell surface receptor Flk1 to isolate cardiac and hematopoietic/vascular lineages by FACS (Kouskoff *et al.*, 2005). These mesodermal lineages possess distinct different temporal patterns in EBs with the cardiac lineage arising from a second wave of Flk1+ mesoderm

that appears subsequent to hemangioblast specification (Kattman *et al.*, 2006). Clonal analysis further indicated this second wave of Flk1+ mesoderm represented multipotent cardiovascular progenitors (MCPs) that generated cardiomyocyte, smooth muscle, and endothelial cells. An equivalent MCP population has since been isolated from human ESCs using Flk1 and c-kit (Yang *et al.*, 2008). Interestingly, when Flk1+ MCPs from both mouse and human ESCs were expanded in culture and allowed to differentiate, endocardial transcripts *NFATc1* and *Nrg1* could be detected. These findings, in addition to our previous observations documenting a close temporal-spatial relationship between endocardium and myocardium in EBs, emphasize the potential of ESC differentiation to clarify the origin and lineage classification of endocardial cells.

In the following studies, we establish that endocardial cells are a specialized cardiac subpopulation, specified independently from hematopoietic and endothelial lineages. Endocardial differentiation is inexorably linked to cardiomyocyte differentiation as early exposure to BMP and Wnt signals, affecting cardiac precursors, enhance cardiomyocyte and endocardial differentiation in at the expense of blood and vasculature. Using flow cytometry to sort mesodermal populations, we isolated a temporally specific population of Flk1+ mesoderm capable of generating both endocardium and myocardium distinct from the Flk1+ mesodermal hemangioblast giving rise to hematopoietic and endothelial cell types. Furthermore, clonal analysis established this population contains cardiovascular progenitors with cardiomyocyte, endocardial, endothelial, and smooth muscle potential. Collectively, these studies provide evidence that endocardium and myocardium are derived from a common cardiovascular progenitor within the cardiac mesoderm.

Experimental Procedures

ESC culture and differentiation

ESCs and PMEF feeders were maintained as described in the Experimental Procedures of Chapter III. ESCs were induced to differentiate in hanging drops and suspension cultures as detailed in the Experimental Procedures of Chapter III. For experiments with growth factor treatment, Wnt3A, Dkk-1, and Noggin/Fc were purchased from R&D systems. Concentrations and timing of administration are discussing the Results section.

Cell staining

Immunostaining, β-gal staining, and dual β-gal /immunoperoxidase staining was performed as described in Chapter III. For area calculations, a single EB at D3-4 was plated into individual wells of a gelatinized 24-well dish and maintained under its specified conditions until D10. The EB was fixed and stained for MHC with the MF20 antibody, followed by single detection using a goat anti-mouse Alexa-555 secondary antibody. Hoechst Dye 33342 (Molecular Probes) was used to stain nuclei and define the borders of the EB outgrowth. MetaMorph v6.1 (Molecular Devices) was used to calculate MHC+ area per EB.

Antibodies

NFATc1 (mouse 7A6, BD Pharmingen, 1:200)

Sacromeric myosin heavy chain (MHC; mouse MF20, DSHB, 1 μg/ml)

Cardiac troponin T (cTnT; mouse CT3, DSHB, 1 μg/ml)

CD31/Pecam-1 (rat MEC13.3, BD Pharmingen, 1:500)

β-Gal (chick, Abcam, 1:1,000 or rabbit, Cappel, 1:5,000)

Smooth muscle myosin heavy chain (SM-MHC; rabbit, Biomedical Technologies Inc., 1:100)

Fluorescence activated cell sorting (FACS)

D3.5 EBs were dissociated using cell disassociation buffer (Gibco) for 30 minutes at 37˚C, then resuspended in ice cold FACS buffer prepared from Hanks Buffered Salt Solution (HBSS) with 2% FBS (HyClone), and 25 mM HEPES, and filtered through a 42 μm sieve to produce a single cell suspension. Cell density was adjusted to $1x10^6$ per 100 μl before treatment with an antibody against CD16/CD32 for 10 minutes (mouse, Ebioscence, 1 μg/ml) to block nonspecific binding. For double staining of D3.5 EBs, biotinylated Flk1 (mouse Avas12.1, BD Pharmingen, 1 μg/ml) and E-cadherin (rat DECMA, Sigma, 1 μg/ml) were applied directly to blocked cells and incubated for 45 minutes on ice. Single staining of D4.5 $ECD^{low}Flk1^{low}$ cell cultured O/N for Flk1 omitted E-cadherin. Cells were washed twice with FACS buffer, and then pelleted by centrifugation for 5 minutes at 500xg. Cells were again resuspended at a density of $1x10^6$ per 100 μl before staining with goat anti-Rat Alexa-488 (Molecular Probes, 0.5 μg/ml) and streptavidin-conjugated APC (Molecular Probes, 0.5 μg/ml) for 30 minutes on ice. Samples were washed and brought to a density of $3x10^6$ per 1ml for FACS and stained with propidium iodide (PI) (Molecular Probes, 1:1000). PI, which crosses the plasma and

nuclear membranes, intercalates into double stranded DNA of dead cells and allows for their exclusion from analysis and collection.

For each sort, an unstained control was prepared consisting of dissociated cells processed without primary antibodies in order to compensate for autofluorescence and for nonspecific binding of secondary antibodies. Single color controls, cells treated with only one secondary antibody, were prepared to optimize the voltages of the photo multiplier tube for each fluorochrome. In addition, a PI control was prepared from the unstained control to adjust for cell death.

Cells were sorted on a FACSAria (Becton Dickinson) using FACSDiva 6.0 for data collection at the VMC Flow Cytometry Shared Resource. The VMC Flow Cytometry Shared Resource is supported by the Vanderbilt Ingram Cancer Center (P30 CA68485) and the Vanderbilt Digestive Disease Research Center (DK058404). Gated cell fractions were collected into DM supplemented with additional 20% FBS and stored on ice.

OP9 culture

OP9 cells were obtained from the American Types Culture Collection (ATCC) and plated on gelatinized 100-mm Poly-D-Lysine treated dishes in Minimum Essential Medium Alpha Modification (α-MEM) supplemented with 10% FBS (HyClone), 2 mM L-glutamine, 100 U/ml Penicillin/Streptomycin, and 100 μM β-mercaptoethanol at 37˚C, 5% CO_2. From a single vial, cells were plated to a single dish, passaged at 90% confluence, and then passaged every two days 1:3 or 1:4. Cells were frozen 1:2 by mixing resuspended cells in OP9 media 1:1 with 2x Freezing media (60% OP9 media,

20% FBS, 20% DMSO). Cryovials were placed in an isopropanol freezing container and stored at -80˚C for 1-3 days before transfer to liquid nitrogen. Prior to their use as feeders, OP9 cells were exposed to 6-7 minutes (10-12 Gyr) of Cesium-137 irradiation to inactivate cell division. The use of irradiated cells increased the number of differentiated cell types from expanded mesodermal populations.

Cardiac and hematopoietic/vascular colony assays

$ECD^{high}Flk1^{low}$, $ECD^{low}Flk1^{high}$, and $ECD^{low}Flk1^{low}$ fractions were plated at a density of $5x10^3$ cells/cm^3 onto irradiated OP9 stromal cells. Cells were cultured for 6 days in ESC differentiation media (DM) consisting of IMDM supplemented with 15% FBS, 2 mM L-glutamine, 100 U/ml Penicillin/Streptomycin, 200 μg/m transferrin, 0.5 mM L-ascorbic acid, and 4.5x10–4 M monothioglycerol. For secondary Flk1 sorting, $ECD^{low}Flk1^{low}$ cells were grown for 24 hours on OP9 stromal cells in serum-free DM with 15% Knockout Serum replacement (Invitrogen) substituted for FBS, as well as bFGF (30 ng/ml) and VEGF (5 ng/ml) (R&D Systems). Resorted Flk1 positive and negative cells were plated at a density of $1x10^3$ cells/cm^3 in serum-free DM supplemented with VEGF (5 ng/ml), bFGF (30 ng/ml), BMP4 (50 ng/ml), and Dkk-1 (150 ng/ml). Contracting colonies were scored after 6 days in culture. For clonal expansion, single Flk1+ cells from the D4.5 $ECD^{low}Flk1^{low}$ population were distributed into 96-well plates seeded with OP9 stromal cells. After 7 days in culture, the cells were fixed, stained, and scored.

Reverse Transcriptase PCR (RT-PCR)

RNA and cDNA were prepared as described in Chapter III. Semi-quantitative RT-PCR was performed using REDTaq (Sigma) and 0.5 μM of each primer gene-specific primers, and 50 ng cDNA under the following cycling conditions: 94°C for 2 minutes, followed by 30 cycles of amplification (94°C denaturation for 30 seconds, 60°C annealing for 30 seconds, 72°C elongation for 60 seconds), then a final incubation at 72°C for 10 minutes. Products were run on a 1.5% agarose gel at 4˚C at 80-90V.

Quantitative real-time PCR (qRT-PCR)

All qRT-PCR was performed using a Light Cycler (Roche) with the Light Cycler DNA FastStart SYBR Green I Kit, 0.5 μM of each primer, and 100 ng cDNA. Gene specific primer sets used for these experiments are listed in Table 4.1. Each sample was done in triplicate and relative expression was calculated as $\Delta^{2\text{-ct}}$ with *HPRT* as the internal control.

Statistics

All statistical analyses performed represent two-tailed Student's t-test carried out using Graphpad Prism for Macintosh 4.0.

Table 4.1. ***Oligonucleotides for RT-PCR gene expression analysis of Flk1 and E-cadherin populations and their derivatives.***

Gene	Forward Primer	Reverse Primer
Rex1	5' CGT GTA ACA TAC ACC ATC CG 3'	5' GAA ATC CTC TTC CAG AAT GG 3'
Pax6	5' GCT TCA TCC GAG TCT TCT CCG TTA G 3'	5' CCA TCT TTG CTT GGG AAA TCC G 3'
Sox17	5' TGC CCT TTG TGT ATA AGC CCG AGA 3'	5' GGG TAG TTG CAA TAG TAG ACC GCT 3'
FoxA2	5' AAG GGA AAT GAG AGG CTG AGT GGA	5' ATG ACA GAT GAC TGT GGC CCA TCT 3'
Brachyury	5' ACA GAT CAT GTT AAA CTC CTT GCA T 3'	5' TAC ATC TTT GTG GTC GTT TCT TTC T 3'
Runx1	5' GCC TCT CTG CAG AAC TTT CC 3'	5' GAC GGC AGA GTA GGG AAC TG 3'
Scl/Tal1	5' GCC GGT CTG CCT ACA CCG GC 3'	5' CCC CGA AGC TGG GTT TCC CGG 3'
Nkx2.5	5' ACC TTT CTC CGA TCC ATC CCA CTT 3'	5' GCG TTA GCG CAC TCA CTT TAA TGG 3'
Tbx5	5' TCT CCT TCT GGT TTG GTT CTG CCT 3'	5' TGT CAC CCA GGG CTC TTT CAG TTT 3'
cTnT	5' CCG GCG TGA GGA GGGA GGA GAA 3'	5' AGG GGG CAC AGC TTT GAC GAG AA 3'
βMHC	5' AGC CGC GCC AGT ACT TCA TAG GTG 3'	5' TGT TCT TTT CCA GCC AGC CCA TAA 3'
GATA4	5' TTC CTT GTC CTC ATC ACC CAC AGA 3'	5' GAC AA TGT TAA CGG GTT GTG GAG G 3'
isl1	5' TGT CAG GAG ACT TGC CAC TTT 3'	5' GCC AAA CGT TTA TTA GTG AAA TAG TCC TG 3'
Mef2c	5' TGT ATA GAG GTT TGG ACA GAC CCG 3'	5' TGT TAG CTC TCA AAC GCC ACA C 3'
NFATc1	5' GGT GGC CTC GAA CCC TAT C 3'	5' TCA GTC TTT GCT TCC ATC TCC C 3'
Nrg1	5' CCA ATG GCC ACA TTG CCA ATA GGT 3'	5' AGC CTG GCC TGT AAT TCT TCC TGT 3'
Flk1	5' GGT TCT CTG TCA AGT GGC GGT AAA 3'	5' AGC ACA CAG GCA GAA ACC AGT AGA 3'
VECAD	5' AAC TCA CCC TCC TTG TGG AAT CCT 3'	5' ACA TCT CAT GCA CCA GGG TGA CTA 3'
CD31/Pecam-1	5' ATC CGG AAG GTC GAC CCT AAT CTC AT 3'	5' ATA CCC AAC ATG AAC AAG GCA GCG 3'
βH1-globin	5' CTC AAG GAG ACC TTT GCT CA 3'	5' AGT CCC CAT GGA CTC AAA GA 3'
GATA1	5' CAT TGG CCC CTT GTG AGG CCA G 3'	5' CGC TCC AGC CAG ATT CGA CCC 3'
HPRT	5' AGT CAA CGG GGG ACA TAA AA 3'	5' TGC ATT GTT TTA CCA GTG TCA A 3'

Results

Serum depletion during ESC differentiation reveals an inverse relationship between cardiac and hematopoietic/vascular populations

The spatial-temporal association between endocardium and myocardium during embryogenesis and in ESC differentiation is suggestive of endocardiogenesis being intrinsically linked to cardiomyocyte differentiation, yet the mechanisms orchestrating this relationship remain unclear. The generation of cardiomyocytes from EBs is inefficient, and it has been hypothesized that serum, while vital to hematopoietic and vascular development, contains factors that inhibit myocardial differentiation. Validating this concept, myocardial differentiation was found to vary indirectly with the percentage of serum present in culture media, where reductions in serum enhanced cardiomyocyte differentiation (Passier *et al.*, 2005). To determine the effect alternations in cardiomyocyte differentiation had on endocardiogenesis, ESCs were differentiated under culture conditions that have been described to enhance myocardial specification.

EBs were formed in suspension with DM containing 15% serum, and at D3 were plated on gelatinized tissue culture dishes in DM containing either 15% serum or DM with only 1% serum. EBs were taken at every two days from D0 until D10 for RNA isolation and qRT-PCR analysis of myocardial, endothelial, and endocardial gene transcripts. Myocardial markers *βMHC* and *cTnT* were increased nearly 2-fold by D8 in the 1% serum condition compared to EBs differentiated in media containing 15% serum (Fig 4.1A). In contrast, vascular markers such as *VE-cadherin* and *Flk1* during its vascular restricted phase, are decreased with reduced serum (Fig 4.1B). *Nkx2.5*, though not different at D6, was enhanced with reduced serum at D8. *NFATc1*, as a marker of

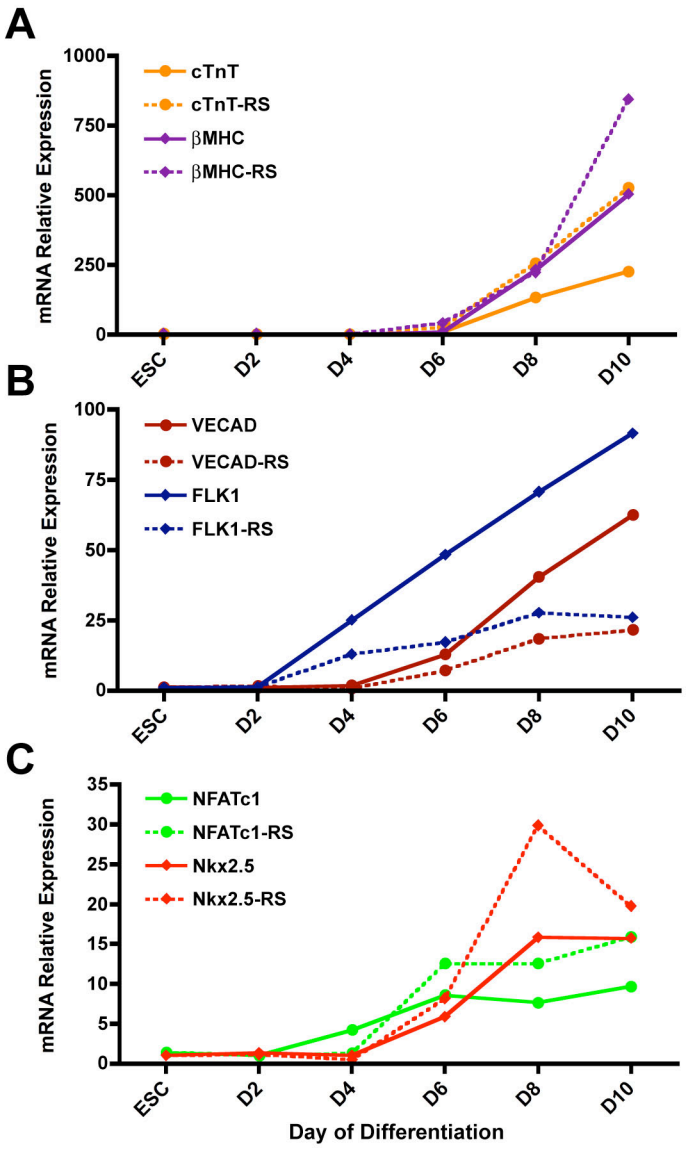

Figure 4.1. ***Endocardial, myocardial, and endothelial differentiation in reduced serum conditions.*** EBs cultured in media containing 15% serum (solid lines) or with reduced serum (RS; 1% serum, dotted lines) were taken at every two days from D0 until D10 for RNA isolation and qRT-PCR analysis of myocardial, endothelial, and endocardial gene transcripts. **A.** Myocardial markers *βMHC* (purple*)* and *cTnT* (orange) were increased nearly 2-fold by D8 in reduced serum. **B.** Vascular genes *VE-cadherin* (dark red) and *Flk1* (blue) were decreased when differentiated in media with reduced serum. **C.** The early cardiac gene *Nkx2.5* (red), though no different at D6, was enhanced with reduced serum at D8, while *NFATc1* expression was elevated at later stages with 1% serum.

endocardium, was elevated at later stages in EBs cultured in media containing 1% serum (Fig. 4.1C). This pattern of differentiation demonstrates that under reduced serum, endocardial and myocardial differentiation in increased, while vascular development is inhibited.

Endocardial cells respond to BMP and Wnt signaling as a cardiac lineage

To further evaluate whether endocardium is a specialized cardiac cell or a spatially distinct endothelial cell, differentiating EBs were treated with soluble factors shown to affect cardiac or hematopoietic/vascular development. For these studies we focused on the BMP and Wnt signaling families, as both have been demonstrated to play vital roles *in vivo* and *in vitro* in cardiovascular cell specification from mesoderm. BMP and Wnt signaling are also remarkable in that activators and inhibits have been found to affect cardiomyocyte specification and blood/vascular specification differently. BMP signaling has been implicated in extraembryonic mesoderm development where it is essential for hematopoiesis, but also is involved in cardiac specification as a growth factor from the ectoderm (Snyder *et al.*, 2004). Noggin, a biologic inhibitor of BMP signaling, has been shown to have a biphasic role in cardiomyocyte specification; Noggin produced by the notochord inhibits cardiac differentiation at the midline, while transient expression of Noggin in the cardiogenic mesoderm and AVE appears to be necessary for myocyte differentiation (Yuasa *et al.*, 2005). In ESC differentiation, early Noggin treatment has been documented to enhance cardiomyocyte differentiation at the determinant of hematopoietic and vascular lineages (Lindsley *et al.*, 2006; Yuasa *et al.*, 2005). Thus while BMP signaling is critical for mesodermal formation and subsequent

cardiomyocyte differentiation, BMP inhibition might also play a role in priming mesoderm towards a cardiac lineage as well as blocking it from progressing to a hematopoietic and vascular lineage. In many cellular contexts, Wnt signaling and its inhibition are effective modulators of gene expression. During embryogenesis, Wnt1, -3A, and -8 produced by the neural tube inhibit cardiogenesis at the midline, while Dkk-1 and Crescent from the endoderm represent inductive signals. These effects have also been documented *in vitro* with ESC differentiation where Wnt inhibition enhanced cardiogenesis, while Wnt receptor activation has an opposing effect, increasing non-cardiac mesodermal derivative and neural cell differentiation. (Naito *et al.*, 2006).

Modifying previously described treatment regimes we dosed EBs during two windows of development, either early or late, and analyzed cardiomyocyte, endocardial, hematopoietic, and endothelial differentiation after 10 days in culture (Fig 4.2A). Under the early treatment paradigm, EBs were treated with recombinant Noggin/Fc (150 ng/ml) in serum containing differentiation media (DM) from day 0 until plating at day 4 (Lindsley *et al.*, 2006). Late treatments with either Wnt3A (100 ng/ml) or the Wnt inhibitor dickkopf-1 (Dkk-1; 200 ng/ml) were added to DM at day 5 until day 7 (Naito *et al.*, 2006). Early Noggin/Fc exposure significantly enhanced cardiomyocyte differentiation, measured by changes in MHC+ area, with an approximate 3-fold increase over controls (16.2%±3.2% vs. 6.0%±1.2%) consistent with previous studies. Dkk-1 treatment at D5 had a similar effect (11.4%±1.6%), while late Wnt activation with Wnt3A suppressed myocyte formation (2.6%±0.5%) (Fig. 4.2B). Quantitative RT-PCR confirmed an inverse relationship between cardiac cells and the hematopoietic/vascular lineage. Markers of cardiomyocyte specification and maturation, *Nkx2.5* and *cTnT*, were

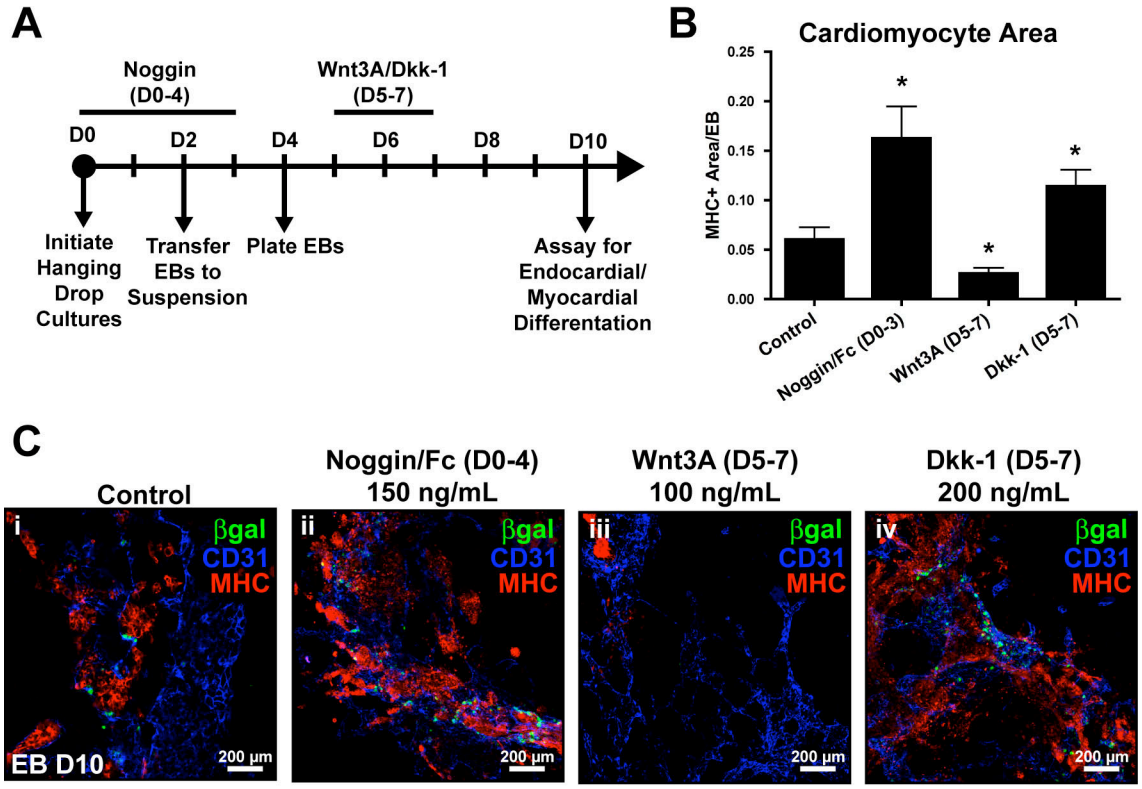

Figure 4.2. ***Effect of BMP and Wnt signals on cardiac, hematopoietic, and vascular specification*.** **A.** Schematic documenting timing of BMP and Wnt treatments compared to EB culture conditions. *NFATc1-nuc-LacZ* derived ESCs were differentiated with recombinant Noggin/Fc (150 ng/ml) from D0 through D4, or Wnt3A (100 ng/ml) or Dkk-1 (200 ng/ml) from D5-D7. **B.** Individual EBs from different treatments were plated into 24-well dishes and subjected to morphometric analysis of MHC at D10. Values represent the ratio of MF20+ area to total EB area. *=p < .05 vs. control, N=8. Error bars indicate SEM. Early Noggin/Fc and late Dkk-1exposure significantly enhanced cardiomyocyte differentiation, while late Wnt activation with Wnt3A suppressed myocyte specification. **C.** Representative images from control **(i)**, Noggin/Fc **(ii)**, Wnt3A **(iii)**, and Dkk-1 **(iv)** treated D10 *NFATc1-nuc-LacZ* derived EBs stained for β-gal (green), MHC (red), and CD31 (blue). β-gal+/CD31+ endocardial cells increased with early addition of Noggin/Fc or late Dkk-1.

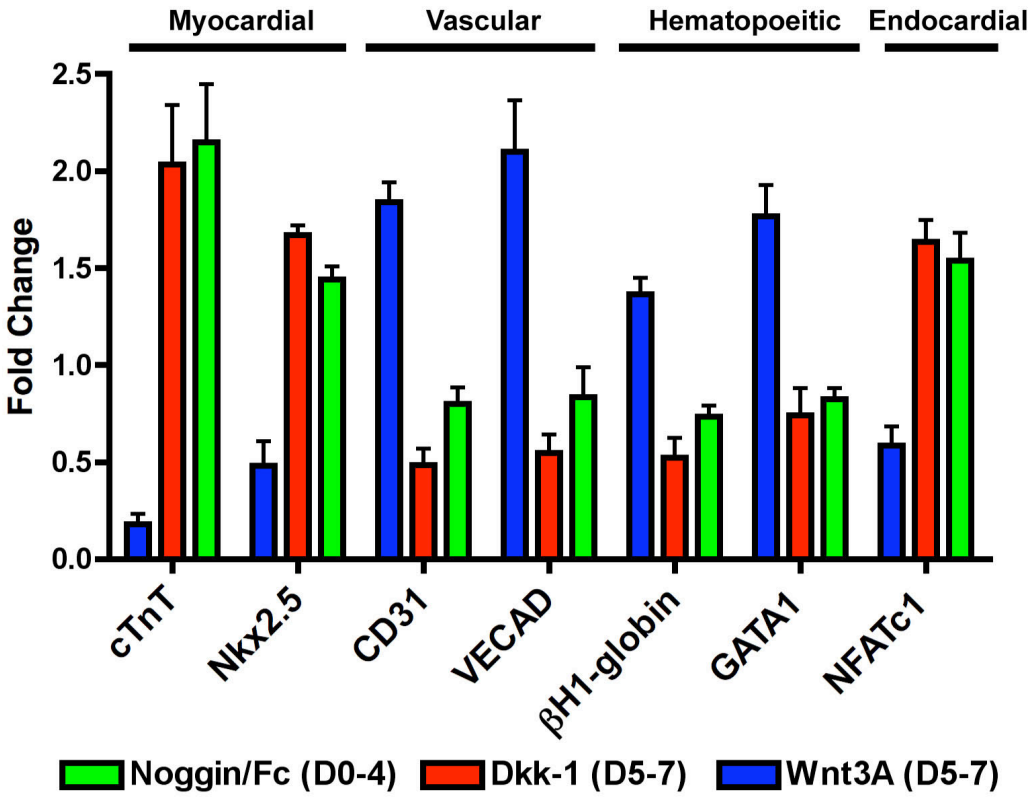

Figure 4.3. ***Molecular expression analysis of cardiac, hematopoietic, and vascular genes in Noggin, Wnt3A, and Dkk-1 treated EBs.*** Fold change in mRNA transcripts by qRT-PCR of endocardial (*NFATc1),* cardiac (*Nkx2.5, cTnT*), vascular (*CD31, VE-cadherin*) and hematopoietic (*βH1-globin, GATA1*) genes in D10 EBs treated with Noggin/Fc (green) from D0 through D4, or Wnt3A (blue) or Dkk-1 (red) from D5-D7. Error bars indicate SEM. Quantitative RT-PCR confirmed an inverse relationship between endocardial cells and the hematopoietic/vascular lineage. With early Noggin/Fc treatment and late Dkk-1, endocardial specification increased with cardiomyocyte markers, corresponding to a reduction in hematopoietic/vascular gene expression. In contrast, late Wnt3A treatment enhanced gene expression from the blood and endothelial lineages and inhibited cardiac gene expression.

upregulated with early Noggin/Fc and late Dkk-1, while suppressed with Wnt3A. Vascular (*CD31, VE-cadherin*) and hematopoietic (*βH1-globin, GATA1*) markers were upregulated with late-phase addition of Wnt3A (Fig. 4.3).

Given the relationship between cardiomyocytes and endocardial cells in EBs, we hypothesized that an increase in endocardium would accompany myocyte enrichment. *NFATc1-nuc-LacZ* BAC ESCs were differentiated to examine endocardiogenesis by immunofluorescence. β-gal+/CD31+ endocardial cells increased with early addition of Noggin/Fc or late Dkk-1. There was a noticeable decrease in vascular plexus formation, though β-gal+/CD31+ endocardial cells were still present (Fig. 4.2C, compare panel i vs. ii & iv). This pattern was reversed with Wnt3a, where myocardium and endocardium were largely absent (Fig. 4.2C, panel iii). *NFATc1*, as a marker of endocardium, increased with Noggin/Fc and Dkk-1 similar to myocytes, not with other endothelial cells (Fig. 4.3). These findings indicate endocardium is specified as a cardiac lineage, not from the hematopoietic/vascular lineage. Also, as the effect of growth factor treatment is effective prior to the emergence of cardiac cell types, it suggests that BMP and Wnt signaling acts on a precursor population of endocardium and myocardium, but this data does not clarify whether endocardial cells are derived from a common precursor as cardiomyocytes or develop in a parallel and dependent pathway.

Endocardium is specified as a cardiac lineage distinct from vascular endothelium

Although our data from Noggin/Fc and Dkk-1 treated EBs indicates endocardium is specified as a cardiac cell type distinct from peripheral vasculature, a level of uncertainty is introduced by conducting these studies using whole EBs. To more

precisely define endocardiogenesis from mesodermal populations as it relates to cardiomyocyte and hematopoietic/vascular differentiation, we sorted EBs at D3.5 with the cell surface markers Flk1 and E-cadherin. Lineage tracing studies have shown components of the cardiovascular system are derived from Flk1+ mesoderm (Ema *et al.*, 2006; Fehling *et al.*, 2003). In addition, Flk1 has been used successfully to isolate hemangioblast and cardiac populations from differentiating ESCs. As an additional marker, we chose E-cadherin (ECD), primarily because exfoliating mesodermal cells downregulate ECD as they exit the primitive streak (Ciruna and Rossant, 2001; Huber *et al.*, 1996). The timing for disassociation of EBs to isolate populations with or without Flk1 and ECD expression was determined from the literature and from pilot studies. For consistency in cell number and size, EBs were formed in hanging drops, and then assayed for Flk1 expression at D2.5, D3.5, D4.5, and D5.5. The number of cells seeded to generate each hanging drop impacted Flk1 expression at these time points, with EBs seeded with 100 cells possessing a greater number of cell expressing Flk1 than those formed from 500 or 1000 cells (Table 4.2). For these experiments, we used 500 cells to initiate EB formation despite exhibiting lower numbers of Flk1+ cells, as EBs formed from 100 cells possessed far fewer cells after 3.5 days. Next we examined ECD expression in undifferentiated ESCs and EBs at D2.5, D3.5, D4.5, and D5.5. ECD was expressed almost alls cells from D0 until D3, however from D2.5 to D3.5 there was a precipitous drop from >90% to 15-20% ECD+ cells (Table 4.3). The timing of this drop, consistent with other studies of ECD in early EBs, marks the transition of mesoderm out of the PS streak stage of gastrulation (Ng *et al.*, 2005). After D3.5, the number of ECD+ cell plateaued at 15-20%.

Table 4.2. ***Percentage of Flk1 positive cells at early time points in embryoid body differentiation.*** EBs were formed in hanging drops with either 100, 500, or 1000 cells per drop. EBs were disassociated at particular time points and analyzed by flow cytometry to determine the number of cells expressing Flk1.

	% Flk1 Positive Cells		
EB Day	**100 cells**	**500 cells**	**1000 cells**
D2.5	3.2 ± 1.5	2.7 ± 2.1	5.1 ± 0.5
D3.5	48.2 ± 5.3	32.2 ± 3.5	11.6 ± 4.1
D4.5	34.5 ± 4.1	17.7 ± 2.5	12.5 ± 1.9
D5.5	19.3 ± 2.2	7.3 ± 2.2	4.2 ± 0.9

Table 4.3. ***Changes in E-cadherin and Flk1 expression during early embryoid body differentiation.*** EBs were formed in hanging drops of 500 cells per drop. EBs were disassociated at particular time points and analyzed by flow cytometry to determine the number of cells expressing Flk1 and E-cadherin. No dual Flk1+ and E-cadherin+ cells were detected.

	% Positive Cells	
EB Day	**E-cadherin**	**Flk1**
ESC	98.6 ± 0.4	0.8 ± 0.3
D2.5	94.1 ± 2.3	3.1 ± 1.1
D3.5	22.8 ± 2.9	33.6 ± 4.9
D4.5	14.1 ± 2.5	19.3 ± 3.1
D5.5	13.6 ± 3.0	12.4 ± 2.9

Three distinct populations of cells were present in D3.5 EBs: $ECD^{high}Flk1^{low}$, $ECD^{low}Flk1^{high}$, and $ECD^{low}Flk1^{low}$; Flk1 and ECD were not co-expressed at high levels (Fig. 4.4A). Isolated $ECD^{high}Flk1^{low}$ cells expressed the primitive ectoderm marker *Rex1*, the neuroectodermal gene, *Pax6*, and markers of endoderm/mesendoderm, *Sox17* and *FoxA2*. The $ECD^{low}Flk1^{high}$ fraction possessed markers of the early hematopoietic and vascular lineage (*Runx1* and *Scl/Tal1*), and the early mesoderm gene *brachyury* (Fig 4.4B). These finding indicate this subpopulation represents the hemangioblast population, present *in vivo* in extraembryonic mesoderm. Cells negative for both Flk1 and ECD at D3.5 expressed *brachyury* and *FoxA2*, but not *Runx1* or *Scl/Tal1*, suggesting these cells represent non-hematopoietic/vascular mesoderm.

To determine the potential of these mesodermal populations, we deposited $ECD^{low}Flk1^{low}$ and $ECD^{low}Flk1^{high}$ cells onto OP9 stromal cells in ESC differentiation media. Isolated from mouse calvaria, OP9 cells have been shown to support differentiation of hematopoietic/vascular and cardiac cell types (Nishikawa *et al.*, 1998; Yamashita *et al.*, 2005). $ECD^{high}Flk1^{low}$ cells were excluded due to the presence of undifferentiated cells and ectodermal/endodermal lineages. After three days in culture, the $ECD^{low}Flk1^{high}$ population developed into "blast-like" groups of cells, while $ECD^{low}Flk1^{low}$ cells formed densely packed colonies (Fig 4.5A,B). After 6 days, contracting colonies appeared from $ECD^{low}Flk1^{low}$ cells, not from $ECD^{low}Flk1^{high}$ cells (Fig. 4.5C,D). In addition, X-gal staining of D3.5 $ECD^{low}Flk1^{low}$ and $ECD^{low}Flk1^{high}$ cell populations cultured for 6 days indicated endocardial differentiation was only detected in cells cultured from the D3.5 $ECD^{low}Flk1^{low}$ fraction (Fig. 4.5D). Immunofluorescence confirmed that $ECD^{low}Flk1^{high}$ cells did not generate any cardiomyocytes (Fig. 4.5E,F).

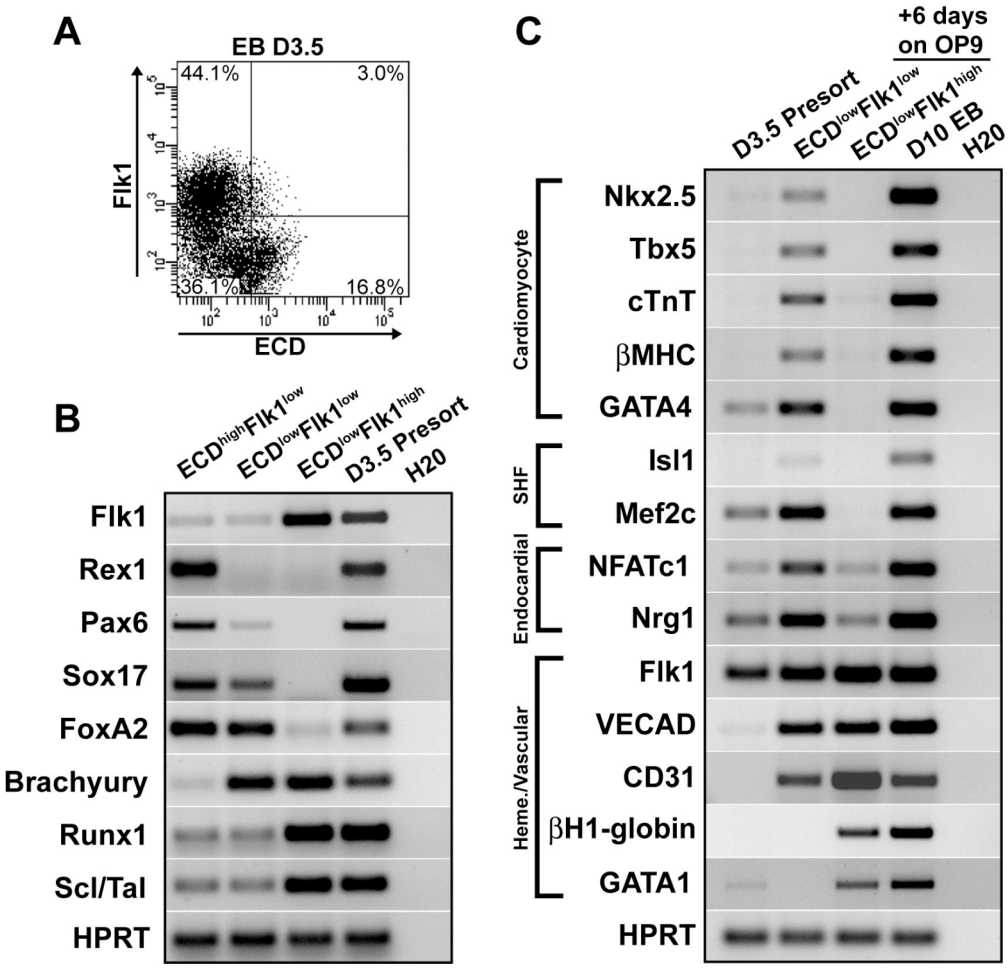

Figure 4.4. ***Isolation of hematopoietic/vascular and cardiac mesodermal precursors from differentiating ESCs.*** **A.** Serum stimulated embryoid bodies were disassociated and sorted at D3.5 by flow cytometry into fractions based on expression of Flk1 and ECD. **B**. RT-PCR of isolated D3.5 populations for markers of primitive ectoderm, neuroectoderm, endoderm, mesoderm, the early hematopoietic/vascular lineage. Controls included D3.5 presort EBs and H_2O. **C**. Gene expression analysis of $ECD^{low}Flk1^{high}$ and $ECD^{low}Flk1^{high}$ populations after 6 days of culture on OP9 stromal cells demonstrating blood and vascular differentiation in the $ECD^{low}Flk1^{high}$ cells, with endocardial and myocardial gene expression restricted to the $ECD^{low}Flk1^{low}$ population. D3.5 presort EBs, D10 EBs cultured intact on gelatin, and H_2O served as controls.

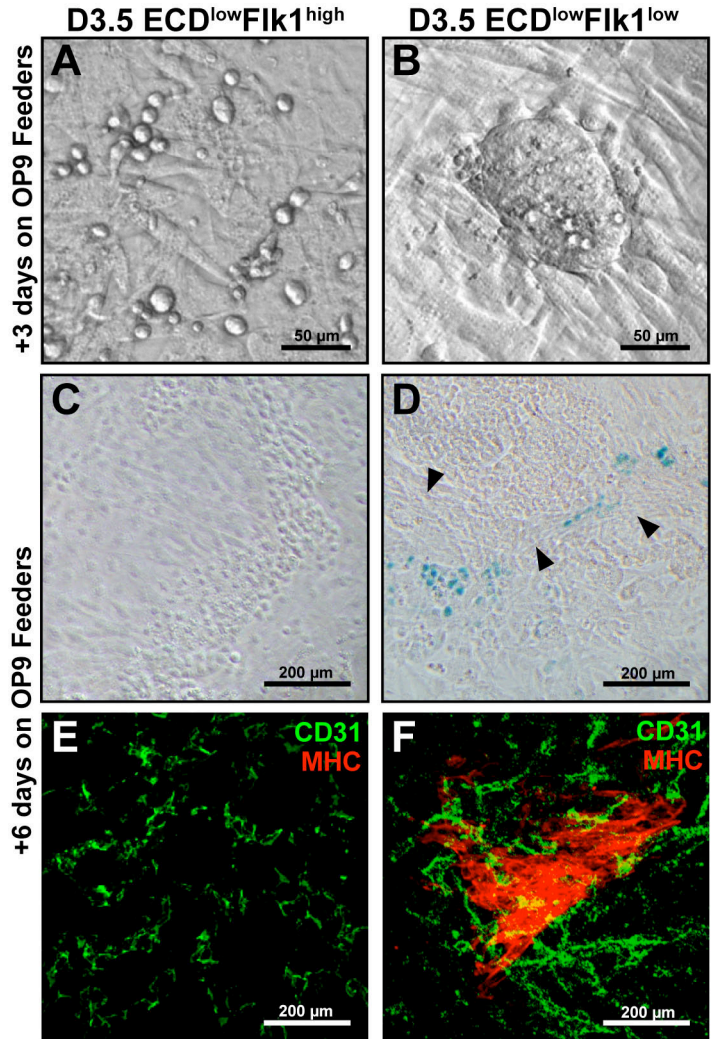

Figure 4.5. ***Characterization of endocardial, cardiomyocyte, and vascular derivatives from D3.5 ECD^{low}Flk1^{high} and ECD^{low}Flk1^{low} cell populations.*** **A,B.** ECD^{low}Flk1^{high} and ECD^{low}Flk1^{low} fractions were deposited onto OP9 stromal cells serum-containing differentiation media. Phase contrast images of characteristic "blast-like" ECD^{low}Flk1^{high} cells **(A)** and densely packed ECD^{low}Flk1^{low} cells **(B)** after 3 days of culture. **C,D**. After 6 days of culture on OP9 feeders, contracting regions (black arrowheads) appeared from ECD^{low}Flk1^{low} cells **(D)**, but not in ECD^{low}Flk1^{high} cells **(C)**. X-gal staining demonstrated endocardial differentiation was only detected in ECD^{low}Flk1^{low} cultured cell fractions. **E,F.** Immunofluorescence of CD31/Pecam-1 (green) and MHC (red) expression in cultured D3.5 ECD^{low}Flk1^{high} and ECD^{low}Flk1^{low} populations after 6 days on OP9 cells. No cardiomyocyte differentiation was detected from the ECD^{low}Flk1^{high} cell population.

Molecular expression analysis of D3.5 ECD^{low}Flk1^{low} and ECD^{low}Flk1^{high} cells after 6 days demonstrated that cardiac genes (*Nkx2.5*, *βMHC, Tbx5, cTnT, GATA4, and Mef2c)* present in ECD^{low}Flk1^{low} colonies, were absent or reduced in the D3.5 presort and ECD^{low}Flk1^{high} fraction (Fig. 4.4C). While both sort groups displayed vascular differentiation, expressing *Flk1*, *VE-cadherin*, and *CD31/Pecam-1*, only the ECD^{low}Flk1^{high} displayed markers of hematopoietic development (*βH1-globin and GATA1*). In contrast, *NFATc1* and *neuregulin1* (*Nrg1*), markers of the endocardium, were only observed in colonies generated from ECD^{low}Flk1^{low} cells with myocardial differentiation. These studies clarify that endocardium is not specified from the mesoderm that generates the hemangioblast population in contrast to zebrafish model where endocardium shares a common precursor with the hematopoietic lineage.

Endocardium and myocardium are derived from an Flk1+ mesoderm population with cardiovascular potential

Specification of cardiac mesoderm follows differentiation of the blood and vascular lineages in murine embryogenesis and EBs (Iida *et al.*, 2005; Kattman *et al.*, 2006; Tam *et al.*, 1997). To determine whether this explained the absence of cardiac derivatives from the D3.5 ECD^{low}Flk1^{high} subpopulation, we re-cultured this fraction in DM with bFGF (30 ng/ml) and VEGF (5 ng/ml) on OP9 stromal cells, and resorted for Flk1 expression 24 hours later (Fig. 4.6A). Isolated cells were cultured on OP9 stromal cells and cultured in serum-free media supplemented with VEGF (5 ng/ml), bFGF (30 ng/ml), BMP4 (50 ng/ml), and Dkk-1 (150 ng/ml), as previously described (Kattman *et al.*, 2006). As discussed in Chapter I, each of these growth factors has been shown to be essential for cardiac specification from mesoderm.

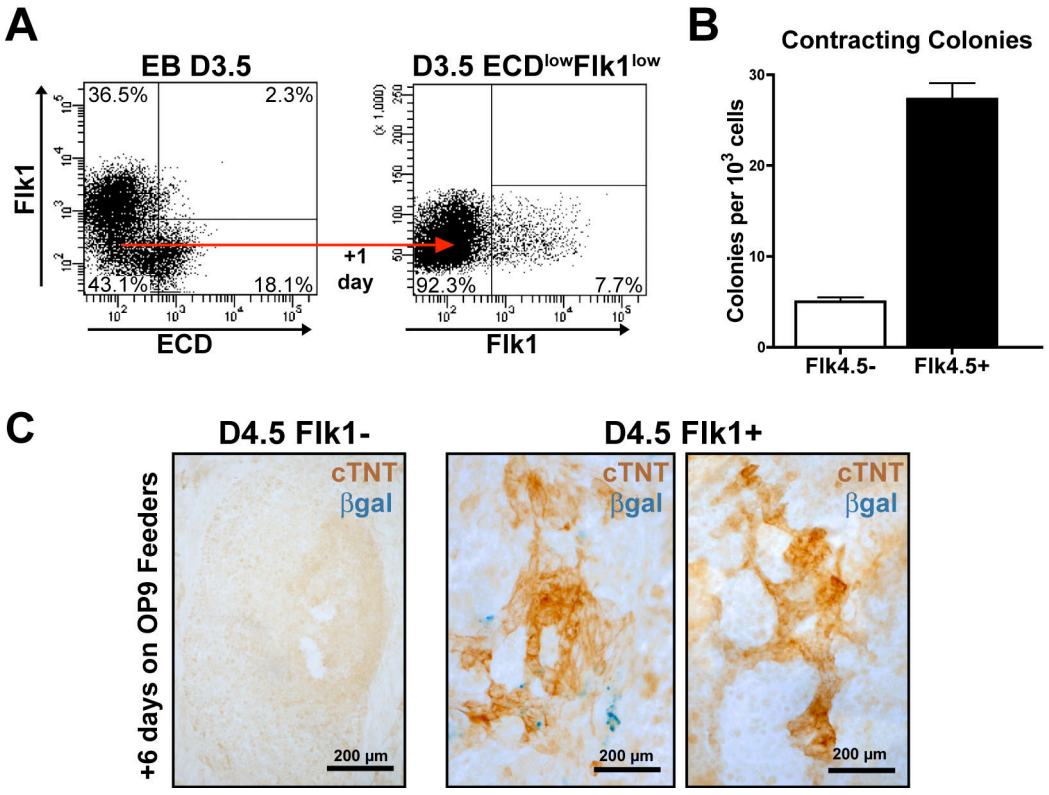

Figure 4.6. ***Isolation and characterization of Flk1+ multipotent cardiovascular progenitors.*** (**A**) D3.5 embryoid bodies were differentiated in serum-containing media, disassociated and sorted with Flk1 and ECD. $ECD^{low}Flk1^{low}$ cells were cultured for 24 hours on OP9 cells in serum-free media with bFGF and VEGF before undergoing a second sort with Flk1. (**B**) Resorted Flk1 positive and negative cells were plated at a density of $1x10^3$ cells/cm^3 onto OP9 cells in a 24-well dish in serum-free media supplemented with VEGF, bFGF, BMP4, Dkk-1. The number of contracting colonies per well was scored after 6 days in culture. *=$p < .05$ vs. control, N=12. Error bars indicate SEM. (**C**) Dual β-gal/immunoperoxidase staining of D4.5 Flk1+ and Flk1- populations from *NFATc1-nuc-LacZ* BAC ESCs after 6 days of culture to demonstrate cardiomyocyte (cTnT, brown) and endocardial (β-gal; blue) differentiation.

The number of contracting colonies present after 6 days of culture was significantly higher in the D4.5 Flk1+ population compared to the D4.5 Flk1- cells (Fig. 4.6B). Dual β-gal/immunoperoxidase staining of D4.5 Flk1+ and Flk1- populations derived from *NFATc1-nuc-LacZ* BAC ESC demonstrated cardiomyocyte differentiation in D4.5 Flk1+ cells with and without endocardial differentiation; no significant endocardial or myocardial differentiation was seen from the D4.5 Flk1- cells (Fig. 4.6C). Examining D4.5 Flk+ cells after 2, 4, and 6 days in culture, we observed early cardiac transcription factors *Nkx2.5* and *isl1* were detectable by day 2 (Fig. 4.7). While *Nkx2.5* expression increased, *isl1* was downregulated at later time points. *Tbx5* and *Mef2c*, markers of the primary and secondary heart fields, respectively, were readily detectable by day 4. This indicated not only that D4.5 Flk1+ cells contain primary and secondary heart field precursors, but also that culture conditions supported their development. In addition, cardiac contractile proteins (*βMHC* and *cTnT*) were present, indicting functional maturation of cardiomyocytes. Most importantly, genes restricted to endocardial endothelium, *NFATc1* and *Nrg1* were also present in cultures derived from D4.5 Flk1+ cells. Vascular markers (*Flk1*, *VE-cadherin*, and *CD31/Pecam-1*) became more pronounced over the course of differentiation, while hematopoietic lineages (*GATA1*) were completely absent. These findings indicate endocardium and myocardium are generated from an Flk1+ multipotent cardiovascular progenitor (MCP) population that arises from a temporally defined mesoderm population.

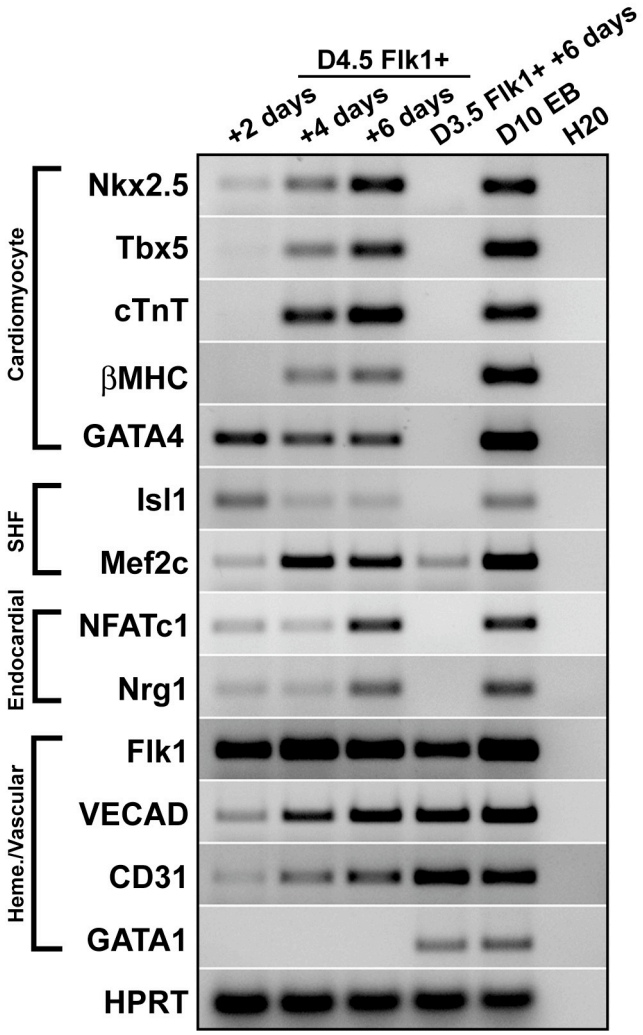

Figure 4.7. ***Temporal gene expression analysis of cultured Flk1+ MCPs.*** RT-PCR expression profile of D4.5 Flk1+ cells after 2, 4, and 6 days in culture examining endocardial, cardiac, vascular, and hematopoietic markers with D3.5 Flk1+ cultured for 6 days, D10 EBs cultured intact on gelatin, and H_2O as controls. Early cardiac transcription factors (*Nkx2.5* and *isl1*) were detected at day 2. *Nkx2.5* expression increased across the period of differentiation, while *isl1* was downregulated. Markers of the primary and secondary heart fields (*Tbx5* and *Mef2c,* respectively) were readily detectable by day 4. Cardiac contractile proteins (*βMHC* and *cTnT*) were present, indicting functional maturation of cardiomyocytes. Endocardial transcripts (*NFATc1* and *Nrg1*) were also present in cultures derived from D4.5 Flk1+ cells. Vascular markers (*Flk1*, *VE-cadherin*, and *CD31/Pecam-1*) became more pronounced over time, but hematopoietic lineages (*GATA1*) were not detected from Flk1+ MCPs.

Clonal analysis of Flk1+ MCPs indicate endocardium and myocardium share a common precursor

As the D4.5 Flk1+ fraction could contain separate Flk1+ endocardial and myocardial precursors, we performed clonal analysis to determine the potential of a given cell. Individual D4.5 Flk1+ cells from the *NFATc1-nuc-LacZ* BAC ESC line were deposited by flow cytometry into wells of a 96-well dish containing irradiated OP9 feeders, and cultured in serum-free media supplemented with VEGF, bFGF, BMP4, and Dkk-1. After 7 days, colonies were immunostained and scored for cardiomyocytes, endothelium, smooth muscle, and endocardium (MHC, CD31/Pecam-1, SM-MHC, and β-gal, respectively). Nearly 50% (42 of 90) of colonies were positive for all four cardiovascular cell lineages (Fig. 4.8A,B). Endocardial differentiation was only detected in the presence of cardiomyocytes, never in their absence. Also, not all endothelial cells that differentiated with cardiomyocytes were endocardial cells. 31 percent of colonies (28 of 90) consisted of only myogenic cell types, cardiomyocytes and smooth muscle, suggesting they were derived from a bipotential myogenic cell population. Colonies of endothelium with or without smooth muscle represented another 15 percent. The ability of individual Flk1+ cells to generate both myocardium and endocardium provides compelling evidence for the existence of a common mesodermal precursor.

Discussion

In these studies, we establish that endocardium and myocardium are derived from a common precursor in the cardiac mesoderm. Using BMP and Wnt signaling to enhance myocardial specification at the expense of blood and vasculature, we demonstrated that endocardium is specified as a specialized cardiac subpopulation, and not spatially distinct

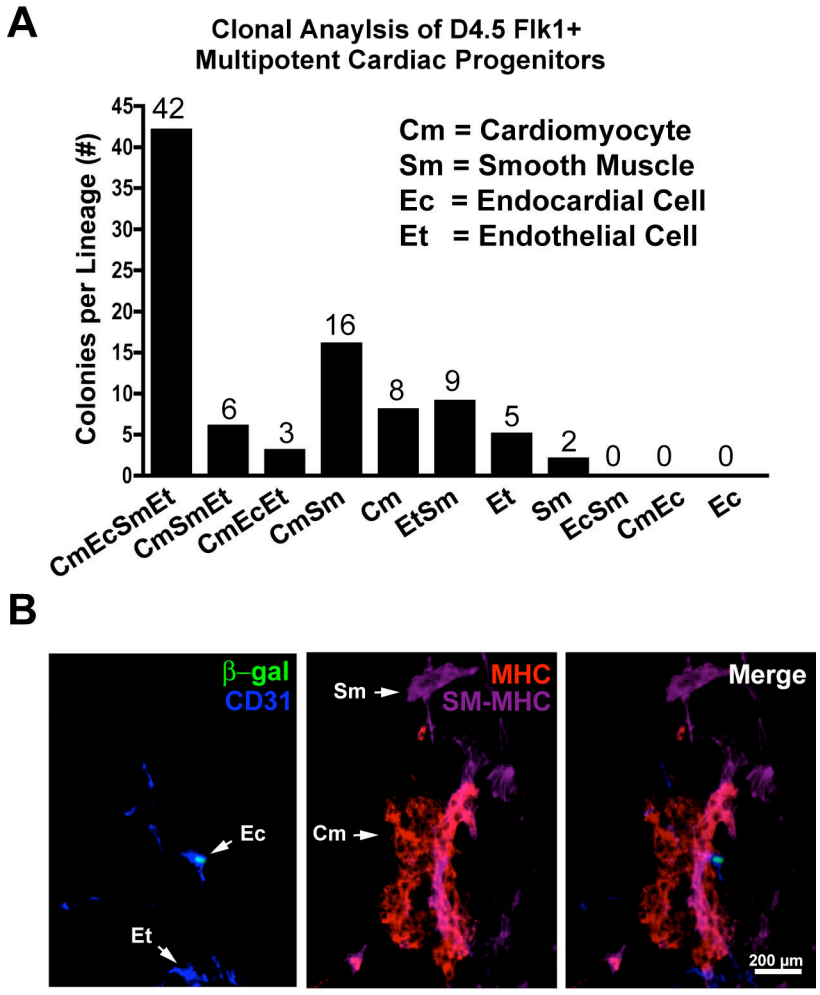

Figure 4.8. ***Clonal analysis of endocardial and myocardial potential in Flk1+ multipotent cardiovascular progenitors (MCPs).*** **A.** Single D4.5 Flk1+ cells from *NFATc1-nuc-LacZ* BAC ESCs were deposited into 96-well plates seeded with OP9 stromal cells in serum-free media supplemented with VEGF, bFGF, BMP4, and Dkk-1. After 7 days, colonies were stained and scored for the presence of endocardium (Ec), cardiomyocytes (Cm), endothelium (Et), smooth muscle (Sm). (**B**) Representative image of Flk1+ multipotent cardiovascular progenitor clone stained for endocardium (β-gal, green), cardiomyocytes (MHC), endothelium (CD31, blue), and smooth muscle (SM-MHC, purple).

endothelial cell that migrates into juxtaposition with cardiomyocytes. Endocardium is not specified from the Flk1+ mesodermal hemangioblast population giving rise to hematopoietic and endothelial lineages, but rather a temporal distinct Flk1+ mesodermal population capable of generating endocardium, myocardium, smooth muscle, and endothelium. Most importantly, we provide evidence through clonal analysis of Flk1+ multipotent cardiovascular progenitors (MCPs) that endocardium and myocardium are derived from a common Flk1+ progenitor, confirming that in the mouse these two lineages do not originate as separate populations.

The lineage classification of endocardium has remained undefined, with its obligatory role in cardiogenesis conflicting with its general classification as apart of the systemic vasculature, expressing pan-endothelial markers. Treatment of differentiating ESCs with the BMP inhibitor Noggin/Fc and Wnt inhibitor Dkk-1 indicate that endocardial cells are specified with other cardiac cell types. With early Noggin/Fc treatment and late Dkk-1, endocardial specification increased along with cardiomyocyte markers, corresponding to a reduction in hematopoietic/vascular gene expression. Conversely, late Wnt3A treatment enhanced gene expression from the blood and endothelial lineages and inhibited cardiac gene expression. Recent studies have demonstrated reciprocal signaling between cardiac and hematopoietic/vascular lineages acts to restrict lineage-specific expression (Schoenebeck *et al.*, 2007). The Ets transcription factor *Er71* has been identified to act on Flk1+ mesoderm to promote hematopoietic and vascular cell specification at the expense of cardiac differentiation (Lee *et al.*, 2008). Our results are consistent with other studies using ESC culture to document an inverse relationship between these two cell lineages, but extend that work

by examining the effect on endocardial specification (Lindsley *et al.*, 2006; Naito *et al.*, 2006; Yuasa *et al.*, 2005). Our observation that endocardial cells are derived from a cardiac lineage would appear to conflict with the recent observation of Lee *et al*., who demonstrated that when *Er71* expression is abolished in the mouse embryo, no endothelial or endocardial cells are formed, but myocardium differentiation still occurs (Lee *et al.*, 2008). However, because of *Er71's* ubiquitous expression in endothelial cells within the embryo, the specific role of *Er71* in endocardial differentiation is difficult to discern. Nonetheless, these findings suggest that similar signaling pathways might induce endocardial and myocardial specification, and that the two lineages could be derived from a common progenitor.

Flk1 identifies mesoderm that contributes to extraembryonic blood and vascular lineages, as well as endocardium and myocardium (Motoike *et al.*, 2003; Shalaby *et al.*, 1995). Progenitor populations of both lineages have been isolated from ESC derived EBs using Flk1 as a surface marker (Fehling *et al.*, 2003; Kattman *et al.*, 2006; Yamashita *et al.*, 2005). Flk1+ cells isolated from D3.5 EBs generated hematopoietic and vascular cells, but did not express endocardial or myocardial transcripts, which were enriched in the $ECD^{low}Flk1^{low}$ fraction. These findings are in agreement of those made by Kouskoff *et al*., where cardiac specification was enriched in Flk1-GFP-Byr+ cells after Flk1 depletion at D3.5, but absent when Flk1+ cells were isolated at D4-D4.5 (Kouskoff *et al.*, 2005). From these observations and our RT-PCR analysis, we concluded that the $ECD^{low}Flk1^{high}$ population at D3.5 represented the mesodermal hemangioblast lineage derived from the anterior primitive streak, while the $ECD^{low}Flk1^{low}$ fraction contained cardiac mesodermal progenitors downregulating ECD as they migrated from the PS.

Given the temporal delay of cardiac progenitors exiting the PS compared to extraembryonic mesoderm, and that Flk1 is expressed only after exiting the PS, we resorted the $ECD^{low}Flk1^{low}$ population a day later (Ema *et al.*, 2006; Kinder *et al.*, 1999). This population of Flk1+ cells was enriched for cells with cardiac potential, forming contracting colonies 6-fold over colonies generated from D4.5 Flk1- cells. Endocardial transcripts, *NFATc1* and *Nrg1*, were detected after 5 or 6 days in culture, relatively late, though still following the onset of *Nkx2.5* and *isl1* expression. We postulate that there is a critical threshold of myocardial cell differentiation necessary to induce endocardial differentiation. After two days in culture expression of early myocardial markers *Nkx2.5* and *isl1* could be detected, indicating both primary and secondary heart fields were represented, but expression of endocardial markers was minimal. Similar to an analogous study of Flk1+ MCPs, *isl1* was downregulated over the course of the course of differentiation, in a process previously attributed to inadequate culture conditions to support secondary heart field derivatives (Kattman *et al.*, 2006). However, we found that *Mef2c*, a gene expressed in secondary heart field derived myocardium, was upregulated at 4 and 6 days of culture. Expressed in secondary heart field progenitors, *isl1* is absent in myocardial later in development (Cai *et al.*, 2003). In addition, the decline in *isl1* could be attributed to the inclusion of Dkk-1 in the culture media, as Wnt signaling has been demonstrated to positive regulates *isl1*+ progenitor self-renewal (Qyang *et al.*, 2007).

Clonal populations derived from single D4.5 Flk1+ MCPs have the potential to form myocardium, endocardium, endothelium, and smooth muscle. While myocardial and endocardial cells are both generated from these progenitors, not all observed endothelial cells are endocardium. This diversity reflects the actual endothelial

heterogeneity seen the developing heart. Interestingly, endocardial cells are only detected in the presence of cardiomyocytes. This suggests that the endocardial cell lineage diverges from the cardiomyocyte lineage soon after the Flk1+ multipotent progenitors arrive at the cardiac mesoderm, as is supported by the early expression of *NFATc1* at E7.5. In addition, the lack of endocardial cells seen in the absence of cardiomyocytes implies that specification/survival of endocardium is dependent on signals from the myocardium, absent in our culture system. While these studies indicate individual Flk1+ MCPs have the ability to generate multiple cell types, the mechanism(s) regulating the divergence of these lineages is unknown. It remains to be seen how endocardial cells retain activate endocardial transcripts, while myocardial cells initiate transcription of contractile proteins.

CHAPTER V

CONCLUSIONS AND FUTURE DIRECTIONS

The primary focus of this work has been to generate novel methods to specifically identify endocardial cells from other endothelium during early development and to establish new model systems to monitor endocardiogenesis *in vivo* and *in vitro*. Previously, the lineage classification of endocardium as either a specialized cardiac cell or a spatially distinct endothelial cell remained undefined, in part due to opposing models differing on whether endocardial cells were derived from a common multipotent progenitor in the cardiac mesoderm or from two distinct precursor populations. In the studies presented here, we demonstrate that endocardium is specified as a cardiac cell lineage independent from other vascular populations. Using a novel *NFATc1-nuc-LacZ* BAC transgenic reporter mouse line, we have specifically labeled endocardial cells as they emerge from the cardiac mesoderm, and tracked their participation in early cardiac morphogenesis. With this reporter, in conjugation with other methods to monitor NFATc1 expression, we have characterized endocardiogenesis in differentiating murine ESCs, demonstrating that the close temporal-spatial relationship seen between endocardium and myocardium in the developing embryo is recapitulated in embryonic stem cell differentiation. By isolating a temporally distinct populations of Flk1+ mesoderm, we show that endocardium is not specified with hematopoietic and endothelial lineages, but rather an Flk1+ mesodermal population capable of generating endocardium, myocardium, smooth muscle, and endothelium. Our clonal analysis of

these Flk1+ multipotent cardiovascular progenitors (MCPs) indicate that endocardium and myocardium are derived from a common mesodermal progenitor and not from two separate, but parallel lineages, addressing a longstanding question in the field of cardiovascular development.

Endocardial differentiation from multipotent cardiovascular progenitors (MCPs)

The findings presented here build on recent work establishing a stepwise, hierarchical model of cardiac lineage diversification analogous to models of hematopoiesis in which all blood cells are derived from a single progenitor population. Gathering from studies of cardiac progenitors isolated from differentiating ESCs and *in vivo* fate mapping combined with our observations, we propose a working model of cardiac lineage specification from MCPs, where endocardial cells are a unique cardiac lineage (Fig. 5.1). As discussed in Chapter I, Flk1+, *Nkx2.5*+, and *isl1*+ MCPs isolated at precise time points from EBs are capable of generating cardiomyocytes, endothelium, and smooth muscle. Although these studies have significantly extended our understanding of cardiac lineage specification, they have either drawn no distinction between endocardium and endothelium or only obliquely addressed endocardiogenesis. In the analysis of expanded D4.5 GFP-Bry+ Flk1+ MCPs, Kattman *et al*. documented expression of the endocardial transcript *Nrg1* in cardiac colonies grown in methylcellulose culture conditions, which was absent in blast colonies formed from the D3.5 GFP-Bry+ Flk1+ population (Kattman *et al.*, 2006). With this finding, the authors speculated that endocardial cells were derived along with cardiomyocytes from Flk1+ MCPs. MCPs isolated from human ESCs with Flk1+ (KDR) and c-kit were also found to

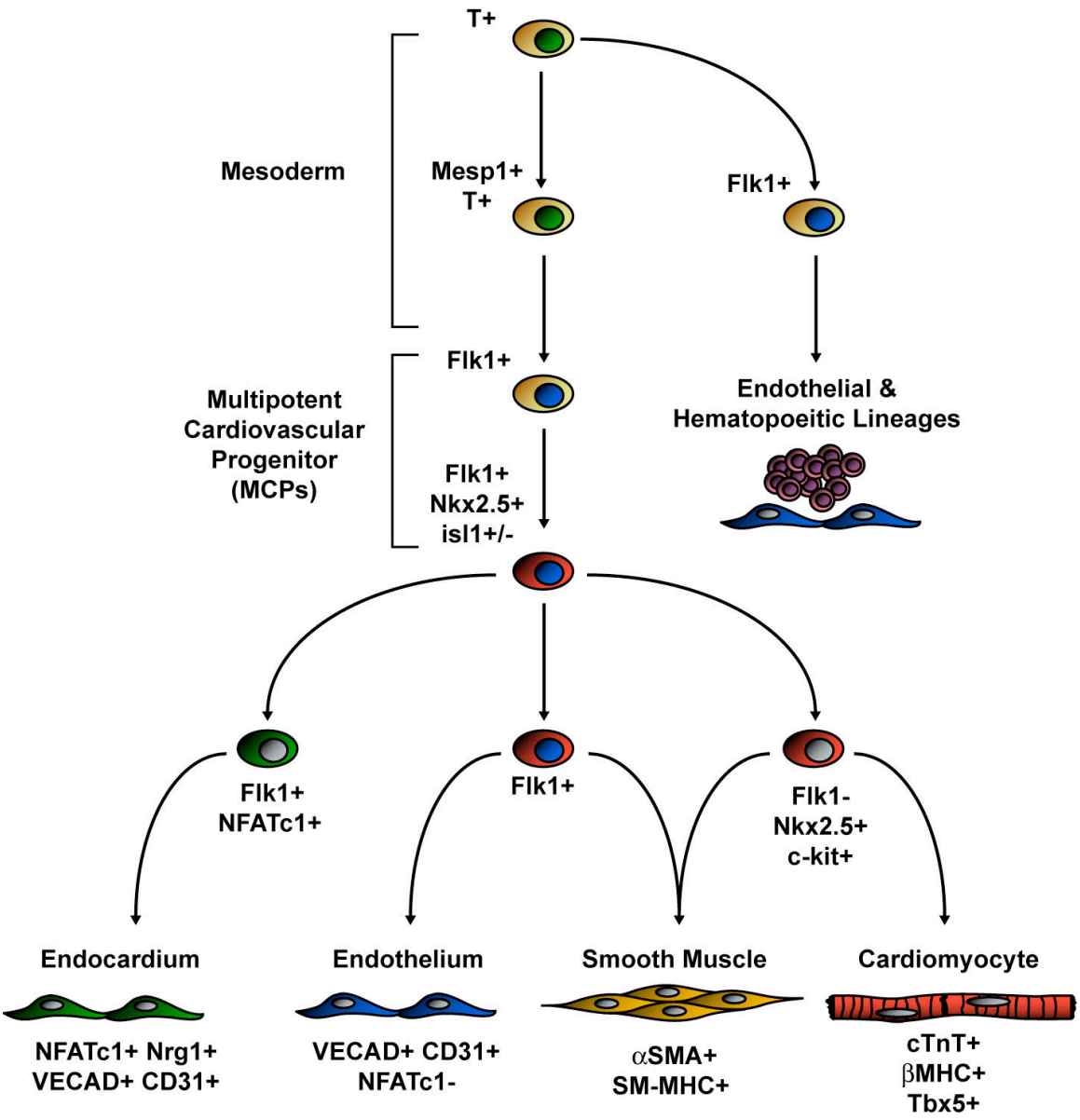

Figure 5.1. ***Working model of endocardial differentiation from multipotent cardiovascular progenitors (MCPs).*** See Chapter V text for further discussion.

express endocardial genes, specifically *NFATc1* and *Nrg1* upon further differentiation (Yang *et al.*, 2008). However, as they assessed endocardial differentiation only through RT-PCR analysis, it could not be definitely stated that endocardial cells were present in these cultures. Our findings validate these assumptions by demonstrating that endocardial cells are derived from the same Flk1+ MCPs that produce the cardiomyocyte lineage.

In agreement with other studies, our findings indicate that vascular and hematopoietic lineages are derived from an Flk1+ hemangioblast specified earlier than the Flk1+ MCP. Contrary to what has been described in zebrafish and avian systems, the endocardial cell lineage is independent from blood cell and other vascular populations. Our model depicts that Flk1+ MCPs are defined prior to *isl1*+ and *Nkx2.5*+ MCPs. Absent at D3-4 as Flk1+ mesoderm emerges, *isl1* and *Nkx2.5* appear within two days in D4.5 Flk1+ MCP-derived colonies (Fig. 4.4). This corresponds to the expression profiles of *Flk1*, *isl1*, and *Nkx2.5 in vivo*, where *Flk1* is detected in mesoderm migrating away from the PS before *isl1* and *Nkx2.5* are upregulated in the PHF and SHF at the cardiac crescent stage. Also, compared to the lineage potential of *isl1*+ MCPs, Flk1+ MCPs are less defined in terms of what type of cells they can generate; while 46% of D4.5 Flk1+ MCPs in our experiments formed cardiomyocytes, smooth muscle, and endothelial cells, only 12% of colonies generated from expansion of *isl1*+ MCPs possessed all three lineages (Moretti *et al.*, 2006).

As studies isolating *isl1*+ and *Nkx2.5*+ MCPs failed to distinguish endocardium from endothelium and examined no endocardial specific transcripts in their characterizations of cell lineages produced from these MCPs, it not possible to conclude

whether these progenitors have the potential to form endocardium (Christoforou *et al.*, 2008; Moretti *et al.*, 2006). However, fate mapping of *Nkx2.5*+ and *isl1*+ cardiac populations and expression analysis of the *NFATc1-nuc-LacZ* BAC transgenic indicates that both the PHF and SHF contribute to the endocardial lineage. Accordingly, the endocardium is depicted in our model as being generated from an Flk1+, *Nkx2.5*+ and *isl1*+ MCP, but will require further analysis for confirmation of this hypothesis.

Further specification of these MCPs establishes the endocardial, myogenic (smooth muscle and cardiomyocyte), and vascular lineages. Aside from colonies containing all 4 lineages, the next most abundant types of colonies either consisted of only myogenic cell types, cardiomyocytes and smooth muscle, or endothelium with or without smooth muscle (Fig 4.8). These findings are supported by work documenting Nkx2.5+ c-kit+ bipotential precursors of the myogenic lineage, as well as Flk1+ progenitors that yield vascular smooth muscle and endothelium (Ema *et al.*, 2003; Wu *et al.*, 2006; Yamashita *et al.*, 2000). In our clonal analysis, myocytes represented the majority of cells in each colony, with endocardial and endothelial cells seen as only a small fraction of the total number of cells. Similarly, in colonies formed from of *isl1*+ MCPs, endothelial cells were the least well represented subpopulation of the three lineages analyzed, and in colonies formed from *Nkx2.5*+ MCPs, endothelial cells made up only 15-20% of the total number of cells per colony with the rest being cardiomyocytes and smooth muscle cells (Christoforou *et al.*, 2008; Moretti *et al.*, 2006). In our model, endocardium has been designated as an independent lineage, without a transitional state as with endothelium and smooth muscle derived from the MCPs. Given the early appearance of endocardium in the cardiac crescent, in addition to its unique

expression profile, and our observation that endocardium, as opposed to endothelium, is never seen in conjugation with smooth muscle cells alone, we hypothesize that the endocardium is an entirely separate cardiac subpopulation.

The transcriptional regulation of early NFATc1 expression in endocardium

The *NFATc1-nuc-LacZ* BAC transgenic mouse described in Chapter II specifically identified endocardial precursors at the earliest stage of cardiac development by faithfully recapitulating endogenous *NFATc1* expression. However, NFATc1's expression profile is dynamic during early cardiogenesis; over time, NFATc1 is restricted from the entire endocardium to the valvular endocardium, before becoming undetectable by late-gestation (Fig. 2.6-8). Thus utilizing a direct transcriptional reporter of *NFATc1* has the inherent drawback of not identifying all endocardial cells across the window of heart development. The most efficient approach to permanently label all endocardial cells, from the earliest progenitors at E7.5 to the adult endocardium, and structural features derived from endocardial cells entails the use of Cre recombinase and a floxed lineage reporter. By crossing an *NFATc1-Cre* BAC transgenic mouse with the *R26R LacZ* reporter, a permanent genetic marker, in this case β-gal, would presumably be expressed in all endocardial cells. It remains unknown whether the adult endocardium is derived from the endocardium of the primitive heart tube or from other sources that contribute to this subpopulation in the mature heart. Lineage analysis as described above could provide a definitive answer to this question.

An *NFATc1-Cre* BAC transgenic mouse could also be employed for tissue-specific gene knockout analyses. Presently, the only option available to excise floxed

alleles to elucidate the function of a particular gene in the developing endocardium relies on transgenic mice with Cre driven by vascular promoters, such as *Tie1* and *Tie2*. However, this approach deletes the gene not only in the endocardium, but also in embryonic endothelium and the yolk sac vasculature, making resulting phenotypes difficult to interpret as endocardial-specific gene deficits (Jiao *et al.*, 2006). A Cre recombinase driven by the *NFATc1* BAC would provide specificity unique among Cre deleter lines, targeting a subpopulation of the embryonic vasculature at its earliest stage of development. An *NFATc1-Cre* BAC transgene was constructed and was injected into mouse pronuclei with the aim of generating a stable mouse line. No PCR+ offspring were born after several rounds of injections. Recently, we have renewed our efforts to generate this mouse line, and if successful, it will represent a powerful new tool for studying the function of genes in the endocardium of the developing heart.

While BACs carry a sizeable amount of the genetic information, including protein encoding regions and a large portion of their surrounding cis-regulatory elements, they still are finite. Thus, the *NFATc1* BAC utilized in these experiments represents a starting point for deletional analysis to locate the regulatory domain necessary to govern expression in endocardial precursors. Two different, but complementary approaches would be appropriate for these studies. Either the *galK* system could be employed to generate large-scale deletions in the BAC, or fragments from the 5' UTR could be subcloned in front of a *HSP* promoter and a reporter gene (Warming *et al.*, 2005). Previous enhancer studies have relied on mouse transgenesis to evaluate fragments for proper expression, and while that is possible in this case, this approach requires significant time and financial commitment. With the characterization of

endocardiogenesis in EBs, fragments could be efficiently evaluated in ESCs prior to final confirmation in mice. Identification of the regulatory region that controls early endocardial expression of NFATc1 could provide valuable information regarding the transcriptional control of endocardial differentiation. An analogous study utilizing the method described here isolated a SHF enhancer from a Mef2c BAC and demonstrated the mechanism by which early cardiac transcription factors, isl1 and GATA4 modulate *Mef2c* expression (Dodou *et al.*, 2004). As virtually nothing is known regarding the transcriptional control of early NFATc1 expression and endocardial differentiation, identification and mutational analysis of putative transcription factor binding sites within this regulatory element might provide new targets for study.

Characterization of ESC-derived endocardial cells

The differentiation of ESCs obtained from *NFATc1-nuc-LacZ* BAC transgenic mice and ESCs carrying stable BAC transgenes provides evidence that the NFATc1+ cells seen in EBs represent endocardial cells. However, as both cardiomyocytes and endothelial cells formed in EBs have been determined to maintain immature phenotypes, it remains unclear whether these ESC-derived endocardial cells are functional. To characterize further endocardial cells generated from EBs, we had planned to utilize ESCs with an *NFATc1* BAC fluorescent reporter to isolate cells by FACS. Though technical issues have prevented significant progress at this time, several lines of investigation are possible in the near future. Given an ESC line with a working *NFATc1-Venus-yfp* BAC transgene, YFP+ cells also positive for CD31/Pecam-1 could be distinguished and isolated from cells only expressing CD31/Pecam-1, allowing direct

comparisons of endocardial cells from endothelium. RNA harvested from these two subpopulations could then be subjected to microarray analysis to compare and contrast their expression profiles. The use of polony multiplex analysis of gene expression (PMAGE), a strategy that combines tagged beads with serial analysis of gene expression (SAGE) sequencing, would be able to detect rare transcripts and avoid issues with cross-hybridization that can lead to errors seen with microarrays (Kim *et al.*, 2007). Transcriptional profiling of these endocardial cells could provide new insights into how the endocardium is specified and identify genes involved in that process.

The functional capacity of ESC-derived endocardial cells would be best examined with *in vitro* collagen gel assays (Camenisch *et al.*, 2002). Endocardial cells of the AVC and OFT are unique among endothelium in their ability to under EMT and migrate into the underlying ECM of the cardiac jelly. The collagen gel assay has been used extensively with cushion explants from avian hearts to assess factors that affect EMT. Depositing YFP+/CD31+ endocardial cells isolated by FACS from differentiating *NFATc1-Venus-yfp* BAC ESCs onto collagen gels could determine their competence to respond to signals that induce EMT. The addition of a marker from endocardial cushion cells would facilitate the identification of a mesenchymal phenotype. *Snail1*, a transcription factor that regulates mesenchymal properties in cells, is expressed in cushion cells but not the overlying endocardium (Timmerman *et al.*, 2004). At present, a *Snail1* reporter transgene is under construction in our laboratory to be used to label cells of the endocardial cushion; combined with the *NFATc1* BAC reporter, this transgene will allow further characterization of mechanisms involved in the EMT of endocardial cells at the initiation of valve development.

While these experiments aim to test whether endocardial cells obtained from EBs are functionally comparable to their *in vivo* counterparts, it does not address the endocardial-myocardial interactions governing cardiac cell differentiation. To ascertain how signals from endocardial cells affect myocardial differentiation and growth in EBs, endocardial cells could be selectively ablated as they differentiate from mesodermal precursors. Differentiating ESCs containing an *NFATc1* BAC transgene driving the *puΔtk* suicide gene, a fusion of puromycin N-acetyltransferase and a truncated Herpes Simplex Virus thymidine kinase (HSVtk), would allow for endocardial ablation at critical periods of differentiation, temporally controlled by administration of the prodrug ganciclovir (GCV) (Chen and Bradley, 2000; Chen *et al.*, 2004). If the dramatic effect of paracrine signaling from endocardium to myocardium seen during latter development *in vivo,* as described in Chapter I, is recapitulated during early cardiac differentiation in EBs, the effect of endocardial ablation on myocardial differentiation would be expected to attenuate either early stages of differentiation and proliferation or progression to latter stages of myocardial maturation.

While murine ESCs are a robust and well-defined system for studying basic processes of development particularly lineage specification, they are not applicable to studying genetic and epigenetic origins of human disease or for use in regenerative treatments. As numerous technical and ethical issues surround the use of human ESCs, a subject beyond the scope of this discussion, it necessitates the identification of alternative sources of progenitor cells. The most radical and exciting alternative to human ESCs came with the recent discovery that human skin fibroblasts virally infected with constructs constitutively expressing *Oct3/4*, *Sox2*, *Klf4*, and *c-Myc* could be converted to

a human ES cell-like state (Takahashi *et al.*, 2007; Yu *et al.*, 2007). Termed induced pluripotent stem cells (iPS), these cells are capable of generating multiple cell lineages upon differentiation *in vitro* and form teratomas *in vivo* similar to human ESCs. Originally obtained from normal human subjects, iPS cells have now also been isolated from human subjects with genetic diseases including adenosine deaminase deficiency-related severe combined immunodeficiency (SCID), Duchenne and Becker muscular dystrophy, Parkinson disease, Huntington disease, and type 1 diabetes mellitus among others (Park *et al.*, 2008). As disease-specific iPS cells can produce genetically comparable tissues of actual patients *in vitro*, they represent a remarkable model to study mechanisms of cell differentiation and function under pathologic conditions. The isolation of iPS cells from patients born with CHD, specifically those with valve defects, could serve to demonstrate how deficit endocardial function might result in this type congenital defect.

Regulation of MCPs and lineage divergence

Flk1+ MCPs isolated from differentiating ESCs possess the ability to generate myocardium, endocardium, endothelium, and smooth muscle under the appropriate culture conditions. However, the mechanism governing the divergence of endocardium and myocardium from these progenitors remains unknown. The transcription factor *Er71* has recently been suggested to act as a regulator of endocardial and endothelial fate from cardiac progenitors (Ferdous & Garry, unpublished). *Nkx2.5* binds to an evolutionarily conserved homeodomain element in the *Er71* promoter to activate transcription. Overexpression of Er71 in EBs consequently results in enhanced endothelial specification

with coincidentally decreases in cardiomyocyte differentiation. Interestingly, Er71 has also been identified as a positive regulator of Flk1+ mesoderm *in vitro* and *in vivo* (Lee *et al.*, 2008). To confirm whether Er71 might regulate the divergence of endocardium and myocardium, Flk1+ MCPs could be procured from ESCs containing the *Er71* coding region under the control of an inducible promoter to determine if *Er71* might direct MCPs towards an endocardial/endocardial fate.

In the clonal analysis of the D4.5 Flk1+ MCPs, no colonies made of endocardial cells with or without other endothelial cells were observed. In fact, endocardium was only detected in the presence of cardiomyocytes, implying that specification/survival of endocardium is dependent on signals from the myocardium or from other factors absent in our culture system. Exposing Flk1+ MCPs to various extracellular growth factors at differentiation concentrations could provide insight into the signals required for endocardial specification. ESCs with the *NFATc1-mCherry* BAC as a marker for endocardium and the *Nkx2.5* or *MHC* promoter driving GFP to designate myocardium would be useful for high throughput analysis of these experiments. To use a candidate gene approach instead a screen, TGF-βs-1/2/3 would be of most interest as they have previously been demonstrated to enhance endocardial specification from mesoderm where BMP-2, FGF-2, and VEGF did not (Sugi and Markwald, 2003). These experiments, in concert with other mentioned here, could clarify the underlying mechanisms of endocardiogenesis and further define how interactions between the endocardium and myocardium shape cardiac morphogenesis.

Concluding remarks

Characterizing cardiac stem cells is foundational to understanding the mechanisms of cardiac lineage specification, and for development of rational therapeutic strategies for the treatment of cardiovascular disease. The work we have described here has relevance not only to the field of cardiac developmental biology, but potentially has significant implications for the field of regenerative medicine. The ability to identify the endocardium at the onset of differentiation and throughout subsequent stages of development will allow for the precise delineation of the critical mechanisms involved in the ontogeny of this unique population. In addition, as an abundance of evidence has emphasized the role of endocardial-myocardial interactions in regulating later cardiac morphogenic events, the models and tools generated in these studies can be used to further elucidate how these two lineages interact at the earliest stages of development is essential. With experimental evidence suggesting that paracrine signals from the endocardium to the myocardium during development can rescue genetic defects of myocardium that are lethal *in utero*, the manipulation of endocardial-myocardial interactions during stem cell differentiation might be a viable strategy to enhance the regenerative potential of stem cell based replacement therapy (Chien *et al.*, 2004; Fraidenraich *et al.*, 2004). In conclusion, these studies provide a framework to further investigate the unique characteristics of endocardial specification and differentiation that are essential for understanding basic processes of heart development and congenital heart disease.

BIBLIOGRAPHY

Akiyama, H., Chaboissier, M. C., Behringer, R. R., Rowitch, D. H., Schedl, A., Epstein, J. A., and de Crombrugghe, B. (2004). Essential role of Sox9 in the pathway that controls formation of cardiac valves and septa. Proc Natl Acad Sci U S A *101*, 6502-6507.

Armstrong, E. J., and Bischoff, J. (2004). Heart valve development: endothelial cell signaling and differentiation. Circ Res *95*, 459-470.

Auerbach, A. B., Norinsky, R., Ho, W., Losos, K., Guo, Q., Chatterjee, S., and Joyner, A. L. (2003). Strain-dependent differences in the efficiency of transgenic mouse production. Transgenic Res *12*, 59-69.

Balconi, G., Spagnuolo, R., and Dejana, E. (2000). Development of endothelial cell lines from embryonic stem cells: A tool for studying genetically manipulated endothelial cells in vitro. Arterioscler Thromb Vasc Biol *20*, 1443-1451.

Baldwin, H. S. (1996). Early embryonic vascular development. Cardiovasc Res *31 Spec No*, E34-45.

Baldwin, H. S., Shen, H. M., Yan, H. C., DeLisser, H. M., Chung, A., Mickanin, C., Trask, T., Kirschbaum, N. E., Newman, P. J., Albelda, S. M., and et al. (1994). Platelet endothelial cell adhesion molecule-1 (PECAM-1/CD31): alternatively spliced, functionally distinct isoforms expressed during mammalian cardiovascular development. Development *120*, 2539-2553.

Barnett, J. V., and Desgrosellier, J. S. (2003). Early events in valvulogenesis: a signaling perspective. Birth Defects Res C Embryo Today *69*, 58-72.

Barron, M., Gao, M., and Lough, J. (2000). Requirement for BMP and FGF signaling during cardiogenic induction in non-precardiac mesoderm is specific, transient, and cooperative. Dev Dyn *218*, 383-393.

Beals, C. R., Clipstone, N. A., Ho, S. N., and Crabtree, G. R. (1997). Nuclear localization of NF-ATc by a calcineurin-dependent, cyclosporin-sensitive intramolecular interaction. Genes Dev *11*, 824-834.

Ben-Shachar, G., Arcilla, R. A., Lucas, R. V., and Manasek, F. J. (1985). Ventricular trabeculations in the chick embryo heart and their contribution to ventricular and muscular septal development. Circ Res *57*, 759-766.

Bishop, C. E., Whitworth, D. J., Qin, Y., Agoulnik, A. I., Agoulnik, I. U., Harrison, W. R., Behringer, R. R., and Overbeek, P. A. (2000). A transgenic insertion upstream of sox9 is associated with dominant XX sex reversal in the mouse. Nat Genet *26*, 490-494.

Bjarnegard, M., Enge, M., Norlin, J., Gustafsdottir, S., Fredriksson, S., Abramsson, A., Takemoto, M., Gustafsson, E., Fassler, R., and Betsholtz, C. (2004). Endothelium-specific ablation of PDGFB leads to pericyte loss and glomerular, cardiac and placental abnormalities. Development *131*, 1847-1857.

Boheler, K. R., Czyz, J., Tweedie, D., Yang, H. T., Anisimov, S. V., and Wobus, A. M. (2002). Differentiation of pluripotent embryonic stem cells into cardiomyocytes. Circ Res *91*, 189-201.

Bondue, A., Lapouge, G., Paulissen, C., Semeraro, C., Iacovino, M., Kyba, M., and Blanpain, C. (2008). Mesp1 acts as a master regulator of multipotent cardiovascular progenitor specification. Cell Stem Cell *3*, 69-84.

Bradley, A., Evans, M., Kaufman, M. H., and Robertson, E. (1984). Formation of germ-line chimaeras from embryo-derived teratocarcinoma cell lines. Nature *309*, 255-256.

Brand, T. (2003). Heart development: molecular insights into cardiac specification and early morphogenesis. Dev Biol *258*, 1-19.

Brannan, C. I., Perkins, A. S., Vogel, K. S., Ratner, N., Nordlund, M. L., Reid, S. W., Buchberg, A. M., Jenkins, N. A., Parada, L. F., and Copeland, N. G. (1994). Targeted disruption of the neurofibromatosis type-1 gene leads to developmental abnormalities in heart and various neural crest-derived tissues. Genes Dev *8*, 1019-1029.

Brown, C. B., and Baldwin, H. S. (2006). Neural crest contribution to the cardiovascular system. Adv Exp Med Biol *589*, 134-154.

Brown, C. B., Boyer, A. S., Runyan, R. B., and Barnett, J. V. (1999). Requirement of type III TGF-beta receptor for endocardial cell transformation in the heart. Science *283*, 2080-2082.

Bruneau, B. G., Nemer, G., Schmitt, J. P., Charron, F., Robitaille, L., Caron, S., Conner, D. A., Gessler, M., Nemer, M., Seidman, C. E., and Seidman, J. G. (2001). A murine model of Holt-Oram syndrome defines roles of the T-box transcription factor Tbx5 in cardiogenesis and disease. Cell *106*, 709-721.

Buckingham, M., Meilhac, S., and Zaffran, S. (2005). Building the mammalian heart from two sources of myocardial cells. Nat Rev Genet *6*, 826-835.

Bussmann, J., Bakkers, J., and Schulte-Merker, S. (2007). Early endocardial morphogenesis requires Scl/Tal1. PLoS Genet *3*, e140.

Cai, C. L., Liang, X., Shi, Y., Chu, P. H., Pfaff, S. L., Chen, J., and Evans, S. (2003). Isl1 identifies a cardiac progenitor population that proliferates prior to differentiation and contributes a majority of cells to the heart. Dev Cell *5*, 877-889.

Camenisch, T. D., Molin, D. G., Person, A., Runyan, R. B., Gittenberger-de Groot, A. C., McDonald, J. A., and Klewer, S. E. (2002). Temporal and distinct TGFbeta ligand

requirements during mouse and avian endocardial cushion morphogenesis. Dev Biol *248*, 170-181.

Chandler, K. J., Chandler, R. L., Broeckelmann, E. M., Hou, Y., Southard-Smith, E. M., and Mortlock, D. P. (2007). Relevance of BAC transgene copy number in mice: transgene copy number variation across multiple transgenic lines and correlations with transgene integrity and expression. Mamm Genome *18*, 693-708.

Chang, C. P., Neilson, J. R., Bayle, J. H., Gestwicki, J. E., Kuo, A., Stankunas, K., Graef, I. A., and Crabtree, G. R. (2004). A field of myocardial-endocardial NFAT signaling underlies heart valve morphogenesis. Cell *118*, 649-663.

Chen, Y. T., and Bradley, A. (2000). A new positive/negative selectable marker, puDeltatk, for use in embryonic stem cells. Genesis *28*, 31-35.

Chen, Y. T., Levasseur, R., Vaishnav, S., Karsenty, G., and Bradley, A. (2004). Bigenic Cre/loxP, puDeltatk conditional genetic ablation. Nucleic Acids Res *32*, e161.

Chien, K. R., Moretti, A., and Laugwitz, K. L. (2004). Development. ES cells to the rescue. Science *306*, 239-240.

Choi, K., Kennedy, M., Kazarov, A., Papadimitriou, J. C., and Keller, G. (1998). A common precursor for hematopoietic and endothelial cells. Development *125*, 725-732.

Christoffels, V. M., Keijser, A. G., Houweling, A. C., Clout, D. E., and Moorman, A. F. (2000). Patterning the embryonic heart: identification of five mouse Iroquois homeobox genes in the developing heart. Dev Biol *224*, 263-274.

Christoforou, N., Miller, R. A., Hill, C. M., Jie, C. C., McCallion, A. S., and Gearhart, J. D. (2008). Mouse ES cell-derived cardiac precursor cells are multipotent and facilitate identification of novel cardiac genes. J Clin Invest *118*, 894-903.

Chuvpilo, S., Avots, A., Berberich-Siebelt, F., Glockner, J., Fischer, C., Kerstan, A., Escher, C., Inashkina, I., Hlubek, F., Jankevics, E*., et al.* (1999a). Multiple NF-ATc isoforms with individual transcriptional properties are synthesized in T lymphocytes. J Immunol *162*, 7294-7301.

Chuvpilo, S., Jankevics, E., Tyrsin, D., Akimzhanov, A., Moroz, D., Jha, M. K., Schulze-Luehrmann, J., Santner-Nanan, B., Feoktistova, E., Konig, T*., et al.* (2002). Autoregulation of NFATc1/A expression facilitates effector T cells to escape from rapid apoptosis. Immunity *16*, 881-895.

Chuvpilo, S., Zimmer, M., Kerstan, A., Glockner, J., Avots, A., Escher, C., Fischer, C., Inashkina, I., Jankevics, E., Berberich-Siebelt, F*., et al.* (1999b). Alternative polyadenylation events contribute to the induction of NF-ATc in effector T cells. Immunity *10*, 261-269.

Ciruna, B., and Rossant, J. (2001). FGF signaling regulates mesoderm cell fate specification and morphogenetic movement at the primitive streak. Dev Cell *1*, 37-49.

Coffin, J. D., and Poole, T. J. (1988). Embryonic vascular development: immunohistochemical identification of the origin and subsequent morphogenesis of the major vessel primordia in quail embryos. Development *102*, 735-748.

Coffin, J. D., and Poole, T. J. (1991). Endothelial cell origin and migration in embryonic heart and cranial blood vessel development. Anat Rec *231*, 383-395.

Cohen, E. D., Tian, Y., and Morrisey, E. E. (2008). Wnt signaling: an essential regulator of cardiovascular differentiation, morphogenesis and progenitor self-renewal. Development *135*, 789-798.

Cohen-Gould, L., and Mikawa, T. (1996). The fate diversity of mesodermal cells within the heart field during chicken early embryogenesis. Dev Biol *177*, 265-273.

Colvin, J. S., White, A. C., Pratt, S. J., and Ornitz, D. M. (2001). Lung hypoplasia and neonatal death in Fgf9-null mice identify this gene as an essential regulator of lung mesenchyme. Development *128*, 2095-2106.

Copeland, N. G., Jenkins, N. A., and Court, D. L. (2001). Recombineering: a powerful new tool for mouse functional genomics. Nat Rev Genet *2*, 769-779.

Court, D. L., Sawitzke, J. A., and Thomason, L. C. (2002). Genetic engineering using homologous recombination. Annu Rev Genet *36*, 361-388.

Crabtree, G. R., and Olson, E. N. (2002). NFAT signaling: choreographing the social lives of cells. Cell *109 Suppl*, S67-79.

David, R., Brenner, C., Stieber, J., Schwarz, F., Brunner, S., Vollmer, M., Mentele, E., Muller-Hocker, J., Kitajima, S., Lickert, H*., et al.* (2008). MesP1 drives vertebrate cardiovascular differentiation through Dkk-1-mediated blockade of Wnt-signalling. Nat Cell Biol *10*, 338-345.

de la Pompa, J. L., Timmerman, L. A., Takimoto, H., Yoshida, H., Elia, A. J., Samper, E., Potter, J., Wakeham, A., Marengere, L., Langille, B. L*., et al.* (1998). Role of the NF-ATc transcription factor in morphogenesis of cardiac valves and septum. Nature *392*, 182-186.

Dell'Era, P., Ronca, R., Coco, L., Nicoli, S., Metra, M., and Presta, M. (2003). Fibroblast growth factor receptor-1 is essential for in vitro cardiomyocyte development. Circ Res *93*, 414-420.

Deng, C. X., Wynshaw-Boris, A., Shen, M. M., Daugherty, C., Ornitz, D. M., and Leder, P. (1994). Murine FGFR-1 is required for early postimplantation growth and axial organization. Genes Dev *8*, 3045-3057.

Dodou, E., Verzi, M. P., Anderson, J. P., Xu, S. M., and Black, B. L. (2004). Mef2c is a direct transcriptional target of ISL1 and GATA factors in the anterior heart field during mouse embryonic development. Development *131*, 3931-3942.

Doetschman, T. C., Eistetter, H., Katz, M., Schmidt, W., and Kemler, R. (1985). The in vitro development of blastocyst-derived embryonic stem cell lines: formation of visceral yolk sac, blood islands and myocardium. J Embryol Exp Morphol *87*, 27-45.

Drake, C. J., Brandt, S. J., Trusk, T. C., and Little, C. D. (1997). TAL1/SCL is expressed in endothelial progenitor cells/angioblasts and defines a dorsal-to-ventral gradient of vasculogenesis. Dev Biol *192*, 17-30.

Eisenberg, C. A., and Bader, D. M. (1996). Establishment of the mesodermal cell line QCE-6. A model system for cardiac cell differentiation. Circ Res *78*, 205-216.

Ema, M., Faloon, P., Zhang, W. J., Hirashima, M., Reid, T., Stanford, W. L., Orkin, S., Choi, K., and Rossant, J. (2003). Combinatorial effects of Flk1 and Tal1 on vascular and hematopoietic development in the mouse. Genes Dev *17*, 380-393.

Ema, M., Takahashi, S., and Rossant, J. (2006). Deletion of the selection cassette, but not cis-acting elements, in targeted Flk1-lacZ allele reveals Flk1 expression in multipotent mesodermal progenitors. Blood *107*, 111-117.

Evans, M. J., and Kaufman, M. H. (1981). Establishment in culture of pluripotential cells from mouse embryos. Nature *292*, 154-156.

Fehling, H. J., Lacaud, G., Kubo, A., Kennedy, M., Robertson, S., Keller, G., and Kouskoff, V. (2003). Tracking mesoderm induction and its specification to the hemangioblast during embryonic stem cell differentiation. Development *130*, 4217-4227.

Ferrara, N., Gerber, H. P., and LeCouter, J. (2003). The biology of VEGF and its receptors. Nat Med *9*, 669-676.

Firulli, A. B., McFadden, D. G., Lin, Q., Srivastava, D., and Olson, E. N. (1998). Heart and extra-embryonic mesodermal defects in mouse embryos lacking the bHLH transcription factor Hand1. Nat Genet *18*, 266-270.

Fraidenraich, D., Stillwell, E., Romero, E., Wilkes, D., Manova, K., Basson, C. T., and Benezra, R. (2004). Rescue of cardiac defects in id knockout embryos by injection of embryonic stem cells. Science *306*, 247-252.

Furuta, Y., and Behringer, R. R. (2005). Recent innovations in tissue-specific gene modifications in the mouse. Birth Defects Res C Embryo Today *75*, 43-57.

Gassmann, M., Casagranda, F., Orioli, D., Simon, H., Lai, C., Klein, R., and Lemke, G. (1995). Aberrant neural and cardiac development in mice lacking the ErbB4 neuregulin receptor. Nature *378*, 390-394.

George, E. L., Baldwin, H. S., and Hynes, R. O. (1997). Fibronectins are essential for heart and blood vessel morphogenesis but are dispensable for initial specification of precursor cells. Blood *90*, 3073-3081.

Giraldo, P., and Montoliu, L. (2001). Size matters: use of YACs, BACs and PACs in transgenic animals. Transgenic Res *10*, 83-103.

Gitler, A. D., Zhu, Y., Ismat, F. A., Lu, M. M., Yamauchi, Y., Parada, L. F., and Epstein, J. A. (2003). Nf1 has an essential role in endothelial cells. Nat Genet *33*, 75-79.

Grego-Bessa, J., Luna-Zurita, L., del Monte, G., Bolos, V., Melgar, P., Arandilla, A., Garratt, A. N., Zang, H., Mukouyama, Y. S., Chen, H*., et al.* (2007). Notch signaling is essential for ventricular chamber development. Dev Cell *12*, 415-429.

Griffin, C., Kleinjan, D. A., Doe, B., and van Heyningen, V. (2002). New 3' elements control Pax6 expression in the developing pretectum, neural retina and olfactory region. Mech Dev *112*, 89-100.

Harvey, R. P. (2002). Patterning the vertebrate heart. Nat Rev Genet *3*, 544-556.

Hatzopoulos, A. K., Folkman, J., Vasile, E., Eiselen, G. K., and Rosenberg, R. D. (1998). Isolation and characterization of endothelial progenitor cells from mouse embryos. Development *125*, 1457-1468.

Hertig, C. M., Kubalak, S. W., Wang, Y., and Chien, K. R. (1999). Synergistic roles of neuregulin-1 and insulin-like growth factor-I in activation of the phosphatidylinositol 3-kinase pathway and cardiac chamber morphogenesis. J Biol Chem *274*, 37362-37369.

Heymann, D., Guicheux, J., Gouin, F., Passuti, N., and Daculsi, G. (1998). Cytokines, growth factors and osteoclasts. Cytokine *10*, 155-168.

Hoch, R. V., and Soriano, P. (2003). Roles of PDGF in animal development. Development *130*, 4769-4784.

Hoffman, J. I., and Kaplan, S. (2002). The incidence of congenital heart disease. J Am Coll Cardiol *39*, 1890-1900.

Hogan, B. (1994). Manipulating the mouse embryo: a laboratory manual, 2nd edn (Plainview, N.Y.: Cold Spring Harbor Laboratory Press).

Hogan, P. G., Chen, L., Nardone, J., and Rao, A. (2003). Transcriptional regulation by calcium, calcineurin, and NFAT. Genes Dev *17*, 2205-2232.

Holtzman, N. G., Schoenebeck, J. J., Tsai, H. J., and Yelon, D. (2007). Endocardium is necessary for cardiomyocyte movement during heart tube assembly. Development *134*, 2379-2386.

Horsley, V., Aliprantis, A. O., Polak, L., Glimcher, L. H., and Fuchs, E. (2008). NFATc1 balances quiescence and proliferation of skin stem cells. Cell *132*, 299-310.

Houweling, A. C., Dildrop, R., Peters, T., Mummenhoff, J., Moorman, A. F., Ruther, U., and Christoffels, V. M. (2001). Gene and cluster-specific expression of the Iroquois family members during mouse development. Mech Dev *107*, 169-174.

Huber, O., Bierkamp, C., and Kemler, R. (1996). Cadherins and catenins in development. Curr Opin Cell Biol *8*, 685-691.

Iida, M., Heike, T., Yoshimoto, M., Baba, S., Doi, H., and Nakahata, T. (2005). Identification of cardiac stem cells with FLK1, CD31, and VE-cadherin expression during embryonic stem cell differentiation. Faseb J *19*, 371-378.

Iwamoto, R., Yamazaki, S., Asakura, M., Takashima, S., Hasuwa, H., Miyado, K., Adachi, S., Kitakaze, M., Hashimoto, K., Raab, G.*, et al.* (2003). Heparin-binding EGF-like growth factor and ErbB signaling is essential for heart function. Proc Natl Acad Sci U S A *100*, 3221-3226.

Jackson, L. F., Qiu, T. H., Sunnarborg, S. W., Chang, A., Zhang, C., Patterson, C., and Lee, D. C. (2003). Defective valvulogenesis in HB-EGF and TACE-null mice is associated with aberrant BMP signaling. Embo J *22*, 2704-2716.

Jaenisch, R., and Young, R. (2008). Stem cells, the molecular circuitry of pluripotency and nuclear reprogramming. Cell *132*, 567-582.

Jiao, K., Langworthy, M., Batts, L., Brown, C. B., Moses, H. L., and Baldwin, H. S. (2006). Tgfbeta signaling is required for atrioventricular cushion mesenchyme remodeling during in vivo cardiac development. Development *133*, 4585-4593.

Kallianpur, A. R., Jordan, J. E., and Brandt, S. J. (1994). The SCL/TAL-1 gene is expressed in progenitors of both the hematopoietic and vascular systems during embryogenesis. Blood *83*, 1200-1208.

Kattman, S. J., Huber, T. L., and Keller, G. M. (2006). Multipotent flk-1+ cardiovascular progenitor cells give rise to the cardiomyocyte, endothelial, and vascular smooth muscle lineages. Dev Cell *11*, 723-732.

Kawai, T., Takahashi, T., Esaki, M., Ushikoshi, H., Nagano, S., Fujiwara, H., and Kosai, K. (2004). Efficient cardiomyogenic differentiation of embryonic stem cell by fibroblast growth factor 2 and bone morphogenetic protein 2. Circ J *68*, 691-702.

Kearney, J. B., Ambler, C. A., Monaco, K. A., Johnson, N., Rapoport, R. G., and Bautch, V. L. (2002). Vascular endothelial growth factor receptor Flt-1 negatively regulates developmental blood vessel formation by modulating endothelial cell division. Blood *99*, 2397-2407.

Kearney, J. B., Kappas, N. C., Ellerstrom, C., DiPaola, F. W., and Bautch, V. L. (2004). The VEGF receptor flt-1 (VEGFR-1) is a positive modulator of vascular sprout formation and branching morphogenesis. Blood *103*, 4527-4535.

Keller, G. (2005). Embryonic stem cell differentiation: emergence of a new era in biology and medicine. Genes Dev *19*, 1129-1155.

Keller, G., Kennedy, M., Papayannopoulou, T., and Wiles, M. V. (1993). Hematopoietic commitment during embryonic stem cell differentiation in culture. Mol Cell Biol *13*, 473-486.

Kelly, R. G., Brown, N. A., and Buckingham, M. E. (2001). The arterial pole of the mouse heart forms from Fgf10-expressing cells in pharyngeal mesoderm. Dev Cell *1*, 435-440.

Kennedy, M., Firpo, M., Choi, K., Wall, C., Robertson, S., Kabrun, N., and Keller, G. (1997). A common precursor for primitive erythropoiesis and definitive haematopoiesis. Nature *386*, 488-493.

Kim, J. B., Porreca, G. J., Song, L., Greenway, S. C., Gorham, J. M., Church, G. M., Seidman, C. E., and Seidman, J. G. (2007). Polony multiplex analysis of gene expression (PMAGE) in mouse hypertrophic cardiomyopathy. Science *316*, 1481-1484.

Kinder, S. J., Tsang, T. E., Quinlan, G. A., Hadjantonakis, A. K., Nagy, A., and Tam, P. P. (1999). The orderly allocation of mesodermal cells to the extraembryonic structures and the anteroposterior axis during gastrulation of the mouse embryo. Development *126*, 4691-4701.

Kirby, M. L. (2002). Molecular embryogenesis of the heart. Pediatr Dev Pathol *5*, 516-543.

Kisanuki, Y. Y., Hammer, R. E., Miyazaki, J., Williams, S. C., Richardson, J. A., and Yanagisawa, M. (2001). Tie2-Cre transgenic mice: a new model for endothelial cell-lineage analysis in vivo. Dev Biol *230*, 230-242.

Kitajima, S., Takagi, A., Inoue, T., and Saga, Y. (2000). MesP1 and MesP2 are essential for the development of cardiac mesoderm. Development *127*, 3215-3226.

Kleinjan, D. A., Seawright, A., Schedl, A., Quinlan, R. A., Danes, S., and van Heyningen, V. (2001). Aniridia-associated translocations, DNase hypersensitivity, sequence comparison and transgenic analysis redefine the functional domain of PAX6. Hum Mol Genet *10*, 2049-2059.

Kleinjan, D. A., and van Heyningen, V. (2005). Long-range control of gene expression: emerging mechanisms and disruption in disease. Am J Hum Genet *76*, 8-32.

Koga, T., Matsui, Y., Asagiri, M., Kodama, T., de Crombrugghe, B., Nakashima, K., and Takayanagi, H. (2005). NFAT and Osterix cooperatively regulate bone formation. Nat Med *11*, 880-885.

Kouskoff, V., Lacaud, G., Schwantz, S., Fehling, H. J., and Keller, G. (2005). Sequential development of hematopoietic and cardiac mesoderm during embryonic stem cell differentiation. Proc Natl Acad Sci U S A *102*, 13170-13175.

Kumar, D., and Sun, B. (2005). Transforming growth factor-beta2 enhances differentiation of cardiac myocytes from embryonic stem cells. Biochem Biophys Res Commun *332*, 135-141.

Ladd, A. N., Yatskievych, T. A., and Antin, P. B. (1998). Regulation of avian cardiac myogenesis by activin/TGFbeta and bone morphogenetic proteins. Dev Biol *204*, 407-419.

Lampugnani, M. G., Resnati, M., Raiteri, M., Pigott, R., Pisacane, A., Houen, G., Ruco, L. P., and Dejana, E. (1992). A novel endothelial-specific membrane protein is a marker of cell-cell contacts. J Cell Biol *118*, 1511-1522.

Lange, A. W., and Yutzey, K. E. (2006). NFATc1 expression in the developing heart valves is responsive to the RANKL pathway and is required for endocardial expression of cathepsin K. Dev Biol *292*, 407-417.

Lavine, K. J., Yu, K., White, A. C., Zhang, X., Smith, C., Partanen, J., and Ornitz, D. M. (2005). Endocardial and epicardial derived FGF signals regulate myocardial proliferation and differentiation in vivo. Dev Cell *8*, 85-95.

Lee, D., Park, C., Lee, H., Lugus, J. J., Kim, S. H., Arentson, E., Chung, Y. S., Gomez, G., Kyba, M., Lin, S.*, et al.* (2008). ER71 acts downstream of BMP, Notch, and Wnt signaling in blood and vessel progenitor specification. Cell Stem Cell *2*, 497-507.

Lee, E. C., Yu, D., Martinez de Velasco, J., Tessarollo, L., Swing, D. A., Court, D. L., Jenkins, N. A., and Copeland, N. G. (2001). A highly efficient Escherichia coli-based chromosome engineering system adapted for recombinogenic targeting and subcloning of BAC DNA. Genomics *73*, 56-65.

Lee, K. F., Simon, H., Chen, H., Bates, B., Hung, M. C., and Hauser, C. (1995). Requirement for neuregulin receptor erbB2 in neural and cardiac development. Nature *378*, 394-398.

Lee, R. K., Stainier, D. Y., Weinstein, B. M., and Fishman, M. C. (1994). Cardiovascular development in the zebrafish. II. Endocardial progenitors are sequestered within the heart field. Development *120*, 3361-3366.

Leveen, P., Pekny, M., Gebre-Medhin, S., Swolin, B., Larsson, E., and Betsholtz, C. (1994). Mice deficient for PDGF B show renal, cardiovascular, and hematological abnormalities. Genes Dev *8*, 1875-1887.

Liao, W., Bisgrove, B. W., Sawyer, H., Hug, B., Bell, B., Peters, K., Grunwald, D. J., and Stainier, D. Y. (1997). The zebrafish gene cloche acts upstream of a flk-1 homologue to regulate endothelial cell differentiation. Development *124*, 381-389.

Lickert, H., Kutsch, S., Kanzler, B., Tamai, Y., Taketo, M. M., and Kemler, R. (2002). Formation of multiple hearts in mice following deletion of beta-catenin in the embryonic endoderm. Dev Cell *3*, 171-181.

Lin, Q., Schwarz, J., Bucana, C., and Olson, E. N. (1997). Control of mouse cardiac morphogenesis and myogenesis by transcription factor MEF2C. Science *276*, 1404-1407.

Linask, K. K. (1992). N-cadherin localization in early heart development and polar expression of Na+,K(+)-ATPase, and integrin during pericardial coelom formation and epithelialization of the differentiating myocardium. Dev Biol *151*, 213-224.

Linask, K. K., and Lash, J. W. (1993). Early heart development: dynamics of endocardial cell sorting suggests a common origin with cardiomyocytes. Dev Dyn *196*, 62-69.

Lindsley, R. C., Gill, J. G., Kyba, M., Murphy, T. L., and Murphy, K. M. (2006). Canonical Wnt signaling is required for development of embryonic stem cell-derived mesoderm. Development *133*, 3787-3796.

Lindsley, R. C., Gill, J. G., Murphy, T. L., Langer, E. M., Cai, M., Mashayekhi, M., Wang, W., Niwa, N., Nerbonne, J. M., Kyba, M., and Murphy, K. M. (2008). Mesp1 coordinately regulates cardiovascular fate restriction and epithelial-mesenchymal transition in differentiating ESCs. Cell Stem Cell *3*, 55-68.

Lints, T. J., Parsons, L. M., Hartley, L., Lyons, I., and Harvey, R. P. (1993). Nkx-2.5: a novel murine homeobox gene expressed in early heart progenitor cells and their myogenic descendants. Development *119*, 969.

Liu, P., Jenkins, N. A., and Copeland, N. G. (2003). A highly efficient recombineering-based method for generating conditional knockout mutations. Genome Res *13*, 476-484.

Lough, J., Barron, M., Brogley, M., Sugi, Y., Bolender, D. L., and Zhu, X. (1996). Combined BMP-2 and FGF-4, but neither factor alone, induces cardiogenesis in non-precardiac embryonic mesoderm. Dev Biol *178*, 198-202.

Mably, J. D., Mohideen, M. A., Burns, C. G., Chen, J. N., and Fishman, M. C. (2003). heart of glass regulates the concentric growth of the heart in zebrafish. Curr Biol *13*, 2138-2147.

Macian, F. (2005). NFAT proteins: key regulators of T-cell development and function. Nat Rev Immunol *5*, 472-484.

Mahdavi, V., Izumo, S., and Nadal-Ginard, B. (1987). Developmental and hormonal regulation of sarcomeric myosin heavy chain gene family. Circ Res *60*, 804-814.

Mann, J. R. (2001). Deriving and propagating mouse embryonic stem cell lines for studying genomic imprinting. Methods Mol Biol *181*, 21-39.

Martin, G. R. (1981). Isolation of a pluripotent cell line from early mouse embryos cultured in medium conditioned by teratocarcinoma stem cells. Proc Natl Acad Sci U S A *78*, 7634-7638.

Marvin, M. J., Di Rocco, G., Gardiner, A., Bush, S. M., and Lassar, A. B. (2001). Inhibition of Wnt activity induces heart formation from posterior mesoderm. Genes Dev *15*, 316-327.

McCloskey, K. E., Smith, D. A., Jo, H., and Nerem, R. M. (2006). Embryonic stem cell-derived endothelial cells may lack complete functional maturation in vitro. J Vasc Res *43*, 411-421.

Meilhac, S. M., Esner, M., Kelly, R. G., Nicolas, J. F., and Buckingham, M. E. (2004). The clonal origin of myocardial cells in different regions of the embryonic mouse heart. Dev Cell *6*, 685-698.

Meyer, D., and Birchmeier, C. (1995). Multiple essential functions of neuregulin in development. Nature *378*, 386-390.

Mikawa, T., and Gourdie, R. G. (1996). Pericardial mesoderm generates a population of coronary smooth muscle cells migrating into the heart along with ingrowth of the epicardial organ. Dev Biol *174*, 221-232.

Miller-Hance, W. C., LaCorbiere, M., Fuller, S. J., Evans, S. M., Lyons, G., Schmidt, C., Robbins, J., and Chien, K. R. (1993). In vitro chamber specification during embryonic stem cell cardiogenesis. Expression of the ventricular myosin light chain-2 gene is independent of heart tube formation. J Biol Chem *268*, 25244-25252.

Mjaatvedt, C. H., Nakaoka, T., Moreno-Rodriguez, R., Norris, R. A., Kern, M. J., Eisenberg, C. A., Turner, D., and Markwald, R. R. (2001). The outflow tract of the heart is recruited from a novel heart-forming field. Dev Biol *238*, 97-109.

Moretti, A., Caron, L., Nakano, A., Lam, J. T., Bernshausen, A., Chen, Y., Qyang, Y., Bu, L., Sasaki, M., Martin-Puig, S*., et al.* (2006). Multipotent embryonic isl1+ progenitor cells lead to cardiac, smooth muscle, and endothelial cell diversification. Cell *127*, 1151-1165.

Motoike, T., Markham, D. W., Rossant, J., and Sato, T. N. (2003). Evidence for novel fate of Flk1+ progenitor: contribution to muscle lineage. Genesis *35*, 153-159.

Murry, C. E., and Keller, G. (2008). Differentiation of embryonic stem cells to clinically relevant populations: lessons from embryonic development. Cell *132*, 661-680.

Nagai, T., Ibata, K., Park, E. S., Kubota, M., Mikoshiba, K., and Miyawaki, A. (2002). A variant of yellow fluorescent protein with fast and efficient maturation for cell-biological applications. Nat Biotechnol *20*, 87-90.

Nagy, A. (2003a). Manipulating the mouse embryo: a laboratory manual, 3rd edn (Cold Spring Harbor, N.Y.: Cold Spring Harbor Laboratory Press).

Nagy, A. (2003b). Manipulating the mouse embryo: a laboratory manual, 3rd edn (Cold Spring Harbor, N.Y.: Cold Spring Harbor Laboratory Press).

Naito, A. T., Shiojima, I., Akazawa, H., Hidaka, K., Morisaki, T., Kikuchi, A., and Komuro, I. (2006). Developmental stage-specific biphasic roles of Wnt/beta-catenin signaling in cardiomyogenesis and hematopoiesis. Proc Natl Acad Sci U S A *103*, 19812-19817.

Narmoneva, D. A., Vukmirovic, R., Davis, M. E., Kamm, R. D., and Lee, R. T. (2004). Endothelial cells promote cardiac myocyte survival and spatial reorganization: implications for cardiac regeneration. Circulation *110*, 962-968.

Narumiya, H., Hidaka, K., Shirai, M., Terami, H., Aburatani, H., and Morisaki, T. (2007). Endocardiogenesis in embryoid bodies: novel markers identified by gene expression profiling. Biochem Biophys Res Commun *357*, 896-902.

Nemer, G., and Nemer, M. (2002). Cooperative interaction between GATA5 and NF-ATc regulates endothelial-endocardial differentiation of cardiogenic cells. Development *129*, 4045-4055.

Nemir, M., Croquelois, A., Pedrazzini, T., and Radtke, F. (2006). Induction of cardiogenesis in embryonic stem cells via downregulation of Notch1 signaling. Circ Res *98*, 1471-1478.

Ng, E. S., Azzola, L., Sourris, K., Robb, L., Stanley, E. G., and Elefanty, A. G. (2005). The primitive streak gene Mixl1 is required for efficient haematopoiesis and BMP4-induced ventral mesoderm patterning in differentiating ES cells. Development *132*, 873-884.

Nishikawa, S. I., Nishikawa, S., Hirashima, M., Matsuyoshi, N., and Kodama, H. (1998). Progressive lineage analysis by cell sorting and culture identifies FLK1+VE-cadherin+ cells at a diverging point of endothelial and hemopoietic lineages. Development *125*, 1747-1757.

Nostro, M. C., Cheng, X., Keller, G. M., and Gadue, P. (2008). Wnt, activin, and BMP signaling regulate distinct stages in the developmental pathway from embryonic stem cells to blood. Cell Stem Cell *2*, 60-71.

Ogawa, S., Tagawa, Y., Kamiyoshi, A., Suzuki, A., Nakayama, J., Hashikura, Y., and Miyagawa, S. (2005). Crucial roles of mesodermal cell lineages in a murine embryonic stem cell-derived in vitro liver organogenesis system. Stem Cells *23*, 903-913.

Park, C., Afrikanova, I., Chung, Y. S., Zhang, W. J., Arentson, E., Fong Gh, G., Rosendahl, A., and Choi, K. (2004). A hierarchical order of factors in the generation of FLK1- and SCL-expressing hematopoietic and endothelial progenitors from embryonic stem cells. Development *131*, 2749-2762.

Park, I. H., Arora, N., Huo, H., Maherali, N., Ahfeldt, T., Shimamura, A., Lensch, M. W., Cowan, C., Hochedlinger, K., and Daley, G. Q. (2008). Disease-Specific Induced Pluripotent Stem Cells. Cell.

Parker, L., and Stainier, D. Y. (1999). Cell-autonomous and non-autonomous requirements for the zebrafish gene cloche in hematopoiesis. Development *126*, 2643-2651.

Passier, R., Oostwaard, D. W., Snapper, J., Kloots, J., Hassink, R. J., Kuijk, E., Roelen, B., de la Riviere, A. B., and Mummery, C. (2005). Increased cardiomyocyte differentiation from human embryonic stem cells in serum-free cultures. Stem Cells *23*, 772-780.

Pearson, S., Sroczynska, P., Lacaud, G., and Kouskoff, V. (2008). The stepwise specification of embryonic stem cells to hematopoietic fate is driven by sequential exposure to Bmp4, activin A, bFGF and VEGF. Development *135*, 1525-1535.

Puri, M. C., Partanen, J., Rossant, J., and Bernstein, A. (1999). Interaction of the TEK and TIE receptor tyrosine kinases during cardiovascular development. Development *126*, 4569-4580.

Qin, Y., Kong, L. K., Poirier, C., Truong, C., Overbeek, P. A., and Bishop, C. E. (2004). Long-range activation of Sox9 in Odd Sex (Ods) mice. Hum Mol Genet *13*, 1213-1218.

Qyang, Y., Martin-Puig, S., Chiravuri, M., Chen, S., Xu, H., Bu, L., Jiang, X., Lin, L., Granger, A., Moretti, A.*, et al.* (2007). The renewal and differentiation of Isl1+ cardiovascular progenitors are controlled by a Wnt/beta-catenin pathway. Cell Stem Cell *1*, 165-179.

Radice, G. L., Rayburn, H., Matsunami, H., Knudsen, K. A., Takeichi, M., and Hynes, R. O. (1997). Developmental defects in mouse embryos lacking N-cadherin. Dev Biol *181*, 64-78.

Ranger, A. M., Gerstenfeld, L. C., Wang, J., Kon, T., Bae, H., Gravallese, E. M., Glimcher, M. J., and Glimcher, L. H. (2000). The nuclear factor of activated T cells (NFAT) transcription factor NFATp (NFATc2) is a repressor of chondrogenesis. J Exp Med *191*, 9-22.

Ranger, A. M., Grusby, M. J., Hodge, M. R., Gravallese, E. M., de la Brousse, F. C., Hoey, T., Mickanin, C., Baldwin, H. S., and Glimcher, L. H. (1998). The transcription factor NF-ATc is essential for cardiac valve formation. Nature *392*, 186-190.

Rao, A., Luo, C., and Hogan, P. G. (1997). Transcription factors of the NFAT family: regulation and function. Annu Rev Immunol *15*, 707-747.

Reiter, J. F., Alexander, J., Rodaway, A., Yelon, D., Patient, R., Holder, N., and Stainier, D. Y. (1999). Gata5 is required for the development of the heart and endoderm in zebrafish. Genes Dev *13*, 2983-2995.

Robson, P., Stein, P., Zhou, B., Schultz, R. M., and Baldwin, H. S. (2001). Inner cell mass-specific expression of a cell adhesion molecule (PECAM-1/CD31) in the mouse blastocyst. Dev Biol *234*, 317-329.

Saga, Y., Kitajima, S., and Miyagawa-Tomita, S. (2000). Mesp1 expression is the earliest sign of cardiovascular development. Trends Cardiovasc Med *10*, 345-352.

Saga, Y., Miyagawa-Tomita, S., Takagi, A., Kitajima, S., Miyazaki, J., and Inoue, T. (1999). MesP1 is expressed in the heart precursor cells and required for the formation of a single heart tube. Development *126*, 3437-3447.

Schmittgen, T. D., and Livak, K. J. (2008). Analyzing real-time PCR data by the comparative C(T) method. Nat Protoc *3*, 1101-1108.

Schneider, V. A., and Mercola, M. (2001). Wnt antagonism initiates cardiogenesis in Xenopus laevis. Genes Dev *15*, 304-315.

Schoenebeck, J. J., Keegan, B. R., and Yelon, D. (2007). Vessel and blood specification override cardiac potential in anterior mesoderm. Dev Cell *13*, 254-267.

Schoonjans, L., Kreemers, V., Danloy, S., Moreadith, R. W., Laroche, Y., and Collen, D. (2003). Improved generation of germline-competent embryonic stem cell lines from inbred mouse strains. Stem Cells *21*, 90-97.

Schroeder, J. A., Jackson, L. F., Lee, D. C., and Camenisch, T. D. (2003). Form and function of developing heart valves: coordination by extracellular matrix and growth factor signaling. J Mol Med *81*, 392-403.

Schultheiss, T. M., Burch, J. B., and Lassar, A. B. (1997). A role for bone morphogenetic proteins in the induction of cardiac myogenesis. Genes Dev *11*, 451-462.

Schultheiss, T. M., Xydas, S., and Lassar, A. B. (1995). Induction of avian cardiac myogenesis by anterior endoderm. Development *121*, 4203-4214.

Sedmera, D., Pexieder, T., Vuillemin, M., Thompson, R. P., and Anderson, R. H. (2000). Developmental patterning of the myocardium. Anat Rec *258*, 319-337.

Shalaby, F., Ho, J., Stanford, W. L., Fischer, K. D., Schuh, A. C., Schwartz, L., Bernstein, A., and Rossant, J. (1997). A requirement for Flk1 in primitive and definitive hematopoiesis and vasculogenesis. Cell *89*, 981-990.

Shalaby, F., Rossant, J., Yamaguchi, T. P., Gertsenstein, M., Wu, X. F., Breitman, M. L., and Schuh, A. C. (1995). Failure of blood-island formation and vasculogenesis in Flk-1-deficient mice. Nature *376*, 62-66.

Sharpe, J., Lettice, L., Hecksher-Sorensen, J., Fox, M., Hill, R., and Krumlauf, R. (1999). Identification of sonic hedgehog as a candidate gene responsible for the polydactylous mouse mutant Sasquatch. Curr Biol *9*, 97-100.

Shaw, J. P., Utz, P. J., Durand, D. B., Toole, J. J., Emmel, E. A., and Crabtree, G. R. (1988). Identification of a putative regulator of early T cell activation genes. Science *241*, 202-205.

Smith, A. G., Heath, J. K., Donaldson, D. D., Wong, G. G., Moreau, J., Stahl, M., and Rogers, D. (1988). Inhibition of pluripotential embryonic stem cell differentiation by purified polypeptides. Nature *336*, 688-690.

Snyder, A., Fraser, S. T., and Baron, M. H. (2004). Bone morphogenetic proteins in vertebrate hematopoietic development. J Cell Biochem *93*, 224-232.

Soriano, P. (1999). Generalized lacZ expression with the ROSA26 Cre reporter strain. Nat Genet *21*, 70-71.

Srivastava, D. (2006). Making or breaking the heart: from lineage determination to morphogenesis. Cell *126*, 1037-1048.

Srivastava, D., Cserjesi, P., and Olson, E. N. (1995). A subclass of bHLH proteins required for cardiac morphogenesis. Science *270*, 1995-1999.

Srivastava, D., and Olson, E. N. (2000). A genetic blueprint for cardiac development. Nature *407*, 221-226.

Stainier, D. Y., Weinstein, B. M., Detrich, H. W., 3rd, Zon, L. I., and Fishman, M. C. (1995). Cloche, an early acting zebrafish gene, is required by both the endothelial and hematopoietic lineages. Development *121*, 3141-3150.

Stanley, E. G., Biben, C., Elefanty, A., Barnett, L., Koentgen, F., Robb, L., and Harvey, R. P. (2002). Efficient Cre-mediated deletion in cardiac progenitor cells conferred by a 3'UTR-ires-Cre allele of the homeobox gene Nkx2-5. Int J Dev Biol *46*, 431-439.

Stenvers, K. L., Tursky, M. L., Harder, K. W., Kountouri, N., Amatayakul-Chantler, S., Grail, D., Small, C., Weinberg, R. A., Sizeland, A. M., and Zhu, H. J. (2003). Heart and liver defects and reduced transforming growth factor beta2 sensitivity in transforming growth factor beta type III receptor-deficient embryos. Mol Cell Biol *23*, 4371-4385.

Sugi, Y., and Markwald, R. R. (1995). Early endocardial formation originates from precardiac mesoderm as revealed by QH-1 antibody staining. Ital J Anat Embryol *100 Suppl 1*, 263-272.

Sugi, Y., and Markwald, R. R. (1996). Formation and early morphogenesis of endocardial endothelial precursor cells and the role of endoderm. Dev Biol *175*, 66-83.

Sugi, Y., and Markwald, R. R. (2003). Endodermal growth factors promote endocardial precursor cell formation from precardiac mesoderm. Dev Biol *263*, 35-49.

Takahashi, K., Tanabe, K., Ohnuki, M., Narita, M., Ichisaka, T., Tomoda, K., and Yamanaka, S. (2007). Induction of pluripotent stem cells from adult human fibroblasts by defined factors. Cell *131*, 861-872.

Takayanagi, H., Kim, S., Koga, T., Nishina, H., Isshiki, M., Yoshida, H., Saiura, A., Isobe, M., Yokochi, T., Inoue, J.*, et al.* (2002). Induction and activation of the transcription factor NFATc1 (NFAT2) integrate RANKL signaling in terminal differentiation of osteoclasts. Dev Cell *3*, 889-901.

Tam, P. P., and Behringer, R. R. (1997). Mouse gastrulation: the formation of a mammalian body plan. Mech Dev *68*, 3-25.

Tam, P. P., Parameswaran, M., Kinder, S. J., and Weinberger, R. P. (1997). The allocation of epiblast cells to the embryonic heart and other mesodermal lineages: the role of ingression and tissue movement during gastrulation. Development *124*, 1631-1642.

Timmerman, L. A., Grego-Bessa, J., Raya, A., Bertran, E., Perez-Pomares, J. M., Diez, J., Aranda, S., Palomo, S., McCormick, F., Izpisua-Belmonte, J. C., and de la Pompa, J. L. (2004). Notch promotes epithelial-mesenchymal transition during cardiac development and oncogenic transformation. Genes Dev *18*, 99-115.

Tomishima, M. J., Hadjantonakis, A. K., Gong, S., and Studer, L. (2007). Production of green fluorescent protein transgenic embryonic stem cells using the GENSAT bacterial artificial chromosome library. Stem Cells *25*, 39-45.

Vintersten, K., Testa, G., and Stewart, A. F. (2004). Microinjection of BAC DNA into the pronuclei of fertilized mouse oocytes. Methods Mol Biol *256*, 141-158.

Vittet, D., Prandini, M. H., Berthier, R., Schweitzer, A., Martin-Sisteron, H., Uzan, G., and Dejana, E. (1996). Embryonic stem cells differentiate in vitro to endothelial cells through successive maturation steps. Blood *88*, 3424-3431.

Waldo, K., Miyagawa-Tomita, S., Kumiski, D., and Kirby, M. L. (1998). Cardiac neural crest cells provide new insight into septation of the cardiac outflow tract: aortic sac to ventricular septal closure. Dev Biol *196*, 129-144.

Waldo, K., Zdanowicz, M., Burch, J., Kumiski, D. H., Stadt, H. A., Godt, R. E., Creazzo, T. L., and Kirby, M. L. (1999). A novel role for cardiac neural crest in heart development. J Clin Invest *103*, 1499-1507.

Waldo, K. L., Kumiski, D. H., Wallis, K. T., Stadt, H. A., Hutson, M. R., Platt, D. H., and Kirby, M. L. (2001). Conotruncal myocardium arises from a secondary heart field. Development *128*, 3179-3188.

Wang, B., Weidenfeld, J., Lu, M. M., Maika, S., Kuziel, W. A., Morrisey, E. E., and Tucker, P. W. (2004). Foxp1 regulates cardiac outflow tract, endocardial cushion morphogenesis and myocyte proliferation and maturation. Development *131*, 4477-4487.

Warming, S., Costantino, N., Court, D. L., Jenkins, N. A., and Copeland, N. G. (2005). Simple and highly efficient BAC recombineering using galK selection. Nucleic Acids Res *33*, e36.

Wei, Y., and Mikawa, T. (2000). Fate diversity of primitive streak cells during heart field formation in ovo. Dev Dyn *219*, 505-513.

Westfall, M. V., Pasyk, K. A., Yule, D. I., Samuelson, L. C., and Metzger, J. M. (1997). Ultrastructure and cell-cell coupling of cardiac myocytes differentiating in embryonic stem cell cultures. Cell Motil Cytoskeleton *36*, 43-54.

White, S. M., and Claycomb, W. C. (2005). Embryonic stem cells form an organized, functional cardiac conduction system in vitro. Am J Physiol Heart Circ Physiol *288*, H670-679.

Williams, R. L., Hilton, D. J., Pease, S., Willson, T. A., Stewart, C. L., Gearing, D. P., Wagner, E. F., Metcalf, D., Nicola, N. A., and Gough, N. M. (1988). Myeloid leukaemia inhibitory factor maintains the developmental potential of embryonic stem cells. Nature *336*, 684-687.

Wilson, V., Rashbass, P., and Beddington, R. S. (1993). Chimeric analysis of T (Brachyury) gene function. Development *117*, 1321-1331.

Winslow, M. M., Pan, M., Starbuck, M., Gallo, E. M., Deng, L., Karsenty, G., and Crabtree, G. R. (2006). Calcineurin/NFAT signaling in osteoblasts regulates bone mass. Dev Cell *10*, 771-782.

Wu, S. M., Fujiwara, Y., Cibulsky, S. M., Clapham, D. E., Lien, C. L., Schultheiss, T. M., and Orkin, S. H. (2006). Developmental origin of a bipotential myocardial and smooth muscle cell precursor in the mammalian heart. Cell *127*, 1137-1150.

Wunsch, A. M., Little, C. D., and Markwald, R. R. (1994). Cardiac endothelial heterogeneity defines valvular development as demonstrated by the diverse expression of JB3, an antigen of the endocardial cushion tissue. Dev Biol *165*, 585-601.

Yamada, G., Kioussi, C., Schubert, F. R., Eto, Y., Chowdhury, K., Pituello, F., and Gruss, P. (1994). Regulated expression of Brachyury(T), Nkx1.1 and Pax genes in embryoid bodies. Biochem Biophys Res Commun *199*, 552-563.

Yamashita, J., Itoh, H., Hirashima, M., Ogawa, M., Nishikawa, S., Yurugi, T., Naito, M., Nakao, K., and Nishikawa, S. (2000). Flk1-positive cells derived from embryonic stem cells serve as vascular progenitors. Nature *408*, 92-96.

Yamashita, J. K., Takano, M., Hiraoka-Kanie, M., Shimazu, C., Peishi, Y., Yanagi, K., Nakano, A., Inoue, E., Kita, F., and Nishikawa, S. (2005). Prospective identification of cardiac progenitors by a novel single cell-based cardiomyocyte induction. Faseb J *19*, 1534-1536.

Yanagisawa, H., Hammer, R. E., Richardson, J. A., Emoto, N., Williams, S. C., Takeda, S., Clouthier, D. E., and Yanagisawa, M. (2000). Disruption of ECE-1 and ECE-2 reveals a role for endothelin-converting enzyme-2 in murine cardiac development. J Clin Invest *105*, 1373-1382.

Yanagisawa, H., Hammer, R. E., Richardson, J. A., Williams, S. C., Clouthier, D. E., and Yanagisawa, M. (1998a). Role of Endothelin-1/Endothelin-A receptor-mediated signaling pathway in the aortic arch patterning in mice. J Clin Invest *102*, 22-33.

Yanagisawa, H., Yanagisawa, M., Kapur, R. P., Richardson, J. A., Williams, S. C., Clouthier, D. E., de Wit, D., Emoto, N., and Hammer, R. E. (1998b). Dual genetic pathways of endothelin-mediated intercellular signaling revealed by targeted disruption of endothelin converting enzyme-1 gene. Development *125*, 825-836.

Yang, L., Soonpaa, M. H., Adler, E. D., Roepke, T. K., Kattman, S. J., Kennedy, M., Henckaerts, E., Bonham, K., Abbott, G. W., Linden, R. M.*, et al.* (2008). Human cardiovascular progenitor cells develop from a KDR+ embryonic-stem-cell-derived population. Nature *453*, 524-528.

Yatskievych, T. A., Ladd, A. N., and Antin, P. B. (1997). Induction of cardiac myogenesis in avian pregastrula epiblast: the role of the hypoblast and activin. Development *124*, 2561-2570.

Ying, Q. L., Nichols, J., Chambers, I., and Smith, A. (2003). BMP induction of Id proteins suppresses differentiation and sustains embryonic stem cell self-renewal in collaboration with STAT3. Cell *115*, 281-292.

Yu, J., Vodyanik, M. A., Smuga-Otto, K., Antosiewicz-Bourget, J., Frane, J. L., Tian, S., Nie, J., Jonsdottir, G. A., Ruotti, V., Stewart, R.*, et al.* (2007). Induced pluripotent stem cell lines derived from human somatic cells. Science *318*, 1917-1920.

Yuasa, S., Itabashi, Y., Koshimizu, U., Tanaka, T., Sugimura, K., Kinoshita, M., Hattori, F., Fukami, S., Shimazaki, T., Ogawa, S.*, et al.* (2005). Transient inhibition of BMP signaling by Noggin induces cardiomyocyte differentiation of mouse embryonic stem cells. Nat Biotechnol *23*, 607-611.

Yutzey, K. E., and Kirby, M. L. (2002). Wherefore heart thou? Embryonic origins of cardiogenic mesoderm. Dev Dyn *223*, 307-320.

Zaffran, S., Kelly, R. G., Meilhac, S. M., Buckingham, M. E., and Brown, N. A. (2004). Right ventricular myocardium derives from the anterior heart field. Circ Res *95*, 261-268.

Zeineddine, D., Papadimou, E., Chebli, K., Gineste, M., Liu, J., Grey, C., Thurig, S., Behfar, A., Wallace, V. A., Skerjanc, I. S., and Puceat, M. (2006). Oct-3/4 dose dependently regulates specification of embryonic stem cells toward a cardiac lineage and early heart development. Dev Cell *11*, 535-546.

Zhou, B., Cron, R. Q., Wu, B., Genin, A., Wang, Z., Liu, S., Robson, P., and Baldwin, H. S. (2002). Regulation of the murine Nfatc1 gene by NFATc2. J Biol Chem *277*, 10704-10711.

Zhou, B., Wu, B., Tompkins, K. L., Boyer, K. L., Grindley, J. C., and Baldwin, H. S. (2005). Characterization of Nfatc1 regulation identifies an enhancer required for gene expression that is specific to pro-valve endocardial cells in the developing heart. Development *132*, 1137-1146.